TPL2 FUNCTIONS IN PULMONARY EPITHELIAL CELLS TO CONSTRAIN INTERFERON PRODUCTION AND PULMONARY FIBROSIS IN RESPONSE TO INFLUENZA A VIRUS INFECTION

by

KARA DIONNE WYATT

(Under the Direction of WENDY T. WATFORD)

ABSTRACT

Tumor progression locus 2 (Tpl2) is a serine/threonine kinase that regulates the expression of inflammatory mediators in response to a variety of TLR, cytokine and G-protein-coupled receptors. Tpl2 negatively regulates the expression of host-encoded interferons (IFNs) within hematopoietic cells, however the regulation of antiviral responses by Tpl2 within the target cells of influenza infection, the lung epithelial cells, has not been investigated. We used *Nkx2.1*-Cre and *Sftpc-CreER*^{T2} to drive Tpl2 deletion within pulmonary epithelial cells to delineate epithelial cell-specific functions of Tpl2 during influenza infection. Tpl2 ablation within lung epithelial cells using *Nkx2.1-Cre Tpl2*$^{fl/-}$ mice caused a significant increase in morbidity, mortality, and pulmonary fibrosis in response to influenza infection. *In vitro* studies confirmed that Tpl2 constrains both type I and type III IFN responses within the type I airway epithelial cell (AECI) line, LET1, as well as primary type II airway epithelial cells (AECII). Overall, these results implicate Tpl2 in the regulation of early innate responses within pulmonary epithelial cells during influenza infection. Using *Sftpc-CreER*^{T2} *Tpl2*$^{fl/-}$ mice, which require tamoxifen treatment to induce Tpl2 deletion within AECII, we report histopathologic changes in the lungs in cre-recombinase-negative mice treated with tamoxifen intraperitoneally. These changes were noted in distal organs such as the lungs which were characterized by the presence of inflammation within the alveolus, perivascular cuff, vasculature, and pleural cavity, resulting in an inflammatory cell

infiltrate. These findings provide a cautionary note that tamoxifen treatment alone leads to histological alterations that may obscure research interpretations and highlights the need for the development of other innovative mouse models for inducible cre-mediated deletion. Collectively, the findings demonstrate that Tpl2 negatively regulates type I and type III IFN production within lung epithelial cells in response to virus sensing *in vitro* and that Tpl2 ablation within lung epithelial cells is sufficient to leads to dyspnea and pulmonary fibrosis in response to influenza infection.

INDEX WORDS: interferons, epithelial cells, influenza, Tumor progression locus 2

TPL2 FUNCTIONS IN PULMONARY EPITHELIAL CELLS TO CONSTRAIN INTERFERON PRODUCTION AND PULMONARY FIBROSIS IN RESPONSE TO INFLUENZA A VIRUS INFECTION

by

KARA DIONNE WYATT

Bachelor of Science, Winthrop University, 2014

A Dissertation Submitted to the Graduate Faculty of The University of Georgia in Partial Fulfillment of the Requirements for the Degree

DOCTOR OF PHILOSOPHY

ATHENS, GEORGIA

2021

TPL2 FUNCTIONS IN PULMONARY EPITHELIAL CELLS TO CONSTRAIN INTERFERON PRODUCTION AND PULMONARY FIBROSIS RESPONSES IN RESPONSE TO INFLUENZA A VIRUS INFECTION

by

KARA DIONNE WYATT

Major Professor:	Wendy Watford
Committee:	Kim Klonowski
	Liliana Jaso-Friedmann
	Lisa Shollenberger
	Ralph Tripp

Electronic Version Approved:

Ron Walcott
Vice Provost for Graduate Education and Dean of the Graduate School
The University of Georgia
May 2021

DEDICATION

For my wonderful husband (Elijah C. Wyatt, MD), my parents (Earl and Doris Hardwick), my in-laws (Bruce, Wendy, and Hannah Wyatt), my sister (Kristen Hardwick), and my dearest friends (Brent and Louise Hardwick and Bailey O. McCarley). I would not have had the strength to continue this process without your constant love, support, encouragement, and faith. I am forever grateful for each of you. Thank you for your patience, love, and prayers.

ACKNOWLEDGEMENTS

My heartfelt thanks to Dr. Wendy Watford for accepting me into her lab and being a wonderful boss, mentor, and friend. Thank you for providing support and training. I am also thankful for my doctoral committee members, Drs. Kim Klonowski, Liliana Jaso-Friedmann, Lisa Shollenberger, and Ralph Tripp for their time, support, and advice throughout my PhD program. Additionally, I would like to thank the current and previous members of the Watford Lab, Krishna Latha and Drs. Chris Slade, Nicole Acuff, and Xin Li for the help in day-to-day activities and encouragement throughout my PhD program. Special thanks to Elijah Caleb Wyatt, MD for his assistance in fixing a wide variety of scientific equipment necessary for my dissertation work. Additionally, I would like to express sincere gratitude to Dr. Demba Sarr, Julie Nelson, Jamie Barber, and Dr. Kaori Sakamoto and the staff at the Coverdell Vivarium who have aided in my dissertation work.

TABLE OF CONTENTS

Page

LIST OF FIGURES

Page

CHAPTER 1

INTRODUCTION AND LITERATURE REVIEW

Host defense against invading pathogens has two main components: innate and adaptive immunity. Both arms of the immune system play critical roles during viral infection and protection. Innate immunity is characterized by a "non-specific", rapid response that impedes pathogen spread and replication. Germline-encoded pathogen recognition receptors (PRRs) recognize either conserved motifs on pathogens termed pathogen-associated molecular patterns (PAMPs) or host-derived danger-associated molecular patterns (DAMPs). These receptors elicit an immediate response by triggering a signaling cascade that culminates in the production of pro-inflammatory mediators, including cytokines. The adaptive immune response is characterized by high specificity, utilizing extensive somatic rearrangement of antigen receptors to generate precise antigen recognition receptors that can discriminate between closely related antigens. Somatic rearrangement of both T and B cell receptors requires time to develop in response to a pathogen; therefore, adaptive responses take days to be fully initiated.

Conventional dendritic cells (cDCs) are considered the bridge between the innate and adaptive immune responses. cDCs are antigen presenting cells (APCs) that can phagocytose pathogens and present antigen on their surfaces within the context of major histocompatibility complex (MHC) class I or MHC class II molecules. The two main cell types that mediate adaptive responses are B and T cells. Naïve T cells that express T-cell receptors (TCRs) specific for the antigen being presented will become activated in the presence of costimulatory molecules. CD4 T cells differentiate into distinct T cell effector lineages [T helper (Th)1, Th2, Th17, follicular helper T cells (Tfh) or regulatory T cells (Tregs)], depending upon local cytokine and other environmental cues. CD8 T cells, or cytotoxic T cells (CTLs), are activated by MHC class I presentation and are responsible for direct killing of infected or transformed host cells. T

cells can also develop into memory cells, which are responsible for inducing a robust and rapid immune response upon reinfection with the same pathogen.

INFLUENZA

Respiratory viruses infect millions annually leading to significant socioeconomic burdens worldwide. Influenza viruses are one of the most common causes of respiratory infections[1]. Individuals most at risk for severe complications to influenza virus include the immunocompromised, children and the elderly[1]. Influenza virus is contracted through contact with virion-containing respiratory droplets via inhalation or fomites[2]. Influenza virus replicates within epithelial cells throughout the upper and lower respiratory tract of humans, specifically within the trachea, bronchi, and pulmonary alveoli[3].

Influenza A (IAV) is a member of the family *Orthomyxoviridae* that affects a broad host range (humans, avian species, swine, and other mammals)[4]. The family *Orthomyxoviridae* contains one genus that includes three Influenza virus types: Influenza A and B, and Influenza C[4]. Influenza has a segmented, negative-sense RNA genome. The genome contains 8 gene segments including: PB2/PB1/PA (polymerase complex for synthesis of viral RNA), HA/NA (surface glycoproteins), M1/M2 (matrix proteins necessary for viral assembly), and NS1 (host immune response regulation) [5,6].

Influenza first interacts with the host cell through the hemagglutinin (HA) located on the surface of the virion which recognizes sialic acid on host cells (Fig. 1). Specifically, the HA1 domain binds to the sialic acid resulting in virion attachment. This interaction also leads to receptor-mediated endocytosis, enabling entry of the virion into the epithelial cell through an endosome. The endosome undergoes an acidification event in order to degrade the virus during which time, the endosome moves along microtubules toward the nucleus [7]. Host endosomal acidification induces a conformational change in the virion's HA protein allowing for the release of the viral genome into the cytoplasm[8910]. The ribonucleoprotein complex (RNP) then uses nuclear localization signals to translocate into the host's nucleus where genome replication and

transcription occur[11]. Influenza virus must utilize the host machinery during replication to produce proteins for infective progeny[10]. Nuclear export signals are utilized to facilitate translocation from the nucleus into the cytoplasm for packaging and assembly. The host's plasma membrane is taken as the envelope for the newly developed virus. Neuraminidase (NA) is crucial for the final export and release of the budding virion due to its role in removing the sialic acid residues on the membrane.[10]

IMMUNE RESPONSE TO INFLUENZA

The two branches of the immune system, innate and adaptive, work together to clear virus within the respiratory tract. The innate response begins with the barrier function of the respiratory epithelium, which produces mucus and surfactants to prevent initial infection of respiratory cells. Respiratory epithelial cells can directly respond to pathogens due to germline-encoded pattern-recognition receptors (PRR) on the cell surface and within endosomes. The most characterized PRRs for influenza detection are toll-like receptors (TLRs), retinoic acid inducible gene-I (RIG-I) and NOD-like receptors (NLRs) [12]. Toll-like receptors (TLRs) are type I integral membrane glycoproteins with an extracellular domain containing leucine rich repeats (LRR) for pathogen recognition and a cytoplasmic toll/interleukin-1R (TIR) domain for signaling[13].

Ligands for 13 TLRs in both human and mice have been well characterized (TLR1-13)[14,15]. The main TLRs involved in viral detection are TLRs 3, 7, 8 (human only), and 9. TLRs 3/7/9 are all located on the endosomal surface within the cell[13] where they detect replicating or released viral nucleic acids within the cytosol. These PRRs are triggered, in the case of influenza, during the pH-dependent fusion event that releases the RNPs. TLR3 and TLR7 recognize double-stranded[16] and single-stranded[17] viral RNA respectively; TLR9 recognizes unmethylated CpG oligonucleotides[18]. The recognition of synthetic oligodeoxynucleotides with unmethylated CpG and RNA (single or double-stranded) is important for significant innate production of antiviral interferons (IFNs) and proinflammatory cytokines such as TNF-α, IL-1β, and IL-1α[19]. The cytokine microenvironment generated by these early innate immune responses

helps to induce Th1 differentiation necessary for appropriate adaptive immune responses that will lead to pathogen clearance.

Retinoic acid-inducible gene I-like-receptors (RLRs) are comprised of receptors that contain a DExD/H box protein motif fused to a caspase activation and recruitment domain (CARD) and C-terminal domain (CTD)[20]. RLRs detect viral RNA within the cytosol and induce type I interferons and proinflammatory cytokines[20] (Fig. 1). The helicase domain of RIG-I is crucial for dsRNA and 5'triphosphate group recognition of viruses. 5' triphosphate groups (5'-ppp) are generated during viral replication and transcription of RNA genomes. RIG-I is able to detect influenza virus, not due to a dsRNA intermediate, but by detecting the uncapped 5'triphosphate viral RNA[21–23]. RIG-I is important for the activation of downstream signaling via caspase, NF-κB, and IRF3 for interferon production[22]. MDA5, although similar in detecting dsRNA, recognizes longer segments of dsRNA (i.e. more than 7 kilobases (kb) long)[14] and therefore is preferentially involved in recognition of *picornaviruses* (encephalomyocarditis virus)[24], *enteroviruses*[25], and Norovirus[26]. In contrast, RIG-I is crucial for the recognition of influenza virus, *paramyxoviruses*, and Japanese encephalitis virus[24].

After recognition of viral ligands by key cytoplasmic and endosomal viral sensors, downstream production of cytokines and chemokines initiates the appropriate microenvironment for cellular recruitment to the site of infection. Neutrophils are polymorphonuclear cells that recruited during the early stages of infection. Neutrophils are capable of sensing virus through cytoplasmic and endosomal TLRs; Neutrophils also contribute to lung immunopathology through the release of ROS and neutrophil extracellular traps (NETs) which can inadvertently damage the epithelium in addition to eliminating virus[27,28]. Natural killer (NK) cells are innate cells that are both recruited to the lung during infection and are also lung resident cells. Lung-resident NK cells are typically suppressed during homeostatic conditions to reduce inflammation[29]. During infection, it is currently unknown the extent of the individual contribution between resident NK cells and recruited NK cells. Regardless, NK cells are important for the

recognition of virally infected cells. NK cells recognize host cells (virally infected or tumor cells) with downregulated MHC I surface expression. In response to decreased MHC I expression, inhibitory receptors fail to receive a "stop" signal from the host cell; instead, activation signals lead to the release of cytotoxic granules (perforin/granzymes) that induce cell death. Additionally, NK cells secrete cytokines that promote Th1 differentiation, increase dendritic cell antigen presentation and induce activation of dendritic cells and macrophages [29].

Alveolar macrophages are the predominant antigen presenting cell (APC) in naïve airways[30]. Similar to lung-resident NK cells, alveolar macrophages are typically tolerogenic and suppress both innate and adaptive responses within the lung to reduce inflammation at homeostasis[30–33]. However, during influenza infection, alveolar macrophages produce proinflammatory cytokines and assist in limiting viral spread by phagocytosing apoptotic host cell cells[30].

Plasmacytoid dendritic cells (pDCs) are an important link between the innate and adaptive immune responses to influenza. pDCs play a vital role by producing large amounts of type I interferons[34] in response to viral ligands detected by TLR7 and TLR9[17,35]. The production of type I interferon leads to the promotion of an antiviral state within the microenvironment and induction of apoptosis in infected cells[36]. Additionally, pDCs can present viral antigen to T cells through MHC Class II signaling; however, pDCs are not as efficient at antigen presentation as conventional dendritic cells [37]. Lung-resident dendritic cells (DCs) can be activated by viral infection through recognition of PAMPs/DAMPs or phagocytosis of virions and virally infected cells. Upon capturing and recognizing antigen, the dendritic cell migrates to a draining lymph node based on a CCR7 chemokine gradient[38]. Antigen presenting DCs and naïve T cells co-localize in the draining lymph nodes for antigen presentation. APCs present antigen to T cells via the major histocompatibility complex I (naïve $CD8^+$ T cells) or II (naïve $CD4^+$ T cells) [39]. The DC-T cell interactions culminate in activation based on a two-signal process: (1) MHC presentation of antigen to the T cell receptor (TCR) (2) Binding of costimulatory molecules (B7.1 and B7.2) expressed by activating

APCs to CD28 expressed on T cells[40].Upon activation of CD4 (MHC II) or CD8 (MHC I) T cells by an antigen-presenting DC, T cells expand, develop an effector phenotype, and leave the draining lymph node to home to the site of infection where they engage the pathogen for clearance [41].

Upon MHC presentation and priming, $CD4^+$ T cells can differentiate into many subtypes for example: Th1, Th2, Th17, Tfh or Tregs. When naïve T cells are activated by viral infection, T cells differentiate into a Th1 phenotype characterized by IFN-γ production and T-bet expression [42]. Th1 polarization requires the presence of IL-12 produced by DCs and macrophages in response to virus. The combination of activation and IL-12 drives the Th1 phenotype by activating signal transducer and activator of transcription 1 (STAT1), STAT4, and T-bet. IFN-γ production further amplifies the Th1 phenotype by autocrine activation via STAT1 and T-bet [43].

$CD4^+$ T cells are also crucial to the development of antibody responses such as isotype switching and affinity maturation during viral infections. CD40 and CD40L costimulatory ligand interactions between B cells and $CD4^+$ T cells generate antibody responses necessary for antiviral activity against influenza virus[44,45]. $CD4^+$ T cells can also enhance the antiviral response by licensing antigen-presenting cells (APCs) using CD40L and CD40 interactions [46,47]. Licensing of APCs enhances their ability to activate antigen-specific $CD8^+$ T cells by upregulating co-stimulatory molecules and antigen processing and presentation machinery; APC licensing can also enhance $CD8^+$ memory generation[48].

Cytotoxic T lymphocytes (CTLs) are $CD8^+$ T cells that target virus-infected host cells for lysis by recognizing virus-specific antigens presented in the context of MHC class I molecules via their T cell receptors (TCRs). CTLs mediate infected cell lysis through the release of cytotoxic granules containing perforins and granzymes or receptor-mediated apoptosis via binding of FasL or TRAIL to the appropriate receptors[49–51]. CTLs can also produce proinflammatory cytokines such as IFNγ and TNF-α[52]. Overall,

virus-specific $CD8^+$ T cells have been shown to be protective, and their cytotoxic abilities are able to control the infection [50,53]. However, lung injury can also result from the release of proinflammatory cytokines [54–56].

During influenza infection, B cells can be activated in either a T cell-independent or T cell-dependent manner. T cell-dependent responses generate high affinity antibodies through affinity maturation, isotype switched antibodies for tailored effector responses to the pathogen and development of memory B cells. Antibody production by B cells is crucial for long-lasting protection and viral clearance. B cells most effectively produce antibodies against two key proteins of influenza: HA and NA. Anti-HA antibodies neutralize the virus and prevent infection by inhibiting the virus' ability to attach and enter the target cell through receptor-mediated endocytosis[57]. Anti-NA antibodies are not neutralizing, however, they are able to limit viral spread and shorten disease severity by preventing virus release from an infected cell[58–60]. Anti-NA antibodies have also been shown to induce antibody-dependent cellular cytotoxicity (ADCC) [61]. Despite production of long-lived antibody responses to influenza viral proteins, continuous antigenic drift and shift leads to changes that inhibit full protection against subsequent infections.

INTERFERONS AND INTERFERON-STIMULATED GENES

There are three known families of interferons (IFN): type I, type II, and type III[62]. Type I (IFN-αs/ IFN-β) and Type II (IFN-γ) interferons are well characterized, whereas type III interferons (IFN-λs) have more recently been discovered [63,64]. Type III IFNs are further divided into four subtypes: IL-29 (IFNλ1), IL-28A(IFNλ2), IL-28B (IFNλ3), and the pseudogene IFNλ4. In mice, IL-29 and IFNL4 are pseudogenes with only IL-28A and IL-28B functionally expressed and produced[63,65,66]. All interferons initiate signaling through the Janus kinase (Jak)-STAT pathway; however, the receptors utilized are genetically distinct[67]. Type I IFNs signal through the heterodimeric interferon-alpha receptor (IFNAR1/2), type II IFNs use the IFNGR1/2[68] and type III IFNs use IL10Rβ and IFNλR1[69,70] (Fig. 3).

Type I receptor distribution is prevalent across tissues and cell-types making type I interferon signaling capabilities widespread in response to viral infection[71]. Type I IFNs are crucial in inducing an antiviral state, which is necessary during early innate immune responses[36]. However, due to the abundant receptor expression of type I IFNs, excessive production of these interferons can lead to immunopathology. Unlike type I IFNs, type III IFNs have a highly restricted receptor expression[72]. The type III IFN receptor is a heterodimer made up of a ubiquitously expressed IL-10Rβ and the restricted IFNλR1[63,64], which is mostly expressed on epithelial cells at mucosal sites[72] (Fig. 3). In mice, some studies have shown that neutrophils and plasmacytoid dendritic cells (pDCs) also express *Ifnlr1* mRNA and respond to IFN-λ [73–75]. Additionally, recent studies suggest that IFN-λ acts on brain microvascular endothelial cells by decreasing permeability of the blood brain barrier in response to West Nile virus infection, however it is currently unknown whether this is an indirect effect or if endothelial cells express functional IFN lambda receptors[76,77].

Upon stimulation of the appropriate interferon receptors, JAK1 and TYK2 molecules are activated and phosphorylate STAT1/2 heterodimers during type I and type III IFN signaling. Once phosphorylated, the STAT1/2 bind to interferon regulatory factor 9 (IRF9), forming the IFN-stimulated gene factor 3 (ISGF3) complex. ISGF3 translocates into the nucleus and binds to the promoters of interferon stimulating genes (ISGs) to induce their expression for antiviral functions (Fig. 1). Interferon-stimulated gene 15 (ISG15) is quickly upregulated after IFN stimulation or viral infection and considered to be one of the most strongly and rapidly induced ISGs [21,78]. ISG15 is a ubiquitin homologue, which enhances IFN-β production[79], NF-κB signaling[80] and directly impedes viral replication[21].

Interferon regulatory factors (IRFs) are crucial positive regulators of the interferon and antiviral immune responses[81]. IRF7 is not only considered a master regulator of interferons, but also acts as an ISG and

drives a positive feedback loop for IFN induction[82–84]. With the exception of pDCs, endogenous IRF7 is present at low levels [81,85]. IRF3 is a ubiquitously expressed cytosolic protein that is activated by viral infection[81,85,86]. IRF7 can homodimerize or heterodimerize with IRF3 to induce type I IFNs [81]. Because IRF7 is necessary for IFN-α and IFN-β gene expression[84], IRF3/7 heterodimers have been shown to be essential for both early and late induction of type I IFNs during viral infections [81,86,87]. Upon phosphorylation of IRF7 during the early stage, phosphorylated IRF7 homo- or heterodimers bind to the interferon-stimulated response element (ISRE) sequence within interferon promoters to promote the expression of type I IFNs [81,88]. The produced type I IFNs bind to the IFNAR receptor and begin the signaling cascade as previous described in which STAT1/2 are phosphorylated and the ISGF3 complex is formed. The ISGF3 complex then binds to the IRF7 promoter, further enhancing IRF7 expression. This facilitates a positive feedback loop that allows for additional IRF7 to be produced that simultaneously continues to induce type I IFNs[81,86,88,89].

Despite similarities in signaling pathways, there are key functional differences between type I and type III interferons. Type III IFNs have been suggested to be responsible for the primary protection against respiratory viral pathogens[90]. IFN-λ inhibits replication of severe acute respiratory syndrome-coronavirus (SARS-CoV) and contributes to influenza[91] and RSV resistance[92]. Additionally, IFN-λ is the predominate interferon produced in response to influenza infection [74,93]. During influenza infection, type I and type III IFNs are temporally induced to clear the viral infection with minimal host damage[74]. Type III IFNs are produced early in order suppress viral replication without initiating a large inflammatory response. They accomplish this, in part, due to the restricted receptor distribution of type III IFNs (as noted above) that restricts inflammation to mucosal sites. Therefore, when a viral replication cannot be controlled by type III IFNs alone, type I IFNs are induced.

IMMUNOREGULATION OF INTERFERONS DURING INFLUENZA INFECTION

The immune response to influenza is a delicate balance between damage to the host and sufficient antiviral potency to induce viral clearance. Influenza-induced cytokine storms are caused by unrestrained proinflammatory cytokine production[94]. Overabundant production of proinflammatory cytokines for an extended period of time leads to significant immunopathology which is indicative of severe influenza infections. Cytokine storms are typically associated with the upregulation of IL-1β, TNF-α, IL-6, IL-18, and type I IFNs [94]. All of these cytokines are crucial in preventing viral dissemination during the initial stages of infection, however continuously amplified responses can lead to severe immunopathology [94–96]. The result of cytokine storms in response to influenza is acute lung injury, which when severe enough, can progress to acute respiratory distress syndrome (ARDS) [97]. During severe influenza infections, the virus disseminates to the lower respiratory tract and destroys the epithelial cells that are indispensable for gas exchange. Once the alveolar epithelial cells are killed, proinflammatory cytokines and virus can invade the endothelium which can significantly increase the levels of inflammation[96]. Overall, ARDS can lead to significant alveolar damage, pulmonary edema, respiratory failure, and death.

Immunoregulation of interferons are crucial in the balancing act between immunopathology and viral clearance. Type I IFN production is crucial for enhancing dendritic cell antigen presentation by increasing MHC and co-stimulatory molecules on the cell surface[69]. Type I IFNs are also necessary for activation of NK cells to induce their cytotoxic functions and IFNγ production necessary to kill virally infected cells [69,98]. However, Type I IFNs can also induced cell-mediated tissue damage by promoting TRAIL-mediated and FAS-L-mediated epithelial cell damage [69,99–101]. In order to prevent overproduction of type I IFNs, there are immunomodulatory mechanisms in place to suppress IFN signaling. The IFNAR receptor can be internalized to halt the feedback loop and prevent additional responses to exogenous IFNs. Casein-kinase II (CK2) phosphorylates a degron sequence in the IFNAR cytoplasmic domain that increases receptor internalization, ubiquitination, and degradation[69]. Additionally, CK2 negatively regulates TLR3/4,

STING, and RIG-I signaling via the phosphatase PP2a which dephosphorylates IRF3 to prevent IFN transcription [102]. CK2 also negatively regulates TBK1 to reduce the downstream immune responses through a currently unknown mechanism [102].

Suppressors of cytokine signaling (SOCS) proteins are also key immunoregulatory molecules that aid in the dampening of interferon (and many other) cytokine responses. Type I IFN signaling induces SOCS1, SOCS3, and USP18 to limit the duration of IFN responses after stimulation. SOCS proteins limit IFN responses by suppressing JAK-STAT signaling. SOCS1 and SOCS3 can inhibit JAK tyrosine kinase activation by binding to the substrate binding groove with their Kinase-inhibitory region (KIR) [103,104]. In addition to binding to the activation loop, SOCS3 can bind to the phosphorylated tyrosine residue on the cytokine receptor chain, thereby inhibiting signaling through the receptor [103]. Additionally, SOCS proteins inhibit Th1 and Th2 differentiation, further dampening downstream adaptive responses and initiating a reduced inflammatory microenvironment [103].

Innate and adaptive cells that aid in viral clearance and resolution of infection can also contribute to severe lung immunopathology. High pathogenic strains of influenza cause increased epithelial cell damage and can also induce high amounts of monocyte chemoattractant protein-1 (MCP-1) production. Increased levels of MCP-1 recruit inflammatory monocytes to the damaged lung where they differentiate into inflammatory macrophages[27]. Recruited inflammatory macrophages and monocyte-derived dendritic cells produce IL-6, NOS2, and TNF-α which are highly associated with immunopathology[30]. Additionally, both cell types can increase TRAIL expression leading to subsequent epithelial cell apoptosis and further destruction of the epithelium[30]. In non-high pathogenic influenza infections, inflammatory macrophages and monocyte-derived dendritic cells develop a suppressive phenotype to aid in restoration of homeostasis[30,105]. Lung epithelial cells assist in facilitating the suppressive phenotype via their expression of CD200. CD200 binds to CD200R on inflammatory macrophages to dampen inflammation [106,107]. Additionally, the activation of peroxisome proliferator-activated receptor-gamma

(PPARγ) controls the differentiation of monocytes into alternatively activated macrophages, which also suppress inflammation after influenza infection[108–110].

Adaptive cells that aid in viral clearance and resolution of infection can also contribute to severe lung immunopathology; therefore, there are multiple mechanisms which prevent immunopathology. As interferons and proinflammatory cytokine production increases during infection, expression of the negative costimulator, PD-L1, is also induced on hematopoietic and non-hematopoietic cells[111]. Additionally, as the virus is neutralized and eliminated throughout the course of infection, the loss of antigen limits the magnitude of the immune response. Therefore, as PD-L1 expression is upregulated, effector T cell functions are downregulated through multiple mechanisms leading to a gradually decreasing inflammatory environment[111]. Tregs are crucial for negatively regulating the immune response[112,113]. Tregs produce anti-inflammatory cytokines (TGF-β and IL-10), sequester IL-2 to force T effector cell death, and block co-stimulation by expressing CTLA-4 which binds with significantly higher affinity to CD80/CD86 [114]. Notably, SOCS1 protects Tregs from pathogenic conversion by supporting retention of FOXP3 expression[112,113]. These cellular mechanisms collectively assist in the regulation and resolution of the immune response to prevent significant immunopathology.

IMMUNE EVASION

IFN signaling leads to the induction of many ISGs for antiviral functions; however, influenza employs multiple tactics to evade the immune response and limit proinflammatory cytokine production and interferon signaling. NS1 is a virus-encoded gene that, when expressed, is able to inhibit IFN-mediated responses [115]. The NS1 protein binds to viral RNA to prevent TLR and RIG-I recognition[6] and significantly impairs functions of protein kinase RNA-activated (PKR), a key ISG produced in response to influenza. PKR proteins are protein kinases that regulate protein synthesis during environmental stress[116]. PKR recognizes viral RNAs that are longer that 30 base pairs and phosphorylates EIF2α to stop

translation[117,118]. Blocking translation inhibits virus-hijacking of host cellular machinery and limits its ability to produce new virions. However, NS1 can bind directly to PKR preventing the phosphorylation of EIF2α leading to continued viral protein translation[6]. The matrix protein (M2) which is required for uncoating RNPs, has also been shown to inhibit PKR[6,119]. Additionally, NS1 degrades eIF4B, a eukaryotic translation initiation factor, to reduce interferon-induced transmembrane protein 3 (IFITM3) production, which inhibits viral entry [6,120].

Genes associated with the polymerase complex encoded by influenza also play important roles in immune evasion. These genes control the synthesis of viral RNA and mRNA and are the mediators of cap-snatching (removal of the 5'-cap) from host mRNA for viral protein translation[121]. Additionally, PB1-F2 and PB2 can interact directly with mitochondrial antiviral signaling (MAVS) and inhibit type I IFN production [6,122–124].

In addition to immune evasion through virus-encoded genes, influenza can undergo antigenic drift in which the virus acquires small mutations over time that can evade cell mediated immunity. Mutations specifically within the HA and NA proteins of influenza can prevent antibody-mediated clearance and prevent memory T cells from being able to recognize the virus, despite prior infection or vaccination [125].

TUMOR PROGRESSION LOCUS 2 (TPL2)

Tumor progression locus 2 (Tpl2 or MAP3K8), also identified as Cancer Osaka Thyroid (*Cot*), is a serine-threonine protein kinase. Tpl2 is widely expressed throughout many tissues including the spleen, thymus, lungs, brain, intestine, kidney, and skeletal muscle[126,127]. Tpl2 was originally identified as an oncogene due to its ability to induce T cell lymphoblastic lymphomas[128]. Tpl2's oncogenic properties can be initiated through truncation of the C-terminus, which induces increased kinase activity[128,129]. However, Tpl2-deficient mice have increased incidence of skin tumors and T cell lymphomas[130], suggesting that it

may also function as a tumor suppressor in a context-dependent manner. Tpl2 protein is expressed as two distinct isoforms (52 and 58 kDa) that result from alternative translation initiation[131].

Tpl2 activation can be induced by: TLRs[132–134], antigen receptors[130,135], G-protein coupled receptors (GPCRs)[136], cytokines[137,138], and the FcγR[139]. Before stimulation, Tpl2 is held in an inactive state with p105 and ABIN-2[140]. Complete activation of Tpl2 requires a two-fold phosphorylation event: First, Tpl2 auto-phosphorylates itself at the T290 residue within the Tpl2 kinase domain[141]. Upon T290 residue phosphorylation, affinity for the p105 subunit decreases[142]. Second, the S400 residue on the C-terminus is directly phosphorylated by IKK[143] or AKT[144]. IKK is also necessary for phosphorylating the p105 subunit bound to Tpl2. IKK phosphorylation induces poly-ubiquitination of p105 by an E3 ligase. This action tags the p105 subunit for degradation by the proteasome. After the release of ABIN-2, Tpl2 becomes fully activated and can phosphorylate its substrates before being quickly degraded. Downstream signals of Tpl2 activation leads to phosphorylation of ERK and the AP-1 complex (*c-Jun* and *c-Fos*), eventually leading to the production of other inflammatory mediators (Fig. 2).

Das *et al.* explored Tpl2-dependent signaling pathways in response to various stimuli within hematopoietic and non-hematopoietic cells, specifically bone marrow-derived macrophages (BMDM) and mouse embryonic fibroblasts (MEFs). In Tpl2-deficient macrophages stimulated with TNF-α or LPS, only ERK phosphorylation was disrupted [133,137,138,145], whereas in MEFs stimulated with TNF-α, Tpl2-deficient macrophages displayed decreased phosphorylation in both ERK and JNK, but p38 phosphorylation was unimpaired[137]. In contrast, when MEFs were stimulated with IL-1β, Tpl2-deficient cells showed impaired ERK phosphorylation only, with JNK, p38, and NFκB being activated similarly to wild type cells [137]. Through exploration of various TLR stimulations and cell types, Das *et al.* 2005 discovered that Tpl2 can function in a cell-type and stimulus-specific manner[137]. Other studies have since shown cell type- and stimulus-specific regulation by Tpl2. In macrophages and conventional dendritic

cells, Tpl2 positively regulates IL-1β production in response to TLR2/3/4 stimulation and during infection with *Listeria monocytogenes*[134]. In addition to regulating proinflammatory cytokines, Tpl2 is also a known regulator of interferons. Tpl2 has also been shown to positively regulate IFNγ production in T cells in response to *Toxoplasma gondii* [135]. Similar to proinflammatory cytokine regulation, there is differential regulation of interferons based on the cell-type and stimulus being studied. In response to TLR9 stimulation, Tpl2 negatively regulates IFN-β in conventional dendritic cells and macrophages [146]. Whereas in plasmacytoid dendritic cells, Tpl2 positively regulates IFN-β. Tpl2 also conversely regulates IL-12 in conventional dendritic cells (negatively) and plasmacytoid dendritic cells (positively) in response to TLR9 stimulation [146].

Depending on the cell-type and stimulus, Tpl2 can activate ERK[145], p38[147], JNK[137] and mTOR[148] pathways. *Tpl2*-deficient mice have enhanced susceptibility and pathogen load with *Toxoplasma gondii*[135], influenza[149], *Listeria monocytogenes*[134], *Mycobacterium tuberculosis*[150], and group B streptococcus infection[151]. Tpl2-deficient mice are also resistant to LPS-induced septic shock[133] due to impairments in TNF-α production. Specifically, Tpl2 promotes TNF-α secretion by increasing TNF-α nucleocytoplasmic transport[133,152]. Additionally, Tpl2-dependent ERK1/2 activation leads to TNF-α converting enzyme (TACE) phosphorylation which is required for the cleavage of pre-TNF-α[145] to produce the mature, secreted form of TNF-α.

Although there is significant expression of Tpl2 in the lung and Tpl2-deficient mice display increased susceptibility to influenza, few studies have investigated a role for Tpl2 during influenza infection. TenOever *et al.* found that Tpl2 is robustly induced during influenza infection in an IRF-7 dependent manner and that lacking Tpl2 leads to significant alterations in the antiviral transcriptome during Vesicular Stomatitis Virus (VSV) infection[153,154]. Kuriakose *et al.* demonstrated that *Tpl2*$^{-/-}$ mice have higher viral titers in the lungs when compared to wild-type mice given a low dose of influenza (H3N2)[149].

Kuriakose *et al.* also determined that Tpl2 functions within non-hematopoietic cells to limit viral replication in response to influenza infection[149]. Tpl2 signaling in non-hematopoietic cells has been shown to mediates leukocyte recruitment in experimental autoimmune encephalomyelitis (EAE)[155]; however, despite high expression of Tpl2 within the lungs[127] few studies have explored the role of Tpl2 specifically within lung epithelial cells during pathogenic infections. During acute pancreatitis, Tpl2 signaling within non-hematopoietic cells increase lung inflammation and proinflammatory cytokines. One study focusing on airway epithelial cells found that Tpl2-dependent ERK activation is crucial in human bronchial epithelial cell, BEAS-2B, in response to *Pseudomonas aeruginosa* infection[156]. These studies suggest that Tpl2 within non-hematopoietic cells contribute to the outcome of immune responses. Despite this, there have been no studies which investigate of how Tpl2 regulates immune responses within non-hematopoietic cells during influenza infection.

COMPONENTS OF THE PULMONARY EPITHELIUM

Mucosal sites namely the respiratory, gastrointestinal, and urogenital tracts are at high risk of exposure to pathogens due to continual contact with foreign antigens [157,158]. Generally, mucosal sites contain a thin epithelial layer that are exposed to many organisms, but a variety of specific mucosal structures aid in regulating the inducible immune response. The respiratory system can be divided into two main anatomical sections: the upper respiratory tract (URT) and the lower respiratory tract (LRT). The upper respiratory tract contains the nasal cavity and all segments of the pharynx (nasopharynx, oropharynx, and laryngopharynx)[159]. The lower respiratory tract contains the trachea, bronchi, and alveoli[160]. The main function of the URT is to aid in respiration by heating, humidifying and filtering the air before it reaches the LRT[161]. Although structurally different, there are many similarities between the epithelial lining and immune responses in the upper and lower respiratory tracts[161].

The conducting airways, including all divisions of the respiratory tract except the alveoli, are comprised of pseudostratified columnar epithelial cells[160]. These cells can produce surfactant proteins,

antimicrobials, and mucins that aid in the movement of pathogens and particles away from the LRT. In mice, the conducting airways mostly consist of secretory cells[162]. The barrier function of epithelial cells in the conducting airways and alveoli is led by mucociliary transport. Mucociliary transport requires a 'mucous blanket' made from secretory mucins that coats the luminal surface of the epithelial cells, binds to pathogens and enhances their clearance from the respiratory tract [161,162]. Submucosal glands, found both in the URT and LRT, are abundant within the conducting airways and are comprised of multiple cell types including myoepithelial, serous, goblet, basal and cilated cells[162,163]. These glands are cellular compartments along the conducting airways where additional antimicrobials can be secreted[162]. Myoepithelial and serous cells both reside within the submucosal glands. Myoepithelial cells make up the lining of the submucosal gland and can also differentiate into cells of the surface epithelium during injury[164,165]. Serous cells are typically found within submucosal glands of the trachea and secrete a thin mucus; the accumulation of serous cells within the trachea are called Acini[163]. Basal cells are progenitors for the cilated and secretory cells of the adult conducting airways[162,166]. Differentiation into lung epithelial subsets is controlled by NOTCH signaling during development and lung homeostasis [166,167]. Basal cells can differentiate into cilated cells without NOTCH signaling. However, high levels NOTCH signaling is required for basal cells to differentiate into goblet cells [166].

The respiratory bronchioles contain cuboidal, non-ciliated cells known as Club cells. Club cells do not produce mucus but can produce other secretions such as Club cell secretory protein (CCSP) also known as club cell protein 16 (CC16), club cell protein 10 (CC10), uteroglobulin, and secretoglobin (SCGB) [168]. CCSP, the major protein produced by Club cells, has been shown to play important roles in limiting susceptibility to RSV infection [169]. Additionally, Club cells secrete glycoproteins for pulmonary surfactant stabilization, however they are unable to secrete surfactants themselves [168]. Club cells are also able to differentiate into cilated cells, however NOTCH signaling is required for differentiation of the secretory club cell into a cilated cell [166].

Goblet cells secrete mucus from conducting airways and submucosal glands; mucus secretion can be induced by cytokine and chemokine production[166,170]. The two major subtypes of mucins that goblet cells produce are MUC5AC and MUC5B [166,171]. MUC5B is most abundantly produced at submucosal glands, whereas MUC5AC is produced predominantly by goblet cells within the conducting airways [171]. Both mucins are produced in response to inflammation[166,171]

Neuroendocrine cells are a relatively rare subset of innervated cells located in clusters, called neuroendocrine bodies (NEBs) and located at branch points within the conducting airways[166,172]. Neuroendocrine cells can sense oxygen, carbon dioxide and various environmental stimuli; malforming NEBs can induce aberrant immune responses due to increased neuropeptides within the lung microenvironment[173]. Lastly, bronchioalveolar stem cells (BASCs) are a controversial subset of cells within the bronchioalveolar-duct junctions of the respiratory tract. These cells produce both Club cell and type II alveolar epithelial cell markers and have been suggested to be a stem cell population capable of replenishing injured cells[174–176].A recent study determined that BASCs are capable of differentiating into Club cells, cilated cells, type I and type II epithelial cells in response to lung damage[174].

The alveoli are comprised of two cell types: type I and type II alveolar epithelial cells. Type I epithelial cells are squamous , cover 90% of the alveolar surface, and make up 10% of the lung cells within the alveoli which equates to only 4% of the entire lung[177,178]. Type I alveolar epithelial (AECIs) cells are thin, branched cells fused to capillary endothelial cells[179]. AECIs mainly function in gas exchange and fluid homeostasis [180]. Despite their prevalence within the alveoli, few studies have been addressed their biological roles due to difficulties in obtaining pure isolations and low yields[181]. However, primary epithelial cell studies have shown that they are immunologically functional and produce TNFα, IL-6, and IL-1β at higher levels that type II epithelial cells when stimulated with LPS[182].

Type II epithelial cells (AECIIs) are cuboidal cells with numerous lamellar bodies and microvilli on their apical surface. These structures play crucial roles in the release of surfactant into the alveolus [162,183]. AECIIs are the only pulmonary cell capable of producing all surfactant protein (SP) components: SP-A, SP-B, SP-C, and SP-D. Other pulmonary cell types can produce SP-A, SP-B, and SP-D[168,184]; however, AECIIs are the only cells capable of producing SP-C [185].

IMMUNOLOGICAL ROLE OF PULMONARY EPITHELIAL CELLS

One major line of defense within epithelial cells is the secretion of the surfactant proteins for opsonization and neutralizing of pathogens. SP-B is a hydrophobic protein which functions during lung homeostasis to lower surface tension within lung[186]. SP-B deficiency causes fatal progressive respiratory failure in both humans and mice[187–189]. SP-C is the only surfactant protein that is solely produced by AECII cells[185]. As with SP-B, SP-C is a hydrophobic protein that functions with surface tension lowering properties as well as additional immunological roles[186]. SP-C has been shown to directly interact with lipopolysaccharides (LPS) from bacteria and reduce cytokine production in a TLR4-dependent manner and is crucial for bacterial clearance during *Pseudomonas aeruginosa* infections[190–192]. During RSV infection in mice, reduced pulmonary inflammation is SP-C mediated through TLR3 signaling[193]. SP-C deficiencies increase lung inflammation during both homeostatic and infection conditions[190].

While SP-B and SP-C mostly function in pulmonary homeostasis, SP-A and SP-D have primary functions in host defense. SP-A and SP-D are found throughout mucosal sites such as the pulmonary, urogenital and intestinal epithelium [194]. Both SP-A and SP-D are collectins[195] and due to their structural conformations are able to opsonize pathogens and enhance uptake by phagocytes[196]. SP-A and SP-D have been shown to regulate the immune system by: binding to TLRs[197], antimicrobial killing[198], aggregation of pathogens[199–201], enhanced phagocytosis of pathogens[199,202–205] and apoptotic cells[206], and regulation of cytokine[207,208] and reactive oxidase species production[209]. During influenza infections, SP-A binds to the HA region and is capable of neutralizing the virion as it binds to the sialic acid receptor on host cells [210].

SP-D has many of the same functions and immunological roles as SP-A, however, structural differences lead to different mechanisms of host defense. During influenza infection, SP-D can induce viral aggregation and enhance binding to neutrophils[211]. SP-D deficiency during viral infection in mice leads to impaired viral clearance and decreased neutrophil recruitment within the lung[212].

Pulmonary epithelial cells express extracellular and intracellular PRRs (TLRs/NLRs/RLRs, and RAGE) to aid in protection of the epithelium [35,213–216]. As previously discussed, PRRs are crucial for immediate detection of PAMPs and DAMPs from invading pathogens and changes to the microenvironment of the lung. Interestingly, it has been shown that NLR signaling leads to the production of antimicrobial peptides rather than cytokines in human pulmonary epithelial cells and is extremely important for mucosal responses[217–220]. *In vitro* stimulation of BEAS-2B cells has shown that epithelial cells produce complement proteins, chemokines, and cytokines in response to TLR3 agonist stimulation, providing evidence that epithelial cells can initiate a variety of host defense mechanisms[221].

In addition to epithelial cells assisting in coordinating other immune cells, studies have shown that RIG-I signaling within the immortalized human epithelial cell line A549s is crucial for initiating an early antiviral response to RSV by activation of NF-κB and interferon-regulating factor 3 (IRF3)[222]. Human AECs and mouse tracheal epithelial cells (mTECs) produce type III IFNs in response to TLR3 stimulation and influenza infection[223]. Bronchial epithelial cells also strongly induce type III IFNs in response to both rhinovirus and influenza A infection[224]. Despite the limited data focusing on epithelial immunological responses, respiratory epithelial cells are capable of responding to pathogens and inducing a substantial immune response to jumpstart viral clearance[3]. Lastly, some studies suggest that there is differential induction and regulation of type I and type III IFNs in alveolar epithelial cells [223].

PULMONARY FIBROSIS

Pulmonary fibrosis occurs because of continuous injury to the alveolar epithelium or endothelium leading to aberrant wound healing, increased inflammatory responses, tissue damage and excess build-up of the extracellular matrix [225]. Pulmonary fibrosis leads to diminishing oxygen within the blood due to the destruction of the alveolar epithelium, ultimately resulting in respiratory failure and death[179,225–227]. There are still many questions revolving around the exact cause of pulmonary fibrosis. Some proposed mechanisms for the development of pulmonary fibrosis include: (1) loss of anti-fibrotic signals in healthy cells, (2) increased pro-fibrotic signals in injured cells or (3) apoptotic alveolar epithelial triggering of fibrotic responses in neighboring cells[228].

Severe respiratory infections, such as influenza, can induce pulmonary fibrosis [229]. Influenza can cause acute lung injury which can progress to ARDS[229]. During ARDS, increased metalloproteinases and proinflammatory cytokines can attract additional immune cells to an already injured epithelium [230]. Increased injury to the alveolus can be exacerbated by endothelial cell injury[230,231]. The destruction of the alveolo-capillary barrier can lead to ongoing injury or failure to initiate appropriate repair responses that drive pathogenic fibrotic responses[230,232–235]. Type I epithelial cells are also considered to play an important role in pulmonary fibrosis pathogenesis due to the ability of type II alveolar epithelial cells to differentiate into type I epithelial cells upon injury[179]. It is possible that the loss of AECIs may trigger the initiation of pulmonary fibrosis.

RECENT ADVANCES IN TPL2 AND PULMONARY FIBROSIS

Bleomycin administration causes fibrosis in both humans and animals, making it a beneficial model for idiopathic and generalized pulmonary fibrosis [236]. Despite intratracheal administration of bleomycin, the mechanism of action and subsequent responses are significantly different from respiratory infections. Bleomycin forms a complex with iron leading to its oxidation and release of free radicals which induces single- and double-stranded DNA breaks [237]. The resulting DNA damage causes cell death of endothelial

and epithelial cells [237]. Although the exact mechanism of lung fibrosis has not been elucidated, alveolar macrophages are identified as key mediators of bleomycin-induced lung fibrosis [238]. Specifically, macrophages are the primary producers of reactive oxygen species, nitric oxides, prostaglandins, and profibrotic cytokines and growth factors after bleomycin administration. Utilizing the bleomycin-lung injury model, Zannikou *et al*. found that Tpl2 has a protective role during bleomycin-induced lung fibrosis[239]. This protection against bleomycin-induced fibrosis was mediated primarily through macrophages. Additionally, they determined that Tpl2 regulates arachidonic acid metabolism, cyclooxygenase-2 (COX-2) and prostaglandin E2 (PGE_2) expression during bleomycin-induced lung injury[239].

Arachidonic acid is a polyunsaturated fatty acid that is present within the phospholipid membrane [240]. Arachidonic acid is released as free arachidonic acids by phospholipase A_2 and phospholipase C after enduring stress within the cellular microenvironment [240]. These free arachidonic acids are now accessible for the initiation of proinflammatory and fibrotic pathways. The COX proteins (COX1/COX2) convert arachidonic acid into prostaglandins [240]. Specifically, COX1/2 oxygenates arachidonic acid to prostaglandin G2 (PGG_2) and then the same COX protein reduces PGG_2 to the unstable intermediate prostaglandin H2 (PGH_2) [241]. Microsomal prostaglandin E synthases (mPGES) couples preferentially with COX2 and utilizes PGH_2 as a substrate to generate prostaglandin E2 (PGE_2) [240] (Fig. 4). Tpl2 has been previously shown to regulate COX2-mediated PGE_2 expression within intestinal myofibroblasts by facilitating ERK-dependent phosphorylation required for COX2 activation[242]; however, this regulatory pathway has previously not been determined within the lung. Zannikou *et al.* found that decreased PGE_2 in *Tpl2*$^{-/-}$ mice was responsible for exacerbated pulmonary fibrosis in response to bleomycin administration. However, the specific mechanism by which Tpl2 negatively regulates arachidonic acid production and positively regulates PGE_2 is currently unknown.

As previously mentioned, bleomycin administration induces a distinct signaling pathway from viral infection. Similarly, various cell-types, stimuli, and signaling pathways induce a wide variety of COX2-PGE_2 mediated responses [243,244]. Specifically, different viruses induce opposing responses to PGE_2. Adenovirus, parainfluenza virus, and measles virus have decreased replication when there is an increased production of PGE_2 [245]. However, cytomegalovirus, vesicular stomatitis virus, bovine leukemia virus, and herpes-simplex 1 virus have enhanced viral replication when PGE_2 production is increased [245]. Additionally, Epstein-Barr virus evades the immune response by impairing PGE_2 production [246]. Finally, in response to influenza infection, decreased COX2 and PGE_2 has been shown to lead to increased influenza replication in human lung epithelial cells and human bronchial epithelial cells [243]. Overall, Zannikou *et al.* demonstrates an important role for Tpl2 during pulmonary fibrosis in the bleomycin model[239]; whether and how Tpl2 may regulate pulmonary fibrosis in response to influenza infection has yet to be determined.

CONCLUSION

Understanding the role of alveolar epithelial cells in the context of both influenza infection and their role in driving pulmonary fibrosis is crucial for a better understanding of respiratory immunity. The respiratory tract is comprised of many cells that can induce a robust immune response, particularly interferons, in response to viral infection. Tpl2 has been previously shown to regulate interferons in a cell-type and stimulus-specific manner. Tpl2 has also been shown to be crucial for viral clearance within the non-hematopoietic compartment during influenza infection, however the role of Tpl2 within respiratory epithelial cells during influenza infection and how Tpl2 is capable regulating the innate response within the epithelium is currently unknown. Understanding how Tpl2 regulates the interferon response may provide additional clarity to the antiviral response within the lung epithelium. The objective of these studies is to define the contribution of Tpl2 to innate immune responses and host resistance within the lung.

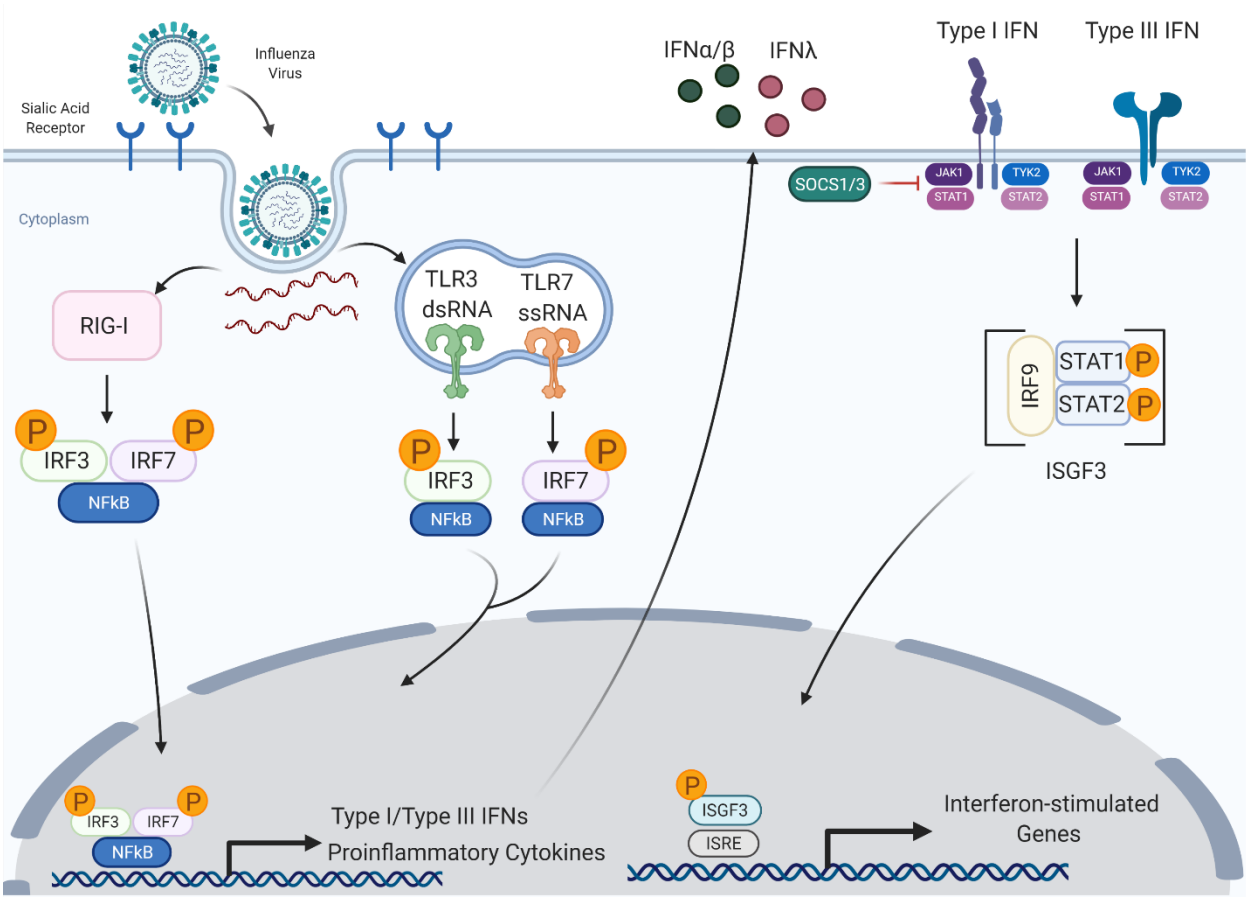

Figure 1. Immune sensing and response to influenza. – Image created with Biorender.com. Influenza first interacts with the host cell through the hemagglutinin (HA) located on the surface of the virion which recognizes sialic acid on host cells. This interaction also leads to receptor-mediated endocytosis, enabling entry of the virion into the epithelial cell via an endosome. Host endosomal acidification induces a conformational change in the virion's HA protein allowing for the release of the viral genome into the cytoplasm. RIG-I, TLR3, and TLR7 are all capable of recognition of the viral genome. RIG-I detects uncapped 5'triphosphate viral RNA of influenza. Upon detection, RIG-I undergoes conformational changes allowing ATP to bind and CARDS to oligomerize. CARD-CARD interactions with MAVS on the mitochondria lead to TBK1 and IKK activation which can phosphorylate IRF3 and IRF7. TLR3, using TRIF as an adaptor protein phosphorylates TRAF3, then recruits TBK1 and IKKε, leading to IRF3 phosphorylation. TLR7 utilizes the MyD88 adaptor protein to recruit IRAK proteins and TRAF3 and lead to downstream phosphorylation of the IKK complex and IRF7. Downstream activation leads to the

phosphorylation of IRF3/IRF7 and NFKB leading to downstream production of IFNs and proinflammatory cytokines. Upon phosphorylation of IRF7 during the early stage, phosphorylated IRF7 homo- or heterodimers bind to the interferon-stimulated response element (ISRE) sequence within interferon promoters to promote the expression of type I IFNs. Once interferons are produced, they can stimulate their appropriate receptors. JAK1 and TYK2 molecules are activated and phosphorylate STAT1/2 heterodimers during type I and type III IFN signaling. Once phosphorylated, STAT1/2 bind to interferon regulatory factor 9 (IRF9), forming the IFN-stimulated gene factor 3 (ISGF3) complex. ISGF3 translocates into the nucleus and binds to the promoters of interferon stimulating genes (ISGs) to induce their expression for antiviral functions. The produced type I IFNs bind to the IFNAR receptor and begin a feedback loop, leading to the production of more interferons.

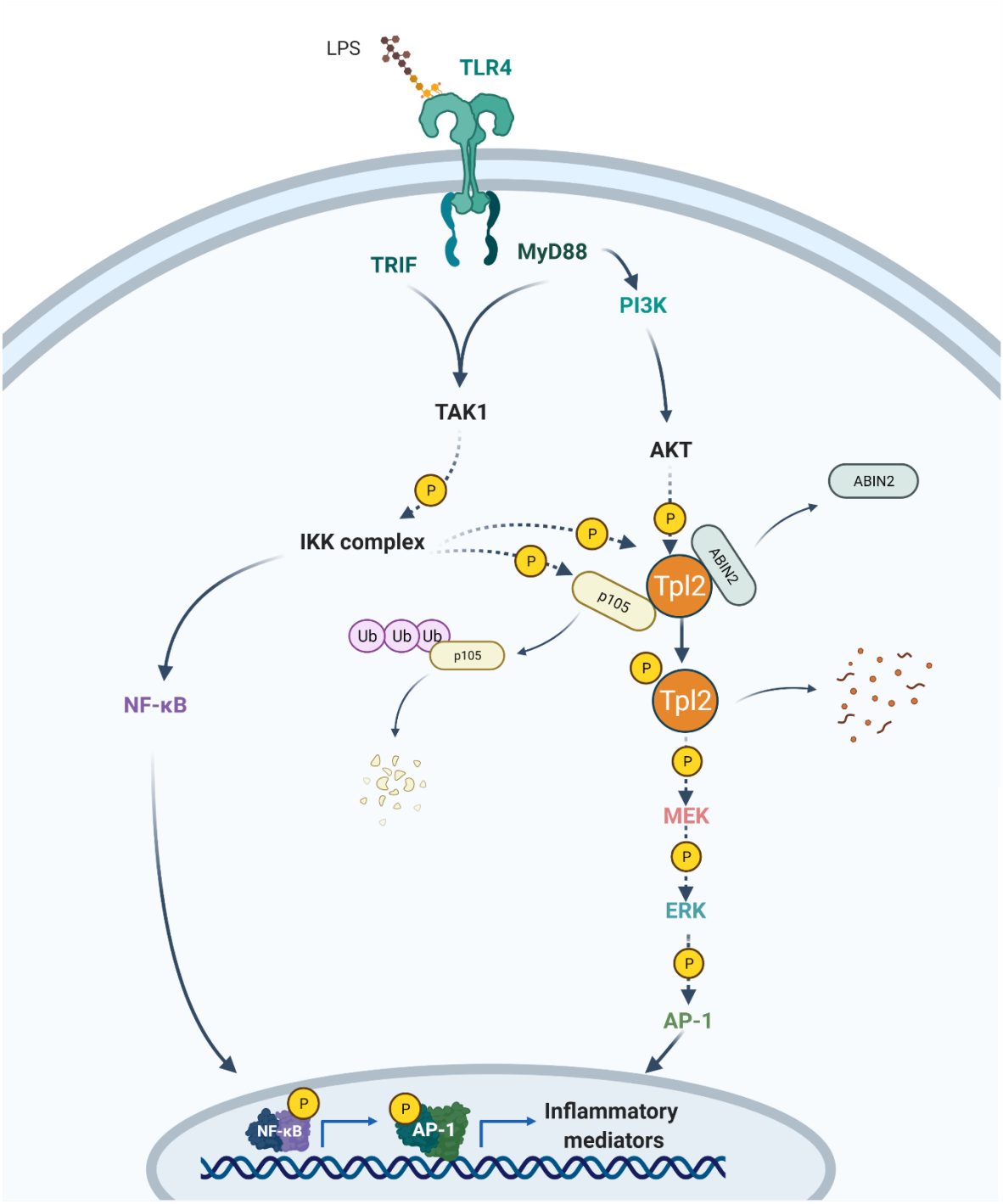

Figure 2. Tpl2 signaling pathway. – Image created with Biorender.com and adapted from: Natalya Odoardi, Clinical Research Coordinator, Children's Hospital of London. Tpl2 activation can be induced by: TLRs, antigen receptors, G-protein coupled receptors (GPCRs), cytokines, and the FcγR[139]. Here,

Tpl2 activation is demonstrated through the TLR4 signaling pathway. TLR4 can utilize either TRIF or MyD88 adaptor proteins to transduce signaling. Both lead to downstream phosphorylation of TAK1 and the IKK complex. TLR signaling also initiates the PI3K/AKT pathway. PI3K converts PIP2 (phosphatidylinositol biphosphate) into PIP3 (phosphatidylinositol triphosphate). PIP3 phosphorylates PDK1 (PIP3-dependent kinase) which leads to the phosphorylation of AKT (not shown). Prior to stimulation, Tpl2 is held in an inactive state with p105 and ABIN-2. Complete activation of Tpl2 requires a two-fold phosphorylation event: First, Tpl2 auto-phosphorylates itself at the T290 residue within the Tpl2 kinase domain. Upon T290 residue phosphorylation, affinity for the p105 subunit decreases. Second, the S400 residue on the C-terminus is directly phosphorylated by IKK or AKT. IKK is also necessary for phosphorylating the p105 subunit bound to Tpl2 and the NF-κB complex. IKK phosphorylation induces poly-ubiquitination of p105 by an E3 ligase. This action tags the p105 subunit for degradation by the proteasome. After the release of ABIN-2, Tpl2 becomes fully activated and can phosphorylate its substrates (MEK) before being quickly degraded. After the phosphorylation of MEK, downstream signals of Tpl2 activation leads to phosphorylation of ERK and the AP-1 complex (*c-Jun* and *c-Fos*) eventually leading to the production of other inflammatory mediators. Additionally, IKK phosphorylation of the NF-κB complex leads to the translocation of NF-κB to the nucleus to produce inflammatory mediators.

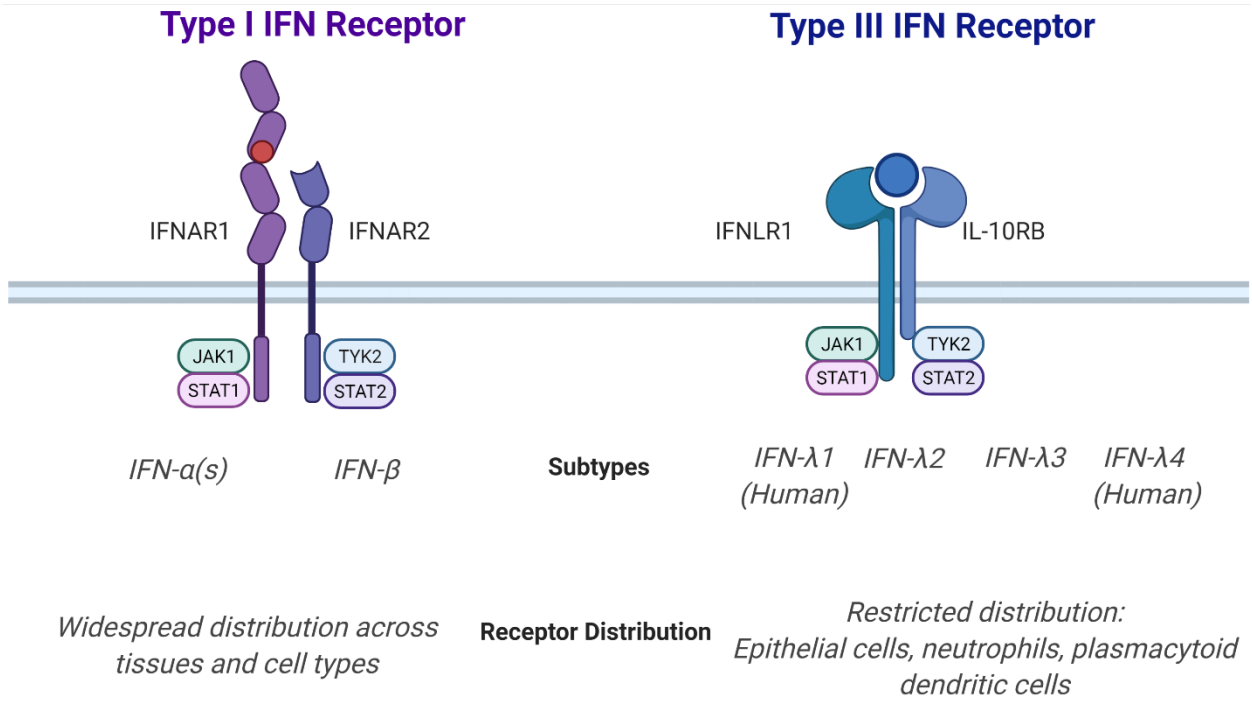

Figure 3. Interferon receptor distribution and composition – Image created with Biorender.com. Type I interferons include the both IFN-αs and IFN-β. Type III IFNs are further divided into four subtypes: IL-29 (IFNλ1), IL-28A(IFNλ2), IL-28B (IFNλ3), and the pseudogene IFNλ4. In mice, IL-29 and IFNL4 are pseudogenes with only IL-28A and IL-28B functionally expressed and produced. All interferons initiate signaling through the Janus kinase (Jak)-STAT pathway; however, the receptors utilized are genetically distinct. Type I IFNs signal through the heterodimeric interferon-alpha receptor (IFNAR1/2), and type III IFNs use IL10Rβ and IFNλR1. Type I receptor distribution is prevalent across tissues and cell-types making type I interferon signaling capabilities widespread in response to viral infection. Unlike type I IFNs, type III IFNs have a highly restricted receptor expression. The type III IFN receptor is a heterodimer made up of a ubiquitously expressed IL-10Rβ and the restricted IFNλR1, which is mostly expressed on epithelial cells at mucosal sites[72]. In mice, neutrophils and plasmacytoid dendritic cells (pDCs) also express *Ifnlr1* mRNA and respond to IFN-λ.

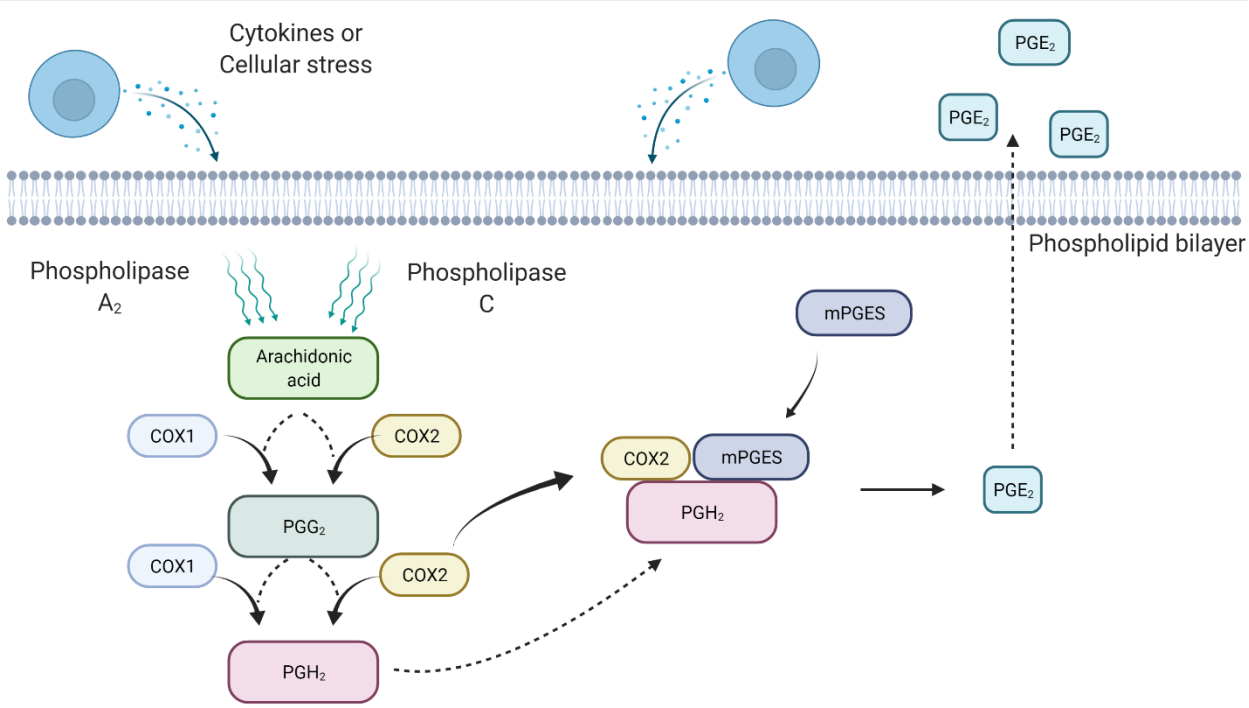

Figure 4. Arachidonic acid metabolism and Prostaglandin E2 production. – Image created with Biorender.com. PGG_2 – prostaglandin G2; PGH_2 – prostaglandin H2; mPGES – microsomal prostaglandin E synthase. Arachidonic acid is released from phospholipids after signals from cytokines or cellular stress. Arachidonic acid is released as free acids by phospholipase A_2 and phospholipase C. COX1 or COX2 can convert arachidonic acid into downstream prostaglandins. Specifically, COX1/2 oxygenates arachidonic acid to prostaglandin G2 (PGG_2) and then the same COX protein reduces PGG_2 to the unstable intermediate prostaglandin H2 (PGH_2). Microsomal prostaglandin E synthases (mPGES) couples preferentially with COX2 and utilizes PGH_2 as a substrate to generate prostaglandin E2 (PGE_2). PGE_2 is then released from the cell to initiate various signaling pathways.

CHAPTER 2

TPL2 FUNCTIONS IN PULMONARY EPITHELIAL CELLS TO CONSTRAIN INTERFERON PRODUCTION AND PULMONARY FIBROSIS DURING INFLUENZA A VIRUS INFECTION [1]

[1] Wyatt, K.D., Sakamoto K.S., and Watford, W.T.W, Submitted to *Journal of Immunology, 3/9/21*.

ABSTRACT

Tumor progression locus 2 (Tpl2) is a serine/threonine kinase that regulates the expression of inflammatory mediators in response to a variety of TLR, cytokine, and G-protein-coupled receptors. Tpl2 negatively regulates the expression of host-encoded interferons (IFNs) within hematopoietic cells; however, the regulation of antiviral responses by Tpl2 within the target cells of influenza infection, the lung epithelial cells, has not been investigated. *In vitro* studies determined that Tpl2 constrains both type I and type III IFN responses within the type I airway epithelial cell line (AECI), LET1, as well as primary type II airway epithelial cells (AECII). We used *Nkx2.1*-cre to drive Tpl2 deletion within pulmonary epithelial cells in order to delineate epithelial cell-specific functions of Tpl2 during influenza infection. Tpl2 ablation across multiple lung epithelial cell types led to enhanced susceptibility to influenza A virus. Despite significantly increased morbidity and mortality in mice with Tpl2-ablated lung epithelial cells, virus replication was controlled normally. Instead, Tpl2 ablation within lung epithelial cells caused a moderate but statistically significant increase in pulmonary fibrosis in response to influenza infection suggesting dysregulated fibrotic pathways may contribute to enhanced morbidity and mortality. Overall, these results implicate Tpl2 in the regulation of early innate responses within pulmonary epithelial cells during influenza infection.

INTRODUCTION

Influenza is one of the most common causes of respiratory infections[1]. Within the United States, approximately 200,000 hospitalizations occur during a typical flu season[1]. Seasonal influenza poses a substantial threat to global health, particularly in high-risk populations, such as pregnant women[247], children[248], elderly[249] and the immunocompromised[250], with global deaths due to seasonal influenza estimated to be between 290,000-650,000 annually[251]. Given the current global coronavirus pandemic, the at-risk population may be even greater, including those with co-morbidities, like COVID-19, who are not typically at risk for influenza complications[252].

The innate immune response is crucial for protection against influenza infection. Pathogen-recognition receptors (PRRs), such as RIG-I and Toll-like receptors, recognize pathogen-associated molecular patterns (PAMPs) that initiate signaling cascades leading to the expression of antiviral molecules. Interferons (IFNs) are host restriction factors that 'interfere' with viral replication[253]. Specifically, IFNs induce the production of IFN-stimulated genes (ISG) that can, through a variety of mechanisms, inhibit viral replication, alert uninfected cells to the surrounding danger by generating an 'antiviral state'[254], and assist in the recruitment of innate immune cells[255]. There are three major subsets of IFNs including type I (IFN-α/IFN-β), type II (IFN-γ), and type III (IFN-λs). It is well-established that influenza infections produce a robust type I (IFN-α/IFN-β) IFN response[256]. However, type III IFNs are a more recently described[63,64] and genetically distinct subset of IFNs[67] now known to be the predominant IFN produced during influenza A infection[257]. Even though they utilize distinct cell surface receptors, type I and type III IFNs have comparable signaling pathways leading to the induction of similar IFN-stimulated genes for the restriction of viral replication[67]. However, type III IFNs have a more restricted receptor expression primarily within epithelial cells and play an essential, non-redundant role in protecting these primary targets of influenza[74,258,259]. Both type I and type III IFNs are crucial for protection against influenza infection, and the loss of both IFN-α/β and IFN-λ receptors increases susceptibility to influenza

infection[74,91,260–262]. IFN-λ has been shown to be the earliest and predominant IFN produced in response to IAV infection[74,257]. Type I IFNs are produced later than type III IFNs and require higher viral loads to drive an earlier appearance[74]. IFN-λ is critical for controlling early viral replication without driving immune activation and tissue damage. Once the viral burden exceeds IFN-λ control, type I IFNs are produced and drive a stronger proinflammatory response to regain control of viral replication[74]. Despite their primary protective role, an imbalance in IFN production can drive immunopathology, which can cause influenza-induced acute respiratory distress syndrome (ARDS)[263]. Regulation of IFNs is crucial to maintaining an appropriate balance between viral control and host-induced pathology. Therefore, understanding what proteins regulate the interferon response is important for delineating the mucosal immune response to influenza.

One known regulator of IFNs is the serine-threonine kinase, Tumor progression locus 2 (Tpl2), also known as Cot or MAP3K8. Tpl2 is broadly expressed in hematopoietic and nonhematopoietic tissues[137]. Tpl2 transduces intracellular signaling through several prominent pathways, such as ERK, JNK, p38, and PI3K-AKT-mTOR [130,135,137,147,264–267], and regulates subsequent cellular responses, including proliferation and gene expression, in a context-dependent manner[137]. For example, Tpl2 regulates IFNs in a cell type-specific manner. Specifically, Tpl2 negatively regulates IFN-β production in macrophages but positively regulates IFN-α production in plasmacytoid dendritic cells (pDCs) in response to TLR stimulation[146]. Tpl2 has also been shown to promote the induction of IFN-λ in pDCs[149]. Previous studies have established an important role for Tpl2 in promoting various inflammatory responses including the production of TNF[133,145], IFN-γ[133,145] and IL-1β[134]. Additionally, Kuriakose *et al.* recently demonstrated that *Tpl2*$^{-/-}$ mice have enhanced susceptibility to a low pathogenic strain of influenza A (x31; H3N2) and that the increased susceptibility was caused by Tpl2 deficiency within the non-hematopoietic cells.[149]

Multiples lines of evidence now support that Tpl2 plays critical regulatory roles within non-hematopoietic cells. For instance, Tpl2 signaling in non-hematopoietic cells mediates leukocyte recruitment in experimental autoimmune encephalomyelitis (EAE)[155]. Additionally, Tpl2 signaling within intestinal subepithelial myofibroblasts modulates hepatocyte growth factor and epithelial cell proliferation during colitis-induced colorectal carcinogenesis[268]. Not only does Tpl2 have known functions within the brain and intestinal stromal compartments, Tpl2 is expressed at high levels within the lungs[127]. However, limited studies have explored the role of Tpl2 specifically within lung epithelial cells. Tpl2 has been shown to increase lung inflammation during acute pancreatitis via non-hematopoietic cells[269], and Tpl2 is essential for ERK activation in the BEAS-2B human bronchial epithelial cell line in response to *Pseudomonas aeruginosa* infection[156]. Despite its designation as a viral restriction factor *in vitro* and *in vivo*[149,154], the role of Tpl2 within lung epithelial cells during a *bona fide* viral infection *in vivo* has not been investigated.

The respiratory tract is divided into two main portions: the upper respiratory tract includes the nasal cavity and pharynx, whereas the lower respiratory tract includes the trachea, bronchi, and alveoli [159]. The pulmonary alveoli are known replicative niches of influenza[3] and are comprised of two major cell types: type I and type II airway epithelial cells (AECI/AECII). Type I epithelial cells are branched cells that cover 95% of the lung with expansive but thin apical surfaces[179]. AECI are fused with capillary endothelial cells to form the alveolo-capillary barrier structure for gas exchange[179,270]. Given their major role in gas exchange, AECI are also key contributors to pulmonary fibrosis, which can lead to fatal deficiencies in lung function[179]. AECII are cuboidal cells that are crucial for surfactant production and lung homeostasis[177,178]. AECII are the only pulmonary cell capable of producing all surfactant proteins and the sole producer of surfactant protein C (*Sftpc*) [168,184,185]; therefore, *Sftpc* has been widely used as a promoter for conditional transgenic mouse strains for targeting AECII[271,272].

Tpl2 has been shown to offer host protection *in vivo* during influenza infection[149]. However, there is still a limited amount of information about the specific cell types that contribute to pathology in the setting of

global Tpl2 ablation. The goal of this study is to gain a more complete understanding of how Tpl2 regulates the innate immune response initiated within virus-infected epithelial cells. In this study, we utilized the immortalized murine lung epithelial type I cell line (LET1) and primary AECIIs to model epithelial cell responses to influenza A virus. Additionally, we generated two lung-specific conditional Tpl2-knockout mouse models to study the contribution of Tpl2 within the epithelial cells of the lower respiratory tract using Nkx2.1 and Sftpc promoters to drive cre expression. *Nkx2.1* is a critical transcription factor for the development of the lower respiratory tract[273,274]. By utilizing *Nkx2.1* as a lung-specific *cre* promoter, we were able to test Tpl2 functionality within a variety of epithelial cells during influenza infection. Additionally, Sftpc-CreER^{T2} mice were used to determine if Tpl2 responses could be localized individually to type II epithelial cells during influenza infection. We demonstrate that Tpl2 constrains interferon responses in vitro and limits morbidity and mortality in vivo to influenza infection. Overall, this study establishes not only the crucial role for Tpl2 in orchestrating interferon responses, but also that Tpl2 limits fibrotic responses in influenza-infected lungs due to its intrinsic function within pulmonary epithelial cells.

Overall, this study establishes not only the crucial role that Tpl2 plays in orchestrating interferon responses, but also that Tpl2 functions within airway epithelial cells to regulate the innate immune response to influenza infection. Specifically, Tpl2 limits the fibrotic response in influenza-infected lungs due to its intrinsic function within pulmonary epithelial cells. These findings are important because few studies have explored the role of Tpl2 within the lung epithelium to determine its contribution to the innate immune response. Gaining a better understanding of how innate immune responses are generated within mucosal sites, including how Tpl2 is regulated within pulmonary epithelial cells, can reveal potential therapeutic targets and pathways for treating lung diseases.

MATERIALS AND METHODS

Mice and viruses

Wild type (WT) C57BL/6J mice were purchased from The Jackson Laboratory. Tpl2-deficient mice were backcrossed to C57BL6/J more than ten generations and kindly provided by Dr. Philip Tsichlis and Thomas Jefferson University[264]. *Tpl2*$^{flox/flox}$ mice were offered by Dr. George Kollias[268] and purchased from EMMA (EM:07150). Mice with conditional ablation of Tpl2 within AECII or broadly within the lung epithelium (AECI, AECII, club cells, bronchial epithelial cells, basal cells, cilated epithelial cells, and goblet cells) were generated by crossing *Tpl2*$^{flox/flox}$ mice with Sftpc$^{tm1(cre/ERT)Blh}$ (Sftpc-CreER^{T2}) and *Nkx2.1*cre, respectively.

To enhance the overall deletion efficiency of Tpl2 (see Results section; Figure 6C and 7C), the resulting *Nkx2.1*cre$^{+/-}$*Tpl2*$^{flox/flox}$ and Sftpc-CreER$^{T2+/-}$*Tpl2*$^{flox/flox}$ mice were further crossed with *Tpl2*$^{-/-}$ mice to generate experimental (cre+) and littermate control (cre-) *Nkx2.1*cre^{+}*Tpl2*$^{flox/-}$ and Sftpc-CreER^{T2+}*Tpl2*$^{flox/-}$ mice. Mice were housed in specific pathogen-free conditions in microisolator cages in the Coverdell Rodent Vivarium within the University of Georgia. Animals were confirmed *Helicobacter*-negative and used between six to nine weeks of age. To prevent sex-biases, both male and female mice were used in all experiments. All experiments involving mice were performed according to the University of Georgia Guidelines for Laboratory Animals and were approved by the UGA Institutional Animal Care and Use Committee. Mouse-adapted influenza virus A/HK-x31 (H3N2) stocks were provided by Dr. Mark Tompkins (University of Georgia).

In vivo influenza infection

Age-matched, six- to nine-week-old mice were sedated with 2.5% Avertin and intranasally infected with 50 µl of influenza A/x31 (10^4 PFU) diluted in PBS. To determine lung viral titers, whole lungs were harvested on 1, 3-, 5-, 7-, and 8.5-days post infection (dpi). Lungs were placed in 1 ml PBS and dissociated with a bead mill homogenizer (Qiagen). Virus titers were quantified by plaque assays

(described below). To assess susceptibility to influenza infection, mice were infected with 10^4 pfu of influenza A/x31 and observed over a period of 14 days. Body weights were recorded daily, and mice exhibiting severe signs of disease or more than 30% weight loss were euthanized. For morbidity and mortality measurements, researchers were blinded to mouse genotype until the end of the experiment.

Epithelial cell isolation

The isolation of lung epithelial cells was adapted from the protocol of Sinha and Lowell[275] as follows: mice were sacrificed by intraperitoneal injection of 2.5% avertin with secondary mode of sacrifice performed by cutting the renal artery. Cardiac perfusion was performed with sterile PBS followed by intratracheal instillation of approximately 1 mL dispase (50 units/mL) followed by 0.6 mls of 1% low-melt agarose. Lungs were harvested and individual lobes cut and incubated in dispase for 45 min at room temperature on a horizontal rocker. Single cell suspensions were prepared by teasing apart the airways in Complete DMEM (DMEM, 10% FBS, 1X Penicillin-Streptomycin, 10 mM HEPES) with DNase (10 μg/mL) and incubated for 10 min at room temperature. Single cell suspensions were serially strained through 70 μM and 40 μM strainers, and centrifuged at 300 x *g* for 10 min at 4°C.

Pellets were resuspended in Complete DMEM without DNase and stained with the following biotinylated antibodies at 1:100 dilution (anti-CD45, anti-CD31, anti-Ter119, and anti-integrin B4/CD104, Biolegend). Magnetic depletion of biotinylated samples was performed using a Mouse Streptavidin RapidSpheres Isolation Kit (StemCell Technologies). After enrichment, cells were washed with Complete DMEM at 300 x *g* and stained for 10 min at 4°C with CD16/32 (purified, ebioscience, 1:100) EpCAM (PE, ebioscience, 1:100), CD45.2 (FITC, ebioscience, 1:100), Podoplanin (APC, ebioscience, 1:100). Cells were washed, stained, then strained through a 35 μm filter cap tube (Falcon) before cell sorting for singlet $EpCAM^+CD45.2^-$ (AECII) or $EpCAM^+CD45.2^-$Podoplanin (AECI) on a Beckman Coulter MoFlo Astrios EQ.

Leukocyte isolation

Naïve splenic T cells were isolated by disaggregating spleens as described previously[276] and cell sorted for CD4s (CD45.2+/CD4+), CD8s (CD45.2/CD8+) using a Beckman Coulter MoFlo Astrios EQ. Bone marrow-derived macrophages (BMDMs) were generated from wild-type age- and sex-matched mice as previously described[134,277]. Briefly, BMDMs were cultured at a concentration of 2×10^6/ml in DMEM low glucose medium containing 10% FBS, 100 µg/mL Penicillin-streptomycin and 2 mM L-glutamine on sterile Petri dishes for 7 days at 37°C. Media was supplemented with 10 ng/ml macrophage colony stimulating factor (M-CSF) (PeproTech). Fresh medium equal to half of the initial culture volume containing 10 ng/ml M-CSF was added on day 5 of the culture. On day 7, after removing the medium and washing the cells with PBS, the adherent cells were incubated with cell dissociation buffer (Invitrogen) for 10 min at 37°C. Peritoneal exudate cells were isolated from WT mice intraperitoneally injected with 1 ml 3% thioglycollate. Peritoneal lavage was collected 4 hr post-injection and adherence purified overnight. After 24 hr, non-adherent cells were washed away, and adherent cells were lysed directly on the plate. Neutrophils were isolated from the bone marrow of wild type, age- and sex-matched mice and purified by negative selection using a neutrophil enrichment kit (Stem Cell). All harvested cells were lysed using TRK lysis buffer (E.Z.N.A. Total RNA kit, Omega Biotek).

In vitro cell culture

Madin-Darby Canine Kidney cells (MDCKs) were cultured in DMEM with 10% FBS, 2 mM L-glutamine, and 100 µM Gentamicin, and plated at 0.5×10^6 cells overnight prior to plaque assays (described below). The immortalized murine lung epithelial type I cell line (LET1) was graciously supplied by Dr. Paul Thomas (St. Jude Children's Research Hospital)[278]. LET1s were cultured without antibiotics in DMEM with 10% FBS, 2 mM L-glutamine, and 100 µM Penicillin-Streptomycin. All cell media was filter-sterilized, and cells were cultured at 37°C and 5% CO_2 until confluency. MLE-12 cells

(American Type Culture Collection) were cultured without antibiotics in DMEM Ham: F12 with 10% FBS and 1% Insulin, Transferrin, Selenium. All cell media was filter-sterilized, and cells were cultured at 37°C and 5% CO_2 until confluency. MDCKs, MLE-12s and LET1s were split using TrypLE Express (Gibco).

In vitro influenza infection

Influenza infection of LET1s or MLE-12s were performed by seeding 12- or 24-well plates at a density of 2.5 x 10^5 cells per well, and cells were infected with influenza A/x31 at a multiplicity of infection (MOI) of 0.5 for 4 or 24 hr. MLE-12s were similarly infected with a MOI of either 0.1 or 1 for 24 hr. Prior to stimulation, cells pre-treated for 30 min with either DMSO or Tpl2 inhibitor (5 μM; Calbiochem, catalog number: 616373). For all stimulation conditions, supernatants were collected at 24 hr, and RNA lysates collected for RT-PCR at 4 hr.

In vitro influenza plaque assay

Lung homogenates were collected from *Nkx2.1*cre*Tpl2*$^{flox/-}$ and Sftpc-CreER^{T2}*Tpl2* $^{flox/-}$ mice at designated timepoints. MDCKs were plated at a density of 0.5 x 10^6/well in a 12-well plate overnight. Once cells reached 90% confluency, lung homogenates were diluted at 1:10 in infection media (1X MEM, 1X Penicillin-Streptomycin diluted in dH_2O with a pH of 7.4) and applied to MDCKs. After a one hr infection, 2.4% Avicel and 2x Overlay Media (2X MEM, 40 mM HEPES, 4 mM L-glutamine, 0.15% Sodium Bicarbonate, 2X Penicillin-Streptomycin- diluted in dH_2O with a pH of 7.4) were combined at a 1:1 ratio and layered onto the cells to induce plaque formation. After three days, the Overlay/Avicel mixture was removed, cells were washed with PBS and fixed with a 60:40 acetone/methanol mixture followed by staining with crystal violet for 15 min[279].

Protein measurements

Lungs were harvested from *Nkx2.1*cre*Tpl2*$^{flox/-}$ and Sftpc-CreER^{T2}*Tpl2* $^{flox/-}$ mice, placed in 1 ml PBS and dissociated with a bead mill homogenizer (Qiagen). Lung homogenates were centrifuged at 500 x *g* for 5 min, and supernatants were aliquoted for protein measurements. Cytokines were quantified using a custom Procartaplex Immunoassay (Thermo-Scientific), IFN-α and IFN-β Luminescent ELISA kits (Invivogen) and Mouse Inflammation Cytometric Bead Array (CBA, BD Bioscience). IFN-λ3 was measured using a colorimetric ELISA (Invitrogen).

mRNA measurements

RNA was isolated from cell lines or lungs using an E.Z.N.A. Total RNA kit (Omega Bio-Tek, Norcross, GA) and converted to cDNA by high-capacity cDNA reverse transcription kit (Life Technologies). Relative expression levels of *c-fos, IFITM3, IFNα1, IFNβ1, IFNλ3, IRF3, IRF7, ISG15, Ptges2*, *Reg3g*, and *TIMP1* were measured using probes from Applied Biosystems (Grand Island, NY) and a SensiFAST Probe Hi-ROX kit (Bioline, Taunton, MA). Samples were run on a StepOnePlus qPCR machine (Applied Biosystems) and results computed relative to wild-type uninfected and actin control using the $\Delta\Delta C_T$ method.

Complete blood count with automated differential

*Nkx2.1*cre*Tpl2*$^{flox/-}$ mice were infected with influenza A/x31 for 8.5 days prior to harvesting. 100-200 µl of blood was collected into EDTA micro-volume tubes (Fisher Scientific) by terminal cardiac puncture from mice sedated with CO_2. A complete blood count with automated differential was analyzed by the Clinical Pathology Lab at the Veterinary Teaching Hospital at the University of Georgia on a Heska Elements HT5. The analysis included: cellular volume and frequency of white blood cells, neutrophils, lymphocytes, monocytes, eosinophils, and basophils. Additional blood parameters included: red blood cell and platelet volume, red blood cell distribution width, hematocrit, hemoglobin, mean corpuscular

hemoglobin concentration, mean corpuscular hemoglobin, mean corpuscular volume, and mean platelet volume.

Tamoxifen administration

100 mg Tamoxifen Citrate (USP-Grade Spectrum Chemical, T1423) was dissolved in 5 ml of corn oil (Millipore Sigma, C8267) at a final concentration of 20 mg/mL and allowed to shake covered in foil overnight at 37°C. Mice were administered 75 mg/kg Tamoxifen intraperitoneally for 5 days consecutively followed by a 9-day chase period. After the chase period, mice were infected with 10^4 PFU influenza A/x31 intranasally.

Pathology Scoring

Lungs from mice infected with influenza A/x31 for 8.5 days were harvested and fixed in 10% neutral-buffered formalin for 24 hr at room temperature. Formalin-fixed lungs were placed in cassettes, embedded in paraffin, sectioned at 4 μm, mounted onto glass slides, and stained with Periodic Acid Schiff (PAS), counterstained with hematoxylin and Masson's trichrome stain or stained with hematoxylin and eosin (H&E) only.

Histological sections were evaluated in a blinded manner by a board-certified, veterinary pathologist (K.S.) and scored according to the following criteria for inflammation: (A) Percent of lung affected; (B) Alveolar score, Alveolar edema score, Pleuritis score; 1 = focal, 2 = multifocal, 3 = multifocal to coalescing, 4 = most of lobule affected; (C) Bronchiolar score: 1 = focal, 2 = multifocal, 3 = most of the bronchioles in a lobule affected, 4 = lobule diffusely affected; (D) PMN score; 1 = neutrophils compose up to 25% of cells in alveoli, 2 = 25-49%, 3 = 50-74%, 4 = 75%+; (E) Perivascular cuffing (PVC) score: 1 = vessel cuffed by 1 cellular layer, 2 = 2-5 cells thick, 3 = 6-9 cells thick, 4 = 10+ cells thick; (F) Vasculitis score: 1 = infiltration of vessel wall by leukocytes, 2 = infiltration and separation of smooth muscle cells, 3 = infiltration and fibrinoid change; (G) Interstitial pneumonia (IP) score: 1 = alveolar

septa infiltrated and thickened by 1 leukocyte layer, 2 = thickened by 2 leukocyte layers, 3 = 3 leukocyte layers, 4 = 4 leukocyte layers. PAS-Masson's Trichrome-stained histological samples were scored according to the following criteria for fibrosis: (A) Distribution of the fibrosis: Perivascular, Peribronchial, or Alveolar; (B) Thickness relative to the wall of the blood vessel (PV), airway (PB), or alveolar septa: 1 = 1x thickness, 2 = 2x thickness, 3 = 3x thickness, 4 = 4x thickness, 5 = 5x thickness.

Confocal microscopy

Wild-type lungs were harvested as described above, and 4 μm sections were mounted onto glass slides. Slides were stained with anti-rabbit IgG isotype control or anti-rabbit Tpl2 (clone M20), followed by goat anti-rabbit IgG AlexaFluor 488 Tpl2 antibody, and imaged using a Nikon Instruments Ti Eclipse microscope with A1R scan head (Melville NY).

Statistics

P values were derived by either paired or unpaired t-tests and two-way ANOVA with Tukey's multiple comparisons test as indicated using PRISM software. Differences were considered statistically significant if $p \leq 0.05$. Data represent means ± SEM. Kaplan-Meier analysis using PRISM software was performed to determine percent survival of *Nkx2.1*cre*Tpl2*$^{flox/-}$ infected with influenza virus, and *p* value was determined using a Mantel-Cox test.

RESULTS

Tpl2 is expressed in pulmonary epithelial cells, and expression increases upon influenza infection

We previously demonstrated that Tpl2 ablation increases morbidity and mortality to influenza A virus infection in mice[149]. Bone marrow chimera experiments suggested that Tpl2 functions within the non-hematopoietic compartment to restrict early virus replication[149]. Therefore, the aim of this study is to define the contribution of Tpl2 within epithelial cells to host defense against influenza infection. Previous studies showed that Tpl2 negatively regulates type I IFNs in macrophages and pDCs in response to TLR

stimulation[146] and that Tpl2 promotes the induction of IFN-λ in pDCs[149]. Therefore, we hypothesized that Tpl2 expression and function within the lung epithelium is essential for viral control and host protection by regulating the induction and amplification of IFNs and IFN-stimulated genes.

To first confirm Tpl2 expression within epithelial cells, the primary target and replicative niche for influenza A virus[3], wild-type (WT) mice were infected with 10^4 plaque forming units (PFU) of mouse-adapted influenza virus A/HK-x31 (H3N2). Lungs were harvested at 3 dpi to determine Tpl2 expression and localization within the lung epithelium by fluorescence microscopy. Tpl2 expression was observed in both type I and type II alveolar epithelial cells (AECI/AECII) (Fig. 5A). In order to confirm Tpl2 expression in alveolar epithelial cells, AECI and AECII were isolated from WT lungs following a previously published protocol[280]. A single cell suspension of alveolar epithelial cells was stained with CD45.2, EpCAM, and Podoplanin (Pdpn). Podoplanin, also known as T1-alpha, is used as a cell surface marker to differentiate AECI (Fig. 5B). Interestingly, AECII displayed higher basal Tpl2 expression than AECI in uninfected mice, which was confirmed by RT-PCR (Fig. 5C). Notably, both pulmonary epithelial cell types exhibited dramatically increased Tpl2 expression by 3 days post influenza infection (Fig. 5A, bottom panels and Fig. 5D). Influenza-induced Tpl2 expression in epithelial cells was replicated using the AECI cell line LET1 (Fig. 5E) and the AECII cell line MLE-12 (Fig. 5F), which corresponded with increased influenza-induced IFNs in both cell lines (Fig. 5G-H).

Tpl2 inhibits type I and type III IFN responses in LET1 cells and primary AECII in response to influenza infection

AECI cells play a vital role in influenza restriction without the influence of the hematopoietic compartment[278], however they are notoriously difficulty to isolate and study *in vitro*. The LET1s AECI cell line shows similar antiviral responses to primary AECI and will therefore be used to explore the function of Tpl2 in alveolar epithelial cells during influenza infection. To define Tpl2-dependent regulation of inflammatory responses within AECI, we infected LET1s with 0.5 MOI of influenza A/x31

for 24 hr in the presence or absence of a selective Tpl2 inhibitor. We found that TNF-α, IL-6, and MCP-1 were not significantly different in Tpl2-inhibited and influenza-infected cells (Fig. 6A). A significant increase in IL-12 secretion was noted in Tpl2-inhibited and influenza-infected LET1s (Fig. 6A), consistent with previous studies showing a negative regulatory role for Tpl2 in IL-12 expression by bone marrow-derived macrophages (BMDM) and bone marrow-derived dendritic cells (BMDC) [281]. However, the most dramatic change observed was the statistically significant increase in type I and type III IFNs in Tpl2-inhibited cells upon influenza infection when compared to vehicle controls, with the greatest fold-change observed for IFN-λ3 (Fig. 6B). This collective increase in IFNs is also consistent with the known negative regulatory role of Tpl2 in IFN-β expression by BMDM and BMDC[281].

Tpl2's negative regulation of IL-12 and IFN-β can occur via IL-10-dependent or –independent mechanisms in macrophages and dendritic cells [281]. However, despite increases in both IL-12 and IFNs upon Tpl2 inhibition (Fig. 6A-B), there was no significant difference in IL-10 (Fig. 6A), suggesting that Tpl2 regulates IL-12 and IFN-β via an IL-10-independent mechanism in LET1s. In macrophages, negative regulation of IFNs and IL-12 relies upon Tpl2-dependent *c-fos* changes[281]. *c-fos* is induced by Tpl2 in macrophages; *c-fo*s in turn, negatively regulates IL-12 and IFN-β production in the presence or absence of IL-10[281]. Therefore, we determined whether Tpl2-dependent *c-fos* also regulated these cytokines in type I epithelial cells. Equivalent *c-fos* expression in LET1s treated with Tpl2 inhibitor or vehicle control (Fig. 6C) demonstrates that the Tpl2-dependent negative regulation of IFNs and IL-12 in LET1s occurs independently of both IL-10 and *c-fos*.

Because of the high production of IFNs in LET1s, we further explored Tpl2-dependent regulation of interferon-stimulated genes (ISGs) by transcriptional analysis. We found that *ISG15*, *IFITM3*, and *IRF7* gene expression were significantly upregulated in Tpl2-inhibited cells when compared to controls upon

influenza infection, whereas IRF3 mRNA expression was unchanged (Fig. 6C). These data are consistent with an elevated interferon signature in LET1s upon Tpl2 inhibition.

To determine whether Tpl2 regulates the immune response to influenza via AECII cell-intrinsic functions, we isolated primary type II epithelial cells from WT and *Tpl2*$^{-/-}$ mice at 3 dpi with influenza A/x31. We found that Tpl2-deficient primary AECIIs expressed trending higher levels for both type I and type III IFNs, although this did not reach statistical significance (Fig. 6D). Overall, these data suggest that Tpl2 plays a prominent role within AECI, and potentially AECII, in the regulation of innate immune responses to influenza.

Tpl2 ablation within the lung epithelium causes increased morbidity and mortality in response to influenza A infection

Given the ability of Tpl2 to constrain interferon responses within immortalized epithelial cells, we generated a lung-specific conditional knockout strain with cre expression under the promoter control of *Nkx2.1*. *Nkx2.1* is a critical transcription factor expressed during early lung development at embryonic day 9 through day 9.5 within the ventral foregut endoderm[273,274]. *Nkx2.1* expression leads to the generation of major lower respiratory structures, including the trachea, bronchioles, and alveoli[273,274]. By utilizing *Nkx2.1* as a lung-specific *cre* promoter, we restricted Tpl2 ablation to the epithelial cells of the lower respiratory tract, including AECI, AECII, pulmonary basal cells, Club cells, and tracheal epithelial cells.

In order to test Tpl2 functionality within the lower pulmonary epithelial cells during influenza infection, *Nkx2.1*cre^{+}*Tpl2*$^{flox/flox}$ mice were infected with 10^4 PFU influenza A/HK-x31 (x31), and weights were monitored over 14 days. We found that there was no significant difference in weight loss between *Nkx2.1cre*$^{+}$*Tpl2*$^{fl/fl}$ mice and *Tpl2*$^{fl/fl}$ control mice (Fig. 7A). Due to the lack of a phenotype observed, we next determined the deletion efficiency of Tpl2 within AECII isolated from *Nkx2.1cre*$^{+}$*Tpl2*$^{fl/fl}$ mice. We

determined that AECII isolated from these mice had an average deletion efficiency of approximately 63% calculated as: (intensity of the defloxed allele / the intensity of the deflox allele + floxed allele) x 100% (Fig. 7B-C). By comparison, Tpl2 was intact (undeleted) in tail DNA where Nkx2.1-cre expression is absent. Notably, mice lacking a single copy of Tpl2 (50% genetic deletion) can lack a phenotype and are sometimes used as negative controls for *Tpl2*$^{-/-}$ mice[282], suggesting that 63% deletion may be insufficient to trigger a phenotype. Additionally, both anecdotal and recent studies have suggested that crossing a null allele onto a cre-line can improve deletion efficiency[283,284]. Therefore, in order to improve the deletion efficiency within the lung epithelium, we crossed *Nkx2.1cre*$^{+}$*Tpl2*$^{fl/fl}$ with *Tpl2*$^{-/-}$ mice to generate *Nkx2.1*cre^{+}*Tpl2*$^{flox/-}$ mice with littermate controls (hereon, referred to as *Nkx2.1*cre^{+}*Tpl2*$^{fl/-}$ and *Tpl2*$^{fl/-}$). A similar deletion efficiency of the single floxed allele was noted in the *Nkx2.1*cre^{+}*Tpl2*$^{fl/-}$ mouse background (data not shown) but given that one allele of Tpl2 was preemptively deleted and contributed 50%, our calculated deletion efficiency within AECII cells improved to 85.5%.

The *Nkx2.1*cre^{+}*Tpl2*$^{fl/-}$ and *Tpl2*$^{fl/-}$ mice were then infected with 10^4 PFU influenza A/HK-x31 (x31), and weights were monitored over 14 days. Over the course of infection, *Nkx2.1*cre^{+}*Tpl2*$^{fl/-}$ mice exhibited significantly more weight loss than *Tpl2*$^{fl/-}$ control mice, with morbidity peaking at 8 dpi (Fig. 8A). Additionally, *Nkx2.1*cre^{+}*Tpl2*$^{fl/-}$ mice had significantly higher mortality when compared to *Tpl2*$^{fl/-}$ (Fig. 8B). During the infection, we observed significant modest weight loss in combination with labored breathing (dyspnea) in the *Nkx2.1*cre^{+}*Tpl2*$^{fl/-}$ mice, which necessitated euthanasia according to humane endpoints of the study. Therefore, we conclude that Tpl2 functions within the lung epithelium to limit morbidity and mortality in response to a low pathogenic strain of influenza.

Primary AECII displayed increase Tpl2 expression in response to influenza infection (Fig. 5D) as well as a trending increase in influenza-induced interferons (type I/type III) in the presence of a Tpl2 inhibitor (Fig. 6D). Therefore, we investigated whether increased susceptibility could be attributed to

Tpl2 functions specifically within AECII. To this end, an inducible type II epithelial cell conditional Tpl2 knockout line was generated using the *Sftpc*-CreER^{T2} promoter[285]. *Tpl2*$^{fl/-}$ littermate controls and *Sftpc*-CreER^{T2+}*Tpl2* $^{flox/-}$ mice were infected with 10^4 PFU of x31, and weights were monitored over 14 days. *Sftpc*-CreER^{T2+}*Tpl2* $^{flox/-}$ mice did not display any significant differences in weight loss (Fig. 9A). Despite intercrossing with the *Tpl2*$^{-/-}$ mouse to preemptively delete one allele, we were unable to improve deletion efficiency in AECII beyond 65% (Fig.9B), a deletion efficiency proven to be insufficient to reveal a *bona fide* phenotype in the *Nkx2.1* model (Fig. 9C). Therefore, subsequent studies focused on the role of Tpl2 in lung epithelial cell types using the *Nkx2.1*cre model.

Lung-specific Tpl2 ablation impairs early viral control but does not alter inflammatory cytokine production

To determine the cause of increased morbidity and mortality in influenza-infected *Nkx2.1*cre^{+}*Tpl2*$^{fl/-}$ mice, we harvested lungs at 1, 3, 5, 7, 8.5 dpi from influenza-infected *Nkx2.1*cre^{+}*Tpl2*$^{fl/-}$ and *Tpl2*$^{fl/-}$ control mice and prepared lung homogenates. We first measured viral titers within the lung homogenates over the time course. We noted that although there was a modest, statistically significant increase in viral titers at 1 dpi in the *Nkx2.1*cre^{+}*Tpl2*$^{fl/-}$ mice, the increase was resolved by 3 dpi and remained comparable to the *Tpl2*$^{fl/-}$ mice through the study's end (Fig. 10A). Therefore, increased morbidity and mortality cannot be attributed to an inability to control viral replication. High pathogenicity influenza infections are proposed to cause mortality due to an overwhelming immune response rather than uncontrolled viral titers[286]. To address this possibility, we measured the abundance of inflammatory mediators in lung homogenates over the same time course. To our surprise, we found no significant differences in cytokine production in *Nkx2.1*cre^{+}*Tpl2*$^{fl/-}$ mice (Fig. 10B).

Increased pulmonary fibrosis in lung-specific Tpl2 knockout mice

To determine if Tpl2 ablation in non-hematopoietic cells indirectly caused systemic hematologic or metabolic effects that could be responsible for increased morbidity and mortality, we examined several

clinical markers of systemic disease at the peak of morbidity (8.5 dpi, Fig. 8A) in one large representative cohort of mice. The circulating number and frequency of immune cells was not different compared to *Tpl2*$^{fl/-}$ mice (Fig. 11A). Many of the clinical markers of anemia in humans are predictive markers of poor outcomes of influenza infections. Patients with increased red blood cell distribution width typically have severe complications with influenza including a higher rate of mechanical ventilation[287]. However, in *Nkx2.1*cre^{+}*Tpl2*$^{fl/-}$ mice, there was no alteration in red blood cell distribution width compared to *Tpl2*$^{fl/-}$ mice (Fig. 11B). Additionally, it has been shown in mice that increased hemoglobin and hematocrit levels are associated with viral pathogenicity[288]; however, there were no significant differences in either marker in the *Nkx2.1*cre^{+}*Tpl2*$^{fl/-}$ mice (Fig. 11B). All of the hematological markers (mean corpuscular hemoglobin concentration, mean corpuscular hemoglobin, mean corpuscular volume, and mean platelet volume) are highly associated with anemia. Based upon analysis of these factors, there was no indication that anemia was a factor leading to the increased morbidity and mortality in *Nkx2.1*cre^{+}*Tpl2*$^{fl/-}$ mice (Fig. 11B).

We consistently observed that the *Nkx2.1*cre^{+}*Tpl2*$^{fl/-}$ mice exhibited dyspnea in response to viral infection, which often necessitated euthanasia according to the humane endpoints. In order to directly address pulmonary changes associated with increased morbidity and mortality, lung samples harvested 8.5 dpi from *Nkx2.1*cre^{+}*Tpl2*$^{fl/-}$ and *Tpl2*$^{fl/-}$ littermate controls were submitted for histopathology to characterize infection-induced pathological changes in the bronchioles, alveoli, and pleura. There was no significant difference in the percent of lung affected; however, the *Nkx2.1*cre^{+}*Tpl2*$^{fl/-}$ mice tended to have a higher percentage of the lung affected compared to *Tpl2*$^{fl/-}$mice. Inflammation in the bronchioles and the severity of interstitial pneumonia also trended to be worse in the *Nkx2.1*cre^{+}*Tpl2*$^{fl/-}$ mice compared to *Tpl2*$^{fl/-}$mice. However, there were no significant differences in inflammation in any major location of the lung (Fig. 11C and Fig. 12A).

Multiple lines of evidence have recently implicated Tpl2 in restraining fibrotic responses, both in intestinal myofibroblast-mediated fibrosis in the gut[268] and in bleomycin-induce lung fibrosis[239]. Because

pulmonary fibrosis impairs lung function during influenza infection [229], we hypothesized that Tpl2 protects against influenza-induced lung injury by inhibiting pulmonary fibrosis. Indeed, a significant increase in alveolar fibrosis was observed in *Nkx2.1*cre^{+}*Tpl2*$^{fl/-}$ mice compared to *Tpl2*$^{fl/-}$ mice (Fig. 11D and 11F). Representative images display increased fibrosis (designated by the blue stain) surrounding blood vessels and airways in the *Nkx2.1*cre^{+}*Tpl2*$^{fl/-}$, with minor accumulation thickening the alveolar septa (Fig 11E). We also noted trending increases in multiple key fibrotic markers, including *Ptges2*, *Reg3g*, and *TIMP1* within the lung at 8.5 dpi (Fig. 11E).

DISCUSSION

We found that pulmonary epithelial cells within the lower respiratory tract (AECIs and AECIIs) express increased Tpl2 expression after influenza infection (Fig. 5A). This data is consistent with previous studies showing that Tpl2 is transcriptionally induced and activated upon influenza infection in the human embryonic kidney cell line, 293T[154]. Additionally, ours and other previous studies show that Tpl2 is an IFN-induced gene in response to viral infection[153,289]. In AECIs, Tpl2 negatively regulates IFNs (type I and type III) and IL-12 consistent with their negative regulation by Tpl2 in macrophages and dendritic cells [281]. We explored the possible mechanism for Tpl2 regulation of IFNs within LET1s (AECI). Tpl2-dependent *c-fos* expression has been shown to negatively regulate IFN-β and IL-12 in the presence or absence of IL-10 in BMDM[281]. Therefore, we hypothesized that Tpl2-dependent *c-fos* expression also negatively regulates type I/III IFNs during influenza infection by the same *Tpl2*/*c-fos*/IL-10 mechanism reported in macrophages[281]. However, *c-fos* levels were unchanged in Tpl2 inhibitor-treated LET1s arguing that Tpl2 inhibits IFNs independently of IL-10 and *c-fos* in these cells. In *Tpl2*$^{-/-}$ BMDMs and BMDCs, impaired Tpl2-dependent ERK induction of *c-fos* permits increases in IL-12[281]. Since we did not observe an increase in either *c-fos* or IL-10, the increase in IL-12 within LET1s appears to be regulated by a mechanism distinct from that observed in BMDMs and BMDCs.

We generated two lung-specific conditional Tpl2 knockout mouse models using *Nkx2.1* and *Sftpc* as lung-specific *cre* promoters. *Sftpc-creER*^{T2} led to the ablation of Tpl2 specifically from AECII in response to tamoxifen administration. Unfortunately, we were unable to distinguish changes in morbidity or mortality within these mice (Fig. 9A). Therefore, we cannot attribute the protective effects of Tpl2 solely within AECII using this model. *Nkx2.1-cre* was used to ablate Tpl2 from a variety of lung epithelial cells, including club cells, basal cells, AECI, and AECII. In this model, Tpl2 ablation within the lung epithelium significantly enhanced morbidity and mortality in response to influenza A infection (Fig. 8A and B). Increased susceptibility to infection was not caused by excessive viral replication within the lungs (Fig. 10A). Increased susceptibility to infection was not caused by excessive viral replication, rather likely resulted from fibrotic buildup within the alveolar spaces. Unlike in the LET1 cell line where Tpl2 negatively regulates type I and type III IFN responses, we did not observe a significant increase in interferons or other proinflammatory cytokines *in vivo* (Fig. 10A-B). This may be due to interferon production from other cell types – including plasmacytoid dendritic cells, natural killer cells, and other hematopoietic cells – which may mask the specific contributions of epithelial cells to interferon production during influenza infection *in vivo.* Altogether, the Nkx2.1-cre model demonstrated that Tpl2 expression broadly within lung epithelial cell types promotes a protective response to influenza infection.

These results of the *Nkx2.1*cre^{+}*Tpl2*$^{fl/-}$ mice are consistent, in part, with our previous study demonstrating enhanced viral replication and increased morbidity and mortality in influenza-infected mice with global Tpl2 ablation[149]. In the prior study, 100% *Tpl2*$^{-/-}$ mice succumbed to infection or met the humane endpoints of the study by approximately 10 dpi[149], whereas in the current study, epithelial-specific ablation of Tpl2 in the lungs resulted in approximately 60% mortality during influenza infection with similar kinetics. Obvious key differences exist between the two animal models that can account for the difference in disease severity. One major difference is that in *Nkx2.1*cre^{+}*Tpl2*$^{fl/-}$ mice, Tpl2 deletion is restricted to lung epithelial cells. Notably, in the previous study, a Tpl2-dependent *decrease* in IFN-λ3 was noted in lungs after influenza infection[149], whereas type I and type III IFNs are unchanged in the

current study with epithelial-restricted Tpl2 ablation. In *Tpl2*$^{-/-}$ mice, global deficiency leads to major defects within hematopoietic cells that have known roles in interferon production and restriction of viral replication, including plasmacytoid dendritic cells (pDCs)[149]. In *Tpl2*$^{-/-}$ mice, decreased IFNλ3 production by Tpl2-deficient pDCs, the major IFN producers, could have overshadowed minor increases in IFNλ3 by epithelial cells, macrophages, and conventional dendritic cells in which Tpl2 has been shown to inhibit IFNs[281], leading to an overall decrease in IFNλ3 noted in the previous study. In contrast, Tpl2 expression in pDCs is unaffected in the current study, which explains the increased IFN production consistent with its negative regulation by Tpl2 observed in AECI and AECII *in vitro*. Influenza viral clearance is managed by natural killer cells (NK) cells[29] and influenza-specific CD8 T cells[290] that target the virally-infected cells for killing. *Tpl2*$^{-/-}$ mice have significantly less antigen-specific CD8 T cells[149], which could also contribute to a more severe phenotype in *Tpl2*$^{-/-}$ mice. It is possible that altered NK functionality during viral infections may contribute to the increased disease severity of the complete knockout model. However, the role of Tpl2 within natural killer cells remains unclear.

In this study, we observed that *Nkx2.1cre*$^{+}$*Tpl2*$^{fl/-}$ mice have a moderate increase in alveolar fibrosis in *Nkx2.1cre*$^{+}$*Tpl2*$^{fl/-}$ compared to controls (Fig. 5D-E) that corresponded to trending increases of known fibrotic markers, including *Ptges2*, *Timp1* and *Reg3g*. Notably, these moderate changes in fibrosis are consistent with moderate changes in morbidity and mortality in mice with epithelial cell-specific ablation of Tpl2. We hypothesize that in response to influenza-induced lung injury, Tpl2 ablation within the respiratory epithelium increases fibrin deposition in the alveolus through an unknown mechanism, which may contribute to increased lung resistance, as evidence by the dyspnea (labored breathing) in *Nkx2.1cre*$^{+}$*Tpl2*$^{fl/-}$ mice.

Pulmonary fibrosis is a relatively common complication of H1N1-induced acute respiratory distress syndrome (ARDS)[291], and pulmonary fibrosis accounts for 40-70% of all ARDS-related deaths[292,293].

Several lines of evidence suggest that Tpl2 may regulate pulmonary fibrosis [239]. Mitogen-activated protein kinase (MAPK) signaling through ERK1/2, which can be directly phosphorylated by Tpl2[294], has been associated with pulmonary fibrosis[295]. However, the literature involving the role of Tpl2/ERK signaling during pulmonary fibrosis is contradictory and stimulus dependent. ERK phosphorylation has been positively correlated with pulmonary fibrosis in a bleomycin acute lung injury model with high-tidal-volume lung ventilation, which suggests that Tpl2 deficiency may be protective[295]. Kannan *et al.* showed that Tpl2 deficiency increases Th2-mediated immunopathology and pulmonary fibrosis after *Schistosoma mansoni* infection by activating pro-fibrotic and immunoregulatory pathways in M2 macrophages[296]. But perhaps most convincing is the definitive report that Tpl2 inhibits pulmonary fibrosis in a model of bleomycin-induced lung injury. Zannikou *et al.* found that Tpl2 has a protective role during bleomycin-induced lung fibrosis[239]. Tpl2 deficiency causes increased lethality and weight loss in response to bleomycin treatment. Unsurprisingly, this protection against bleomycin-induced fibrosis was mediated through macrophages rather than nonhematopoietic cells. Although the exact mechanism has not been fully elucidated, alveolar macrophages are identified as key mediators of bleomycin-induced lung fibrosis[238]. Bleomycin administration directly kills endothelial and epithelial cells after contact; whereas, macrophages are the primary producers of reactive oxygen species, nitric oxides, prostaglandins, and profibrotic cytokines and growth factors after bleomycin administration[237,238]. Therefore, Tpl2 has been implicated in pulmonary fibrosis, however the exact cell types (somatic versus hematopoietic) involved in limiting fibrosis progression may be context dependent as with previous models[137] and its specific role in IAV-induced fibrosis needs to be addressed in future studies.

In conclusion, Tpl2 functions within epithelial cells to constrain interferon production in response to influenza infection *in vitro*; *in vivo* Tpl2 protects against influenza-induced alveolar fibrosis. Increased IFN-λ3 levels, as we observed in our Tpl2-inhibited LET1s, have previously been associated with liver and pulmonary fibrosis[297,298]. Prior to the onset of fibrosis in the *Nkx2.1cre*$^{+}$*Tpl2*$^{fl/-}$ mice, we were unable

to measure global changes in IFN-λ production. Together, our *in vitro* and *in vivo* data suggests that local increases in IFN-λ at the alveolar surface may still contribute to increases in fibrosis, but not other pulmonary regions. Future studies will examine the causal link between the trending increase in fibrotic markers, cytokines levels, pulmonary fibrosis, and compromised lung function in influenza-infected *Nkx2.1cre*$^{+}$*Tpl2*$^{fl/-}$ mice. Overall, a better understanding of how immune responses are generated within the pulmonary mucosa can reveal novel therapeutic strategies for treating a variety of pathogens.

ACKNOWLEDGEMENTS

The authors thank the University of Georgia (UGA)'s Coverdell Rodent Vivarium for animal care; our laboratory animal veterinarian, Dr Stephen Harvey; UGA's Veterinary Diagnostic Laboratories; and UGA's Veterinary Pathology Department and University of Georgia's Clinical Pathology Lab at the Veterinary Teaching Hospital for blood analysis. Julie Nelson (Cytometry Shared Resource Laboratory, UGA) for flow sorting and James Barber (College of Veterinary Medicine Cytometry Core) for assistance with confocal microscopy. Research reported in this publication was supported by the National Institute of Allergy and Infectious Diseases of the National Institutes of Health under Award Number R21AI147003-01 to WTW. The content is solely the responsibility of the authors and does not necessarily represent the official views of the National Institutes of Health.

FIGURES

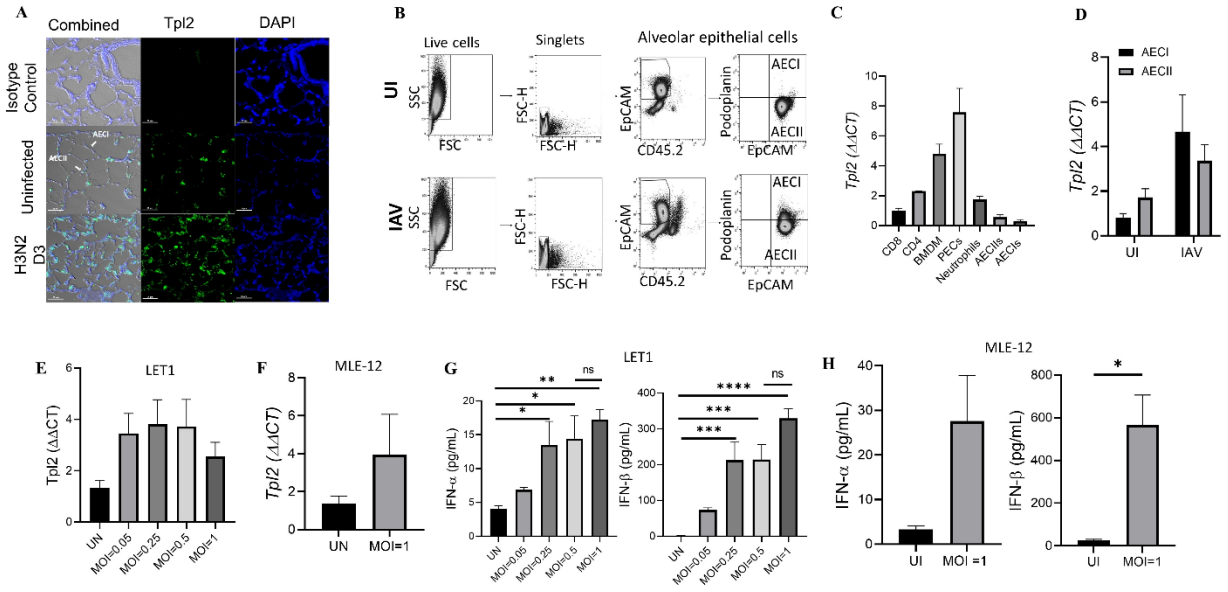

Figure 5. Tpl2 is expressed in pulmonary epithelial cells, and expression increases upon influenza infection. (A) Wild type (WT) mice were either uninfected or infected with 10^4 PFU influenza A/x31 (H3N2) for 3 days. Lung sections were mounted onto glass slides and stained with anti-rabbit IgG isotype control or anti-rabbit Tpl2 (Santa Cruz Biotechnology, clone M20) followed by goat anti-rabbit IgG AlexaFluor 488, and the nucleus was counterstained with DAPI. Slides were imaged using confocal microscopy. Representative images of Tpl2 expression within 4 μm lung sections from WT mice. Data are representative of 3 experiments. (B) Representative flow plot of AECII ($EpCAM^+CD45.2^-$) or AECI ($EpCAM^+CD45.2^-Podoplanin^+$) isolated from mice were either uninfected or infected with 10^4 PFU influenza A/x31 for 3 days. (C) Naïve splenic $CD4^+$ and CD8+ T cells, bone marrow-derived macrophages (BMDM), adherence-purified peritoneal exudate cells (PECs), neutrophils, and lung alveolar epithelial cells (AECI and AECII) were isolated from WT, age- and sex-matched mice. Tpl2 expression was measured by RT-PCR relative to an actin control. All samples were normalized to $CD8^+$ T

cells, which were arbitrarily designated a value of 1. Data are representative of 3 experiments. (D) Isolated alveolar epithelial cells (AECI and AECII) from WT, age- and sex-matched mice that were uninfected or infected with 10^4 PFU influenza A/x31 for 3 days. N=4. Cells, LET1s (E) or MLE-12s (F) were cultured for 24 hours prior and left uninfected or infected with a MOI of 0.05, 0.25, 0.5, or MOI 1 of influenza A/x31 (H3N2) for 24 hours. RNA lysates collected after 24 hours and Tpl2 expression measured by RT-PCR. IFNα and IFNβ secretion were measured by luminescent ELISA from supernatants collected from LET1s (G) or MLE-12s (H) uninfected or infected across a dose-curve (MOI 0.05, 0.25, 0.5, 1) for 24 hours. Pooled data from 3 experiments. Error bars represent means ± sem. Error bars represent means ± sem. *$p<0.05$, **$p<0.01$, ***$p<0.001$, ****$p<0.0001$; one-way ANOVA.

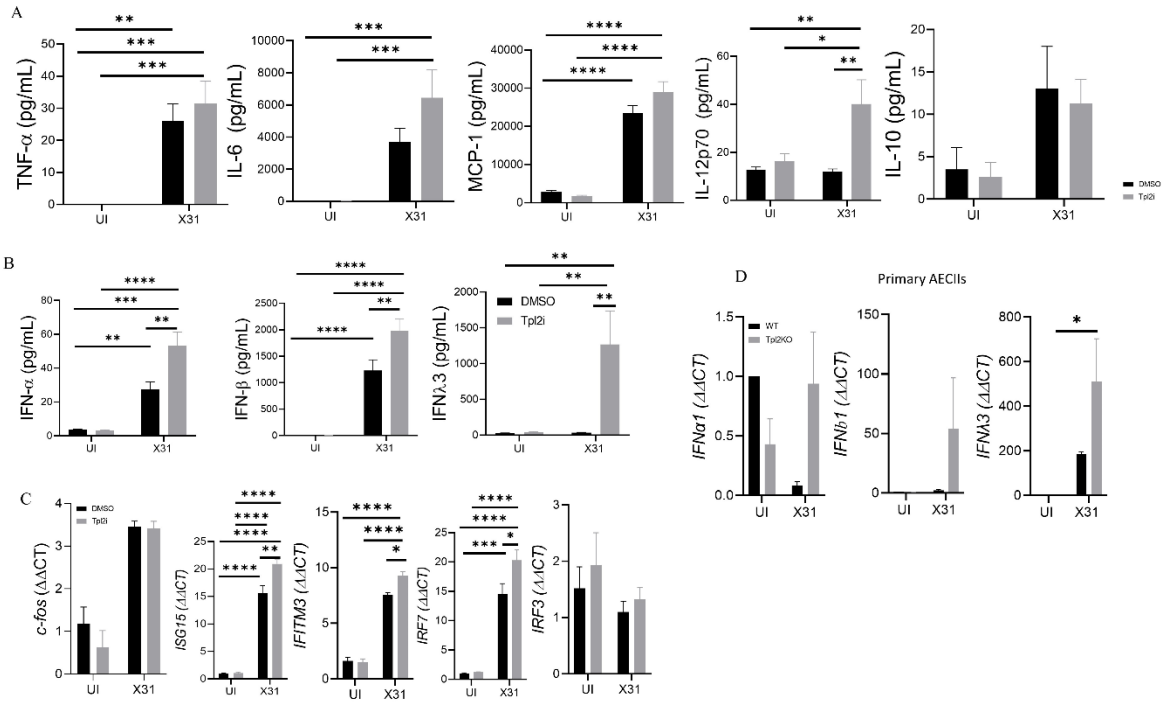

Figure 6. Tpl2 tempers type I and type III IFN responses in LET1s and primary AECII in response to influenza infection. LET1s were cultured for 24 hours prior to stimulation with a MOI of 0.5 of Influenza A/x31 (H3N2) for 24 hours after a 30-minute pre-treatment with DMSO vehicle control or Tpl2 inhibitor (5 μM). (A) Cytokine expression measured by CBA analysis from supernatants collected 24 hpi. Pooled data from 3 experiments. (B) *IL-10, fos, IRF3, IRF7, ISG15,* and *IFITM3* expression levels were quantified by RT-PCR from RNA lysates collected 24 hpi. Pooled data from 3 experiments. (C) IFN-α, IFN-β, and IFN-λ3 secretion was measured by ELISA from supernatants collected 24 hpi. Pooled data from 3 experiments. (D) *IFN-α1, IFN-β1,* and *IFN-λ3* expression levels were quantified by RT-PCR from RNA lysates collected from primary type II alveolar epithelial cells (AECII). N=4. Error bars

represent means ± sem. Undetermined CT values were set to 40. *p<0.05, **p<0.01, ***p<0.001, ****p<0.0001; one-way ANOVA.

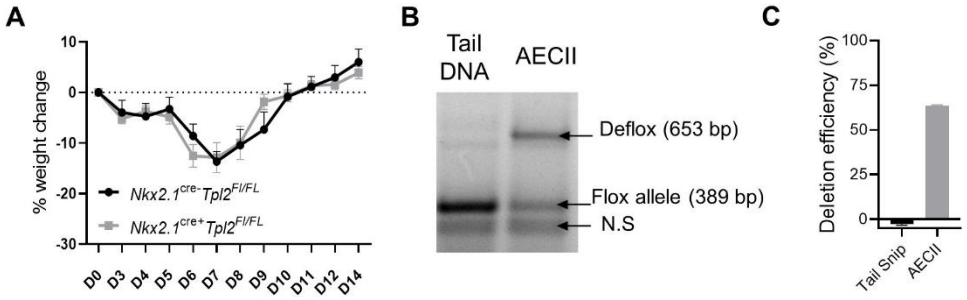

Figure 7. Determination of Tpl2 expression in alveolar epithelial cells and deletion efficiency of conditional knockout strain *Nkx2.1*. (A) *Tpl2*$^{fl/fl}$ and *Nkx2.1*cre^{+}*Tpl2*$^{fl/fl}$ conditional knockout mice were infected intranasally with 10^4 PFU influenza A/x31. Morbidity was assessed by daily weight loss. Cre- N=8, Cre+ N=10. Data representative of 2 experiments. Symbols and error bars represent means ± sem. (B) Representative image from 3 mice in which tail snip DNA and DNA from isolated AECII was subjected to genomic amplification of the defloxed allele versus the intact floxed allele. (C) Deletion efficiency from *Nkx2.1*cre^{+}*Tpl2*$^{fl/fl}$ (left panel) N=3 mice.

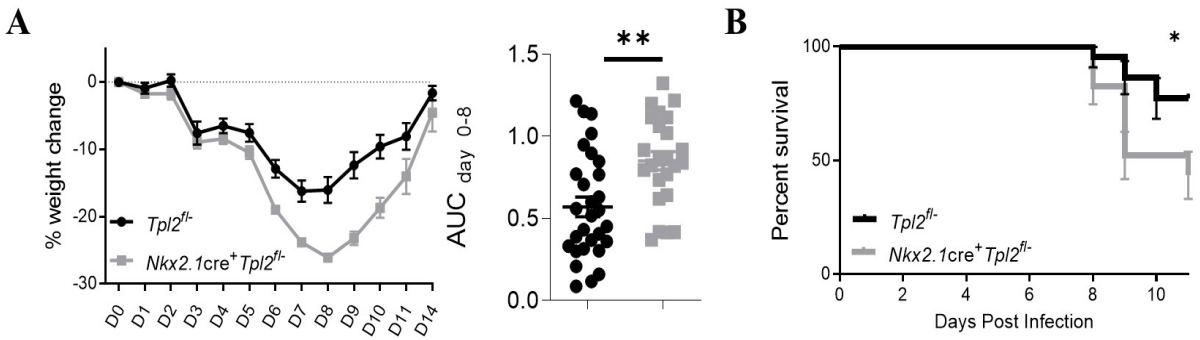

Figure 8. **Tpl2 ablation within the lung epithelium causes increased morbidity and mortality in response to influenza A infection.** (A) *Tpl2*$^{fl/-}$ and *Nkx2.1*cre^{+} *Tpl2*$^{fl/-}$ conditional knockout mice were infected intranasally with 10^4 PFU influenza A/x31. Morbidity was assessed by daily weight loss. Significance of weight loss was determined by area under the curve (AUC) analysis with an unpaired two-tailed T-test. Cre- N=29, cre+ N=24. Pooled data from 3 experiments. (B) Survival curve of mice in (A) after IAV infection. *p-value=0.0199, mean survival= 77.2% *Tpl2*$^{fl/-}$ and 43.3% *Nkx2.1*cre^{+} *Tpl2*$^{fl/-;}$ Log-rank (Mantel-Cox) test. Cre- N=22, cre+ N=23. Pooled data from 3 experiments, Error bars represent means ± sem. *p<0.05, **p<0.005

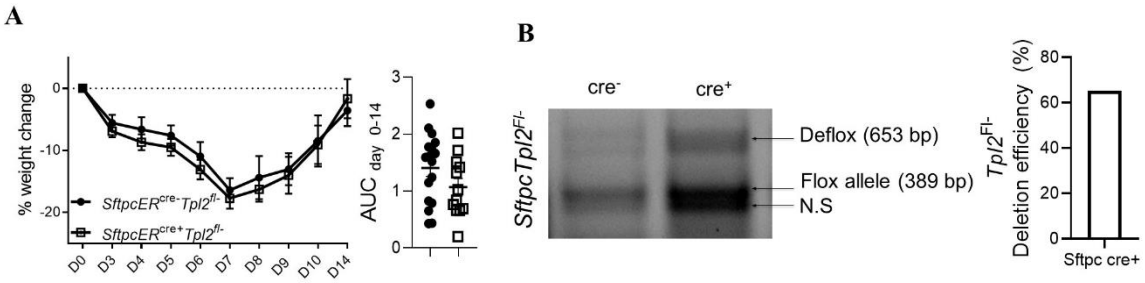

Figure 9. Insufficient Tpl2 deletion within AECII of *Sftpc-CreER^{T2} Tpl2$^{fl/-}$* mice. (A) Influenza-induced morbidity measured by weight loss in *Sftpc-cre^{-}ER^{T2}* and *Sftpc-cre^{+}ER^{T2} Tpl2$^{fl/-}$* conditional knockout mice. Significance determined by AUC analysis. Cre-N=17, cre+ N=12. Data pooled from 2 experiments. Symbols and error bars represent means ± sem. Unpaired two-tailed T-test; not significant (N.S.) (B) Representative image of isolated AECII from *Sftpc-cre^{-}ER^{T2}* and *Sftpc-cre^{+}ER^{T2} Tpl2$^{fl/-}$* mouse deflox allele amplification (left panel). *Sftpccre^{+}Tpl2$^{fl/-}$* calculated deletion efficiency (right panel).

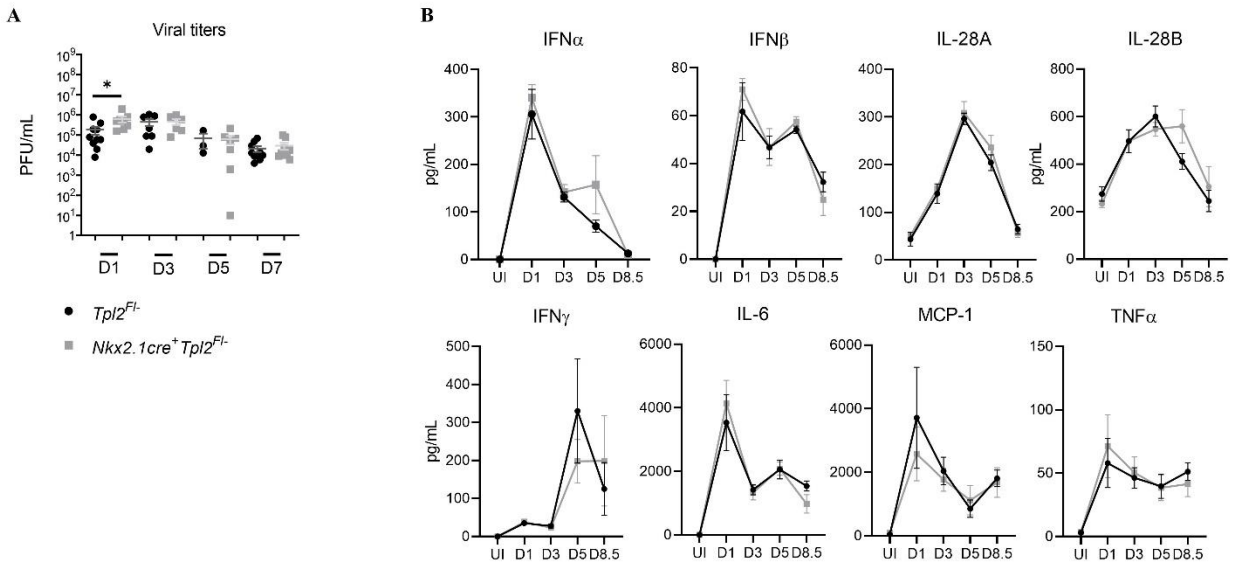

Figure 10. Lung-specific Tpl2 ablation impairs early viral control but does not alter inflammatory cytokine production (A) Viral titers determined by plaque assay. Pooled data from 4 separate experiments, 1 experiment per time point. Mice per group- D1: cre-, N=10. cre+, N=8; D3: cre-, N=7. cre+, N=6; D5: cre-, N=3, cre+ N=7. D8.5: cre-, N=8. cre+, N=6. (B) Cytokine expression determined by Procartaplex immunoassay; data representative of 2 experiments.

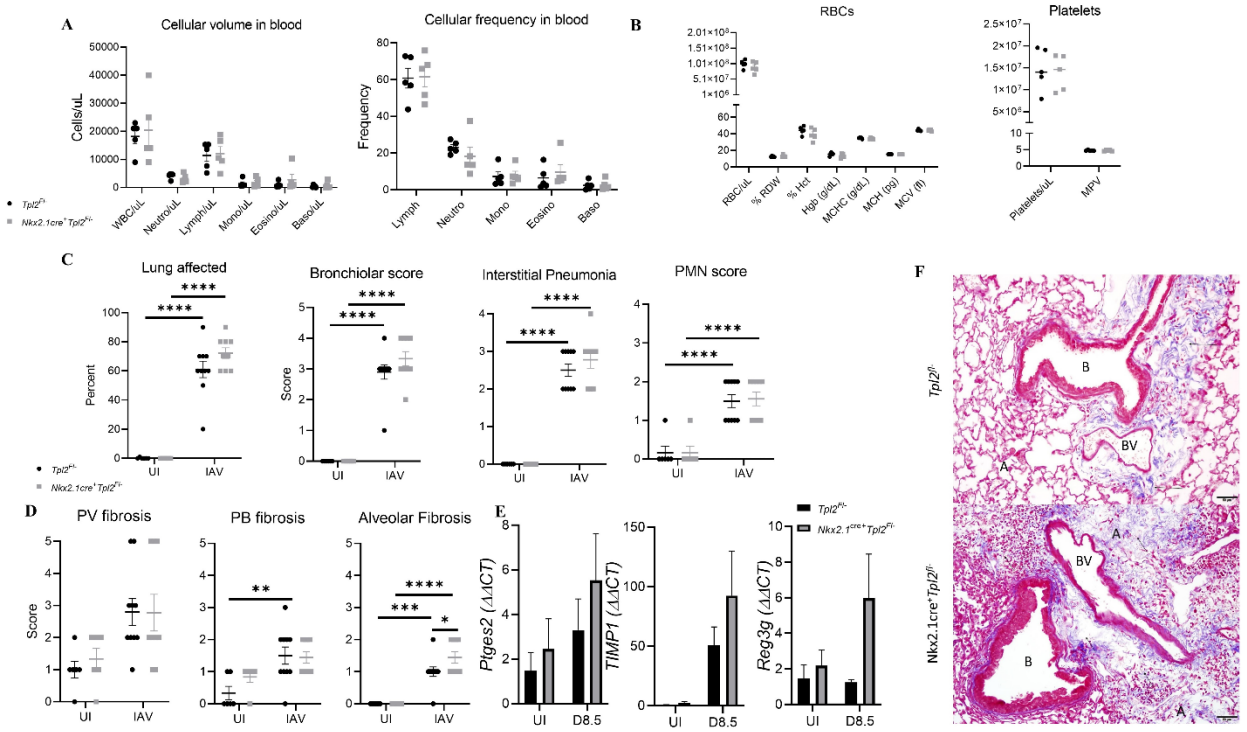

Figure 11. Increased pulmonary fibrosis in lung-specific Tpl2 knockout mice. (A) Complete blood count (CBC) from *Tpl2*$^{fl/-}$ and *Nkx2.1*cre^{+}*Tpl2*$^{fl/-}$ mice at 8.5 dpi with 10^4 PFU influenza A/x31 measuring immune cell volume and frequency collected by terminal cardiac puncture (N=1). (B) Anemia-associated markers analyzed by CBC: RDW (red blood cell distribution width), Hct (hematocrit), Hgb (hemoglobin), MCHC (mean corpuscular hemoglobin concentration), MCH (mean corpuscular hemoglobin), MCV (Mean corpuscular volume), MPV (Mean platelet volume). N=5 mice per group. (C) Inflammation scoring of *Tpl2*$^{fl/-}$ and *Nkx2.1*cre^{+}*Tpl2*$^{fl/-}$ mice at 8.5 dpi with 10^4 PFU influenza A/x31. Lungs sections were stained with hematoxylin and eosin and scored by a pathologist blinded to sample identity. *Tpl2*$^{fl-}$, N=16 (6 controls, 10 experimental). *Nkx2.1*cre^{+}*Tpl2*$^{fl/-}$ N=15 (6 controls, 9 experimental). (D) Fibrosis scoring of *Tpl2*$^{fl/-}$ and *Nkx2.1*cre^{+}*Tpl2*$^{fl-}$ mice at 8.5 dpi with 10^4 PFU influenza A/x31. Lungs sections were stained with Masson's-Trichrome stain and scored for fibrosis by a pathologist blinded to sample identity.

Scoring was on a scale of 1-5 comparing surrounding fibrosis relative to normal thickness of the structure. Perivascular (PV), Peribronchiolar (PB), Alveolar fibrosis. *p<0.05; unpaired one-tailed T-test, null hypothesis: Tpl2 inhibits pulmonary fibrosis. Tpl2fl- , N=16 (6 controls, 10 experimental). Nkx2.1cre+Tpl2fl-, N=15 (6 controls, 9 experimental). (E) Ptges2, Reg3g, TIMP1 expression levels were quantified by RT-PCR from RNA lysates collected from uninfected and D8.5 lung homogenates. unpaired one-tailed T-test, null hypothesis: Tpl2 inhibits pulmonary fibrosis. Data representative of 2 experiments. (F) Representative image of Tpl2Fl- and Nkx2.1cre+Tpl2Fl- lung sections stained with Periodic Acid Schiff, counterstain with hematoxylin and Masson's trichrome stain 8.5 dpi. Alveoli (A), B (Bronchiole), BV (Blood Vessel). Arrows pointing to blue areas of fibrotic-positive stain. Data representative of 2 experiments. Error bars represent means ± sem. *p<0.05, **p<0.01, ***p<0.001, ****p<0.0001; one-way ANOVA unless otherwise noted.

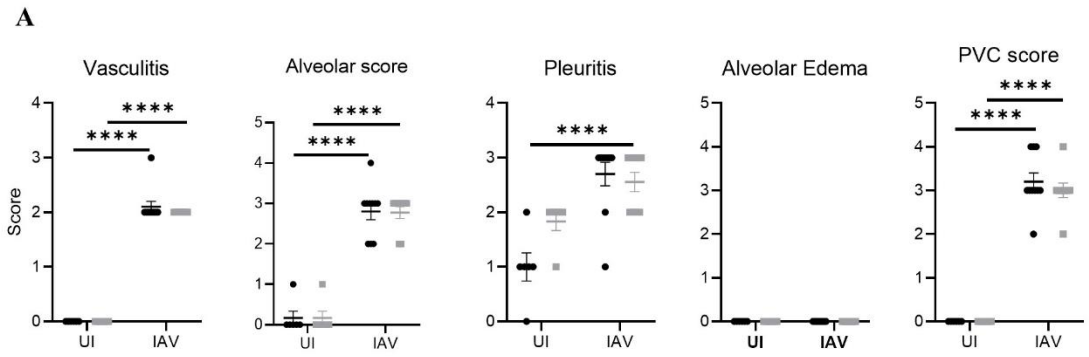

Figure 12. Histological analysis in Tpl2-ablated lungs shows similar inflammation levels to control mice. (A) Histological sections were evaluated in a blinded manner by a veterinary pathologist (K.S.) and scored according to the following criteria: Vasculitis score: 1 = infiltration of vessel wall by leukocytes, 2 = infiltration and separation of smooth muscle cells 3 = infiltration and fibrinoid change; Alveolar score, Alveolar edema score, Pleuritis score: 1 = focal, 2 = multifocal, 3 = multifocal to coalescing, 4 = most of lobule affected; Perivascular cuffing (PVC) score: 1 = vessel cuffed by 1 cellular layer, 2 = 2-5 cells thick, 3 = 6-9 cells thick, 4 = 10+ cells thick. *Tpl2*$^{fl/}$, N=16 (6 controls, 10 experimental) and *Nkx2.1cre*$^{+}$ *Tpl2*$^{fl/}$, N=15 (6 controls, 9 experimental).

CHAPTER 3

TAMOXIFEN-TREATMENT INDUCES HISTOPATHOLOGIC CHANGES WITHIN CRE-RECOMBINASE NEGATIVE MICE[2]

[2] Wyatt, K.D., Sakamoto K.S., and Watford, W.T.W, Submitted to *Laboratory Animals*, 01/22/21.

ABSTRACT

Tamoxifen is a selective estrogen receptor modulator (SERM) that is commonly used as a cancer treatment in humans and for inducing genetic alterations using cre-lox mouse models in the research setting. Side effects within human patients have been well-documented; however, the extent of tamoxifen off-target effects in animal research is underappreciated. Here we report significant changes in cellular infiltration in cre-recombinase-negative mice treated with tamoxifen intraperitoneally. These changes were noted in distal organs such as the lungs, which were characterized by the presence of inflammation within the alveoli, vasculature, and pleura, as evidenced by an inflammatory cell infiltrate. Despite significant immunological changes in response to tamoxifen-treatment, clinical signs were not observed. This study provides a cautionary note that tamoxifen treatment alone leads to histologic alterations that may obscure research interpretations and further highlights the need for the development of alternative mouse models for inducible cre-mediated deletion.

INTRODUCTION

Tamoxifen is a selective estrogen receptor modulator (SERM), a derivative of a class of molecules called triphenylethylenes, which outcompetes estradiol for estrogen receptor binding and forms a nuclear complex that inhibits downstream transcriptional activity[299,300]. The most prominent usage of tamoxifen in human medicine is as a hormone therapy for breast cancer, where it is commonly used in women to treat early-stage invasive breast cancer and advanced breast cancer [299,301]. Tamoxifen is also used as an off-label treatment for breast cancer in men or gynecomastia resulting from prostate cancer treatments [302].

Tamoxifen has been shown to be highly effective against breast cancer, although patient non-compliance due to side effects is a significant issue. One study suggests that between 30-80% of women do not take tamoxifen daily as prescribed [303]. The side effects for tamoxifen treatments in humans have been well-documented and range from hot flashes to increased risk for endometrial cancer and uterine sarcomas [299]. In addition to an increased cancer risk, tamoxifen administration has also been associated with an increased risk of fatty liver disease and cholestasis[304,305]. Tamoxifen treatment in humans also induces immune modulation[306]. Recent studies have found other endocrine therapy options, such as aromatase inhibitors, to be superior to tamoxifen for use in post-menopausal patients [301,307,308]. However, in humans, the data overwhelmingly support that the benefits of tamoxifen outweigh the risks due to the significant efficacy against cancer progression.

In animal research, tamoxifen is typically used in conjunction with the cre-lox system to facilitate inducible site-specific gain- or loss-of-function for genes targeted by *loxp* sites. Classically, the ligand-binding domain of the estrogen receptor has been directly fused to cre-recombinase to trigger tamoxifen-inducible deletion of a gene flanked by *loxp* sites. However, leaky deletion in this model, likely due to binding of CreER to endogenous estrogens, may complicate experimental interpretations[309]. In the new $CreER^{T2}$ systems, endogenous estrogens bind only weakly to ER^{T2} compared to tamoxifen, such that the fusion protein remains in the cytoplasm of the cell until tamoxifen binds, driving the cre recombinase

enzyme to translocate into the nucleus, where it can access the *loxp* sites[309]. The inducible cre-lox system is widely used in animal research; however, a wide range of tamoxifen doses have been published with little uniformity[310]. This is an issue because a variety of off-target effects can occur in response to tamoxifen usage across multiple organs. It is appreciated that tamoxifen has multiple immune modulatory effects *in vivo* [306]. One study has shown that a single dose of tamoxifen can cause reproductive changes in male rodents that are detectable both transiently and long-term[310]. Tamoxifen side effects are not always detrimental; in SLE-like mouse models, tamoxifen-treated mice had increased survival rates[306,311–313]. In experimental autoimmune encephalitis (EAE) mouse models, tamoxifen-treated mice displayed a protective Th2 bias that increased survival[314].

The indisputable efficacy of tamoxifen outweighs the potential negative off-target side effects of the drug in human cancer patients. However, animal researchers must be aware of the myriad off-target effects that may occur outside the scope of their expected phenotype when tamoxifen is used for inducible gene ablation. In the current report, we observed that intraperitoneal tamoxifen treatment induces distal histopathologic changes even in the absence of cre-recombinase activity. Abnormal histologic findings within the lungs of tamoxifen-treated mice included the presence of inflammation within alveoli, surrounding and in the vasculature, and in the pleura; inflammation within these regions was evidenced by significant leukocyte infiltration. Overall, a greater appreciation of how tamoxifen dosing impacts the immune response in laboratory animal models is required to ensure appropriate interpretation of results.

MATERIALS AND METHODS

Mice and viruses

Tpl2$^{flox/flox}$ mice were offered by Dr. George Kollias[268]and purchased from EMMA (EM:07150). *Tpl2$^{flox/flox}$* mice were crossed with *Sftpc$^{tm1(cre/ERT)Blh}$ (Sftpc-CreER^{T2})* mice. Because of poor deletion efficiency within this line, *Sftpc-CreER$^{T2+/-}$Tpl2$^{flox/flox}$* mice were further crossed with *Tpl2$^{-/-}$* mice to enhance deletion efficiency and resulted in littermate *Sftpc-CreER^{T2+}Tpl2$^{flox/-}$* and *Tpl2$^{flox/-}$* mice. *Tpl2$^{-/-}$*

mice were backcrossed to C57BL6/J more than ten generations and kindly provided by Dr. Philip Tsichlis and Thomas Jefferson University[264]. For the purposes of this study, only cre-negative *Tpl2*$^{flox/-}$ mice were used.

Mice were housed in specific pathogen-free conditions in microisolator cages in the Coverdell Rodent Vivarium within the University of Georgia (Athens, GA) according to the UGA Institutional Animal Care and Use Committee (IACUC)-approved guidelines for laboratory animals. Mice were maintained in accordance to the standards established by the *Guide for the Care and Use of Laboratory Animals*[315]. The central animal facility at the University of Georgia monitors all mouse cages daily and routinely tests for the presence of pathogenic infection in female sentinel cages. Throughout this study, sentinels consistently tested negative for various endoparasites, ectoparasites, and viral infections including mouse parvovirus, mouse hepatitis virus, Sendai virus, pneumonia virus of mice, *Mycoplasma pulmonis*, and lymphocytic choriomeningitis virus. Animals were confirmed *Helicobacter*-negative and used between six to nine weeks of age.

To prevent sex-biases, both male and female mice were used in all experiments. All experiments involving mice were performed according to the University of Georgia guidelines for laboratory animals and were approved by the UGA IACUC. Mouse-adapted influenza virus A/HK-x31 (H3N2) stocks were provided by Dr. Mark Tompkins (University of Georgia).

Tamoxifen administration

100 mg tamoxifen citrate (USP-Grade Spectrum Chemical, T1423) was dissolved in 5 ml of corn oil (Millipore Sigma, C8267) at a final concentration of 20 mg/mL and allowed to shake covered in foil overnight at 37°C. Mice were administered 75 mg/kg tamoxifen intraperitoneally for 5 days consecutively followed by a 9-day chase period. After the chase period, mice were infected with 10^4 PFU influenza A/x31 intranasally.

Pathology Scoring

Lungs from mice either uninfected and not tamoxifen-treated (UI/NT), uninfected and tamoxifen-treated, or infected with influenza A/x31 and tamoxifen-treated were harvested and fixed in 10% neutral-buffered formalin for 24 hr at room temperature. Formalin-fixed lungs were placed in cassettes, embedded in paraffin, sectioned at 4 μm, mounted onto glass slides, and stained with hematoxylin and eosin (H&E) stains. Histologic sections were evaluated in a blinded manner by a board-certified, veterinary pathologist (K.S.) at the University of Georgia (Athens, GA) and scored according to the following criteria: (A) Percent of lung affected, (B) Alveolar score, Alveolar edema score, Pleuritis score: 1 = focal, 2 = multifocal, 3 = multifocal to coalescing, 4 = most of lobule affected. (C) PMN score: 1 = neutrophils compose up to 25% of cells in alveoli, 2 = 25-49%, 3 = 50-75%, 4 = 75%+ (D) Perivascular cuffing (PVC) score: 1 = vessel cuffed by 1 cellular layer, 2 = 2-5 cells thick, 3 = 6-9 cells thick, 4 = 10+ cells thick. (E) Vasculitis score: 1 = infiltration of vessel wall by leukocytes, 2 = infiltration and separation of smooth muscle cells, 3 = infiltration and fibrinoid change. (F) Interstitial pneumonia (IP) score: 1 = alveolar septa infiltrated and thickened by 1 leukocyte layer, 2 = thickened by 2 leukocyte layers, 3 = 3 leukocyte layers, 4 = 4 leukocyte layers.

In vivo influenza infection

Age-matched, six- to nine-week-old mice were sedated with 2.5% Avertin and intranasally infected with 50 μl of influenza A/x31 (10^4 PFU) diluted in PBS. Body weights were recorded daily, and mice exhibiting severe signs of disease or more than 30% weight loss were euthanized.

Statistics

P values were derived by unpaired *t*-tests or two-way ANOVA with Dunnett's multiple comparisons test as indicated using PRISM software. Differences were considered statistically significant if $p \leq 0.05$. Data represent means ± SEM. Analyses were completed using PRISM software.

RESULTS

We initially generated *Sftpc-creER^{T2} Tpl2$^{fl/-}$* mice to study the role of Tpl2 specifically within type II alveolar epithelial cells in a murine model of influenza infection. However, it quickly became apparent that immune alterations occurred in cre-negative mice in response to intraperitoneal tamoxifen treatment. Specifically, uninfected cre-negative mice displayed grossly obvious white nodules dispersed across the lung (Fig. 13A). These nodules were immediately visible upon opening the chest cavity and resembled inducible bronchus-associated lymphoid tissue (iBALT), suggesting an ongoing immune response. Therefore, a controlled study was initiated in cre-negative mice to detail tamoxifen-dependent immunological changes to the lungs.

Five days of intraperitoneal tamoxifen-treatment, followed by a nine-day chase period, induced histologic evidence of inflammation within the alveoli, surrounding and within the vasculature, and within the pleura in uninfected mice (Fig. 13B). Uninfected, tamoxifen-treated mice display inflammation scores which trend higher than non-treated mice, specifically with regard to perivascular inflammation scores which resemble mice that were tamoxifen-treated and infected with influenza at the peak of infection (day 7) and after resolution (day 28) (Fig. 13B, 13E). As expected, influenza-infected mice displayed more widespread histopathologic effects and more alveolar edema than uninfected, tamoxifen-treated mice. (Fig. 13C, 13E). In influenza-infected mice, lung samples denoted significant changes within the alveoli, including type 2 pneumocyte hyperplasia, the presence of foamy macrophages, and cellular debris (Fig. 13E). The extent of neutrophil recruitment and interstitial pneumonia were significantly increased in the influenza-infected tamoxifen-treated mice (Fig. 13C). Despite the presence of trending signs of increased inflammation throughout their lungs, uninfected tamoxifen-treated mice displayed normal body weights comparable to uninfected, non-treated mice (Fig. 13D), and we were unable to discern any clinical signs induced by tamoxifen treatment. These data suggest that tamoxifen treatment alone induces an

inflammatory phenotype that trends higher in the lungs of uninfected mice and that in some respect, mimics the inflammatory phenotype of an antiviral response in the absence of clinical signs.

Characterization of the cellular infiltrate induced by tamoxifen treatment

We next characterized the cellular infiltrates in the lungs of the cre-negative, tamoxifen-treated mice. Forty percent of tamoxifen-treated mice showed cellular infiltration within the alveoli, lung vasculature, interstitium, and pleura (Fig. 14A). Sixty percent of tamoxifen-treated mice showed perivascular cuffing by leukocytes compared to non-treated mice (Fig. 14A). Between non-treated mice (UI/NT) and tamoxifen-treated mice, there was a significant increase in the cells present in the alveoli, perivascular cuff (PVC), and the interstitium (Fig. 14B).

The cellular populations recruited to the lungs included macrophages, plasma cells, eosinophils, neutrophils, and lymphocytes. These cells were seen in similar distribution in mice that were influenza-infected and remained present past the normal 14-day resolution period for influenza (Fig. 14B). Additionally, other abnormal histologic findings included epithelioid and foamy macrophages present in tamoxifen-treated mice. Collectively, these data suggest that tamoxifen treatment not only induces abnormal cellular recruitment in organs distal to the site of tamoxifen administration, but this happens independently of cre-recombinase and is therefore not an off-target effect driven by inappropriate recombination.

Discussion

This study shows that intraperitoneal tamoxifen administration induces significant alterations within the distal lung microenvironment in mice. Excessive recruitment of various hematopoietic cell types was noted throughout major regions of the lung even in the absence of cre-recombinase activity. Cellular infiltrates were varied and included: macrophages, plasma cells, eosinophils, neutrophils, and lymphocytes, suggesting global inflammation of the lung rather than targeted alteration of a single

pathway. Consistent with this, epithelioid macrophages were detected in the lungs of tamoxifen-treated mice (Fig. 14B). This was unexpected, given that they are typically associated with granuloma formation during bacterial infections such as tuberculosis[316] and *Brucella* spp. [317], fungal infections[318] or after inhalation of foreign materials [319]. The presence of inflammatory infiltrates like epithelioid macrophages in tamoxifen-treated mice suggests an abnormal microenvironment driven by chronic inflammation. In tamoxifen-treated mice infected with influenza, foamy macrophages were seen within the alveoli at 7 and 28 dpi, (Fig. 13C and Fig. 14B), and multinucleated giant cells were observed at 7 dpi with influenza. These etiologies more closely resemble tuberculosis rather than influenza infection[316,320]. Notably, neither foamy macrophages nor multinucleated giant cells are commonly observed during influenza infection, and their presence here may be a consequence of tamoxifen treatment [321].

Tamoxifen toxicity, as we have noted, has been observed anecdotally in a variety of organs. For example, dramatic changes occur within the gastric mucosa in response to tamoxifen administration via intraperitoneal injection or oral gavage[322,323]. This toxicity was found to be independent of mouse strain or sex and observed even in the absence of estrogen[322]. In some studies, this can likely be attributed to excess tamoxifen administration. However, long term alterations to spermatogenesis has been noted in mice given a single dose of either 250 μg or 1 mg tamoxifen [310].

There is no general consensus on the appropriate dosage or routes of administration for tamoxifen. In a meta-analysis that examined 50 studies from 1998 onward, remarkably, there were 85 different tamoxifen dosing regimens published [310]. Uniformity within the field would help to alleviate many of the confounding effects. This is challenging, because tamoxifen doses must be determined empirically for each cell type and tissue-specific cre-system to ensure appropriate deletion efficiency[309]. For our study, the tamoxifen dose of 75 mg/kg was chosen based upon recommendations from JAX where our cre-strain was purchased and upon consideration of several studies, which collectively gave a range for administration route, dosage, and injection timeline[324–326]. Notably, airway epithelial cells were previously

shown to undergo recombination using conditions approximating JAX recommendations [324]. However, the tamoxifen dose used in this study, which caused significant confounding effects within the lungs, only achieved 30% deletion efficiency of the floxed allele in *Sftpc-creER^{T2} Tpl2$^{fl/-}$* mice. Given the known immune modulating effects of tamoxifen[306], there may be no way to use tamoxifen without triggering off-target effects. Our analysis focused on lung immunopathology; however, it is likely that systemic alterations occur in response to tamoxifen administration, and that changes may be present in multiple major organ systems.

We reported the similarities in histological changes and cellular infiltrates between uninfected tamoxifen-treated mice and influenza-infected mice. It should be noted that all mice were separated by group and housed in individual microisolator cages with no chance of cross-infection between uninfected and infected mice. These data highlight the confounding effects of tamoxifen treatment that make it difficult to distinguish bona fide infection-driven phenotypes versus the lasting off-target effects of tamoxifen-treatment. Interestingly, mice that were infected with influenza and tamoxifen-treated show sustained levels of inflammation within the lung through 28 dpi, a time at which inflammation would normally be resolved. This again likely points to long-lasting changes in influenza-infected mice that result from prior tamoxifen treatment.

Despite routine usage in humans, tamoxifen effects within mice need to be examined further. In addition to inclusion of tamoxifen treatment alone "baseline" controls, a more comprehensive understanding of tamoxifen-induced side effects in mice will help to inform researchers who are considering the use of tamoxifen-inducible models. Overall, this study describes tamoxifen-induced histopathologic alterations of the lungs that may obscure research interpretations and highlights the need for the development of optimized mouse models for inducible cre-mediated deletion.

Acknowledgements

The authors thank the University of Georgia (UGA)'s Coverdell Rodent Vivarium for animal care; our laboratory animal veterinarian, Dr Stephen Harvey; the Athens Veterinary Diagnostic Laboratory; and the UGA Histology Laboratory. Research reported in this publication was supported by the National Institute of Allergy and Infectious Diseases of the National Institutes of Health under Award Number R21AI147003-01 to WTW. The content is solely the responsibility of the authors and does not necessarily represent the official views of the National Institutes of Health.

FIGURES

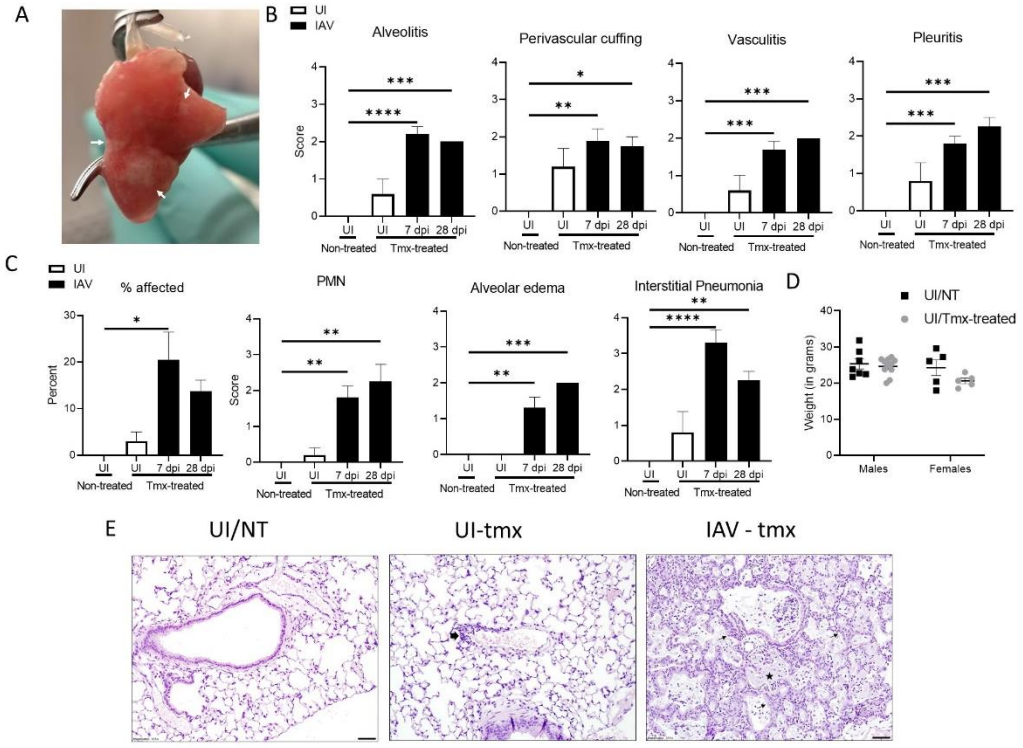

Figure 13. Tamoxifen-treatment alone shows increased histopathologic findings similar to influenza infection conditions. (A) Representative photograph of white nodules seen in tamoxifen-treated mouse lungs. White arrowheads denote white nodules. (B) Histology scoring of H&E-stained lungs performed by a board-certified, veterinary pathologist blinded to sample identity. UI/NT (N=5), UI (N=5), 7 dpi (N=10), 28 dpi (N=4). Scoring was based off the following criteria: Alveolar, Pleuritis, and Alveolar edema score; 1 = focal, 2 = multifocal, 3 = multifocal to coalescing, 4 = most of lobule affected. Perivascular cuffing (PVC) score; 1 = vessel cuffed by 1 cellular layer, 2 = 2-5 cells thick, 3 = 6-9 cells thick, 4 = 10+ cells thick. Vasculitis score; 1 = infiltration of vessel wall by leukocytes, 2 = infiltration and separation of smooth muscle cells 3 = infiltration and fibrinoid change. (C) Scoring based off the following criteria: Percent of lung affected; PMN score; 1 = neutrophils compose up to 25% of cells in alveoli, 2 = 25-49%, 3 = 50-75%, 4 = 75%+; Interstitial pneumonia (IP) score; 1 = alveolar septa infiltrated and thickened by 1 leukocyte layer, 2= thickened by 2 leukocyte layers, 3 = 3 leukocyte layers,

4 = 4 leukocyte layers. (D) Weights recorded from UI/NT males (N=7) and UI/NT females (N=5) or Tamoxifen-treated males (N=11) and Tamoxifen-treated females (N=5). (E) Representative images from UI and IAV (7dpi) infected lungs. Black arrow denotes mild perivascular cuffing. Star denotes alveoli filled with foamy macrophages, neutrophils, and cell debris. Black arrowhead denotes type 2 pneumocyte hyperplasia.

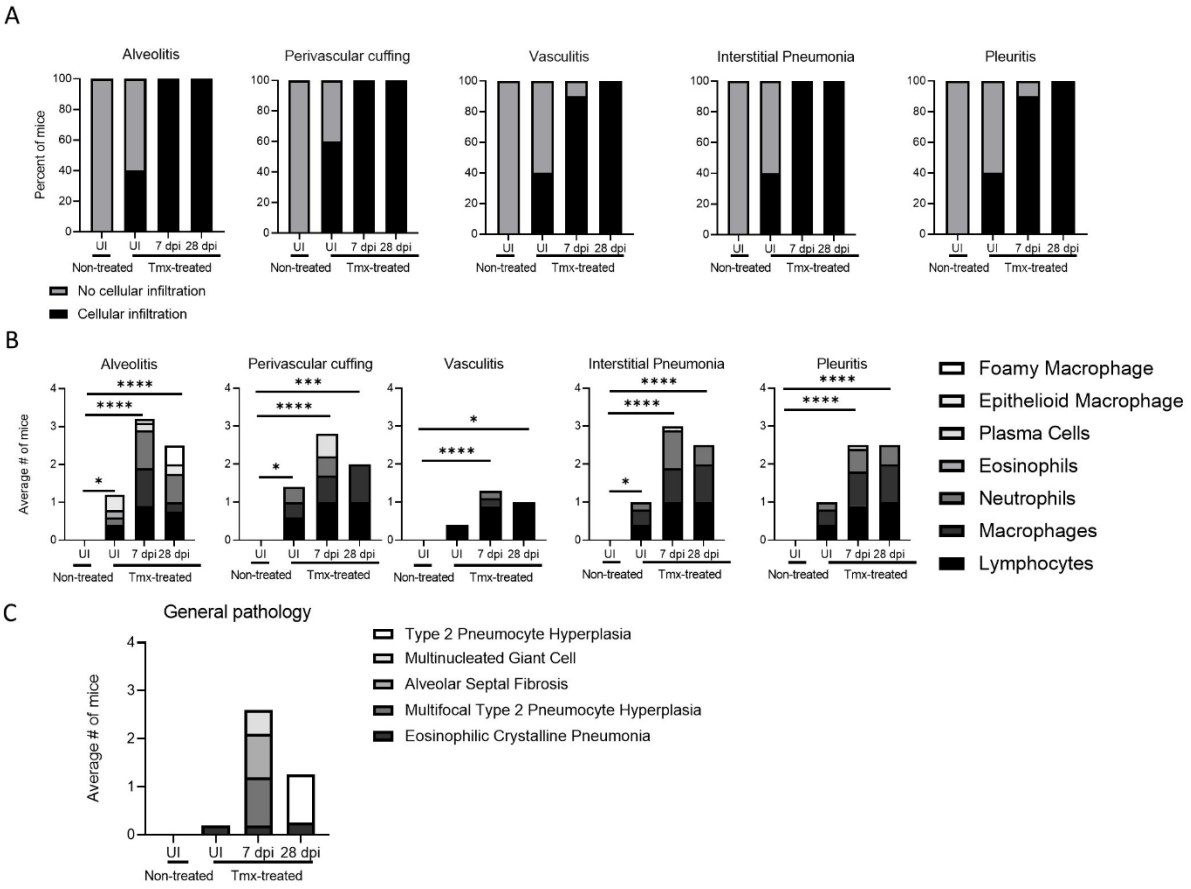

Figure 14. Tamoxifen-treatment alone induces aberrant cellular infiltration without recombination. (A) Percent of mice showing the presence or absence of cellular infiltration within the lung sections. Specifically, alveolitis, perivascular cuffing (PVC), vasculitis, interstitial pneumonia, and pleuritis. Cellular infiltration determined by H&E staining of lungs from Sftpc-cre^{ERT2} Tpl2$^{fl/-}$ mice characterized by the following groups: uninfected and non-tamoxifen treated (UI/NT), uninfected and treated (UI), infected with 104 PFU influenza A/x31 for 7 days post infection (dpi), and 28 dpi. Lungs sections were scored for cellular infiltration by a pathologist blinded to sample identity. (B) Leukocyte types within the cellular infiltrate were assessed by the pathologist for each lung sample. (C) Other histologic findings of H&E-stained lungs isolated from UI/NT mice, and influenza-infected 7dpi and 28 dpi tamoxifen-treated mice. Samples were analyzed for notable histopathologic features present by a pathologist blinded to sample identity. Graphs represent the average number of mice displaying each lesion. *p<0.05, **p<0.01, ***p<0.001, ****p<0.0001; two-way ANOVA, Dunnett's multiple comparisons test.

CHAPTER 4

CONCLUSIONS AND FUTURE DIRECTIONS

Our previous study showed that Tpl2 is crucial for viral clearance within the non-hematopoietic compartment during influenza infection[149], however the role of Tpl2 within respiratory epithelial cells during influenza infection and how Tpl2 is capable regulating the innate response within the epithelium is currently unknown. We sought to understand how Tpl2 regulates the interferon response during influenza infection. Based on our previous studies, we believed that Tpl2 was essential for viral control and host protection in the somatic cell compartment[149]. Herein, we show that Tpl2 acts as a negative regulator of type I and type III IFN production in lung epithelial cells *in vitro*. By utilizing a tissue-specific deletion of Tpl2, we were able to demonstrate that in lung non-hematopoietic cells Tpl2 limits early virus replication but that ultimately virus control occurred with kinetics similar to WT mice. Additionally, *in vivo* studies show that there is a modest increase in alveolar fibrosis within the mice with Tpl2-deficient lung epithelial cells (Fig. 15).

Pulmonary fibrosis is a consequence of aberrant fibrotic reparative responses to injury or insult within the lung epithelium. Type III IFNs, along with other cytokines (TNF-α, IL-6, MCP-1) have been associated with fibrotic responses and can potentially drive abnormal responses during viral infection Our data suggests that Tpl2-deficiency within immortalized lung epithelial cells drives significantly increased production of type III IFNs, suggesting that Tpl2 acts normally to constrain type I and type III IFNs, TNF-α, IL-6, IL-12, and MCP-1 production within this cell type. To determine Tpl2's effect on type III IFNs globally, utilization of recently available kits that distinguish IL-28A and IL-28B could help define contributions of individual IFN lambda subtypes and Tpl2 signaling. Additionally, expansion to human cell

lines would allow for broader application, but also necessitate a reliance on Tpl2 inhibitors in order to identify Tpl2-specific regulatory pathways.

Further studies are needed to fully elucidate the involvement of Tpl2 on acute lung injury-induced pulmonary fibrosis. It is possible that type III IFNs may play a role in the induction of pulmonary fibrosis, given the significant negative regulation shown when alveolar epithelial cells are directly stimulated without the presence of hematopoietic cells. Therefore, the role of type III IFNs could be assessed by blocking IFNLR1 signaling at the peak of cytokine induction (day 3) in *Nkx2.1cre*$^{+}$*Tpl2*$^{fl/-}$ mice to potentially reduce the occurrence of fibrosis within the alveoli. Additionally, lung function studies would allow us to determine whether blocking type III IFN signaling improves respiration and significantly decreases morbidity and mortality during influenza infection. Future studies are also needed to definitively pinpoint the cause of mortality in *Nkx2.1cre*$^{+}$*Tpl2*$^{fl/-}$ mice infected with influenza. Based on dyspnea observed late in the disease course at approximately 7 dpi, we hypothesize that decreased lung function, secondary to pulmonary fibrosis, is responsible for mortality. However, due to limitations in equipment to study lung function in small rodents, we were unable to confirm this in the present study.

Such studies will need to examine both lung mechanics and pulmonary gas exchange in *Nkx2.1cre*$^{+}$*Tpl2*$^{fl/-}$ mice and controls to pinpoint the nature of the impairment to lung function. Analysis of lung mechanics and function can utilize either invasive or non-invasive techniques within small rodents. Invasive lung mechanics analysis requires anesthetizing, providing a paralytic agent, followed by intubation and mechanical ventilation per mouse to gather accurate pulmonary mechanic parameters [327,328]. Obstructive lung dysfunction is characterized by decreased force expiratory volume, impaired gas exchange, and increased levels of carbon dioxide[329]. Restrictive lung dysfunction is characterized by reduced lung capacity, compliance, and volume[330]. Invasive pulmonary function studies, specifically the low frequency forced oscillation technique (LFOT), would allow for key differences between obstructive and restrictive pathologies to be determined. LFOT would provide the most detailed measurement of lung mechanics

(including pulmonary resistance in the conducting airways versus lung parenchyma and elasticity of the lung parenchyma); however, the technical requirements for the experiment make this method less feasible [327]. In addition to significant technical difficulty, the longitudinal studies that would be most beneficial for influenza-induced changes would be difficult to complete using this method.

Instead, whole-body plethysmography would allow for lung mechanics and overall function to be more easily determined. Whole-body plethysmography allows for mice to remain unanesthetized and unrestrained and analysis to be repeated on the same mouse over multiple time periods. Thus, allowing for a more consistent model for measuring infection-induced lung function changes over time[327]. This method can also distinguish between obstructive and restrictive lung disorders based on the measurement of key parameters including: functional residual capacity (FRC), residual volume (RV), total lung capacity (TLC), airway resistance (Raw) and specific airway resistance (sRaw)[331]. These parameters are associated with either being elevated (in obstructive airway diseases) or reduced (in restrictive lung disorders)[331]. In addition to separating the type of lung dysfunction into broad categories, whole-body plethysmography allows for the assessment of respiration rate. Measurements of the respiration rate include the length of time for inspiration and expiration which could be correlated with our current observed dyspnea[332].

Additionally, we would assess arterial blood gas levels within infected mice. Arterial blood is a standard parameter to measure impaired lung function in humans and frequently used to evaluate oxygenation during severe sepsis, respiratory failure, and ARDS[333]. However, due to lack of available equipment, we were unable to obtain these measurements. Arterial blood gas would provide the partial pressure of carbon dioxide within the blood which can be indicative of acute or chronic respiratory failure[333]. This data could potentially correlate changes in inspiration rate to the amount of carbon dioxide within the blood[333]. Additionally, lung function analysis studies could be correlated to the levels of type III IFNs over the course of infection and in mice given anti-IFNλ antibodies. These experiments would help determine if lung mechanics and functionality change with significantly reduced IFNλ during infection. Overall, these

parameters would allow us to analyze the extent of respiratory distress and progression of lung dysfunction over the course of infection.

To further explore the role of Tpl2-specific functions within epithelial cells, we utilized a Sftpc-cre^{ERT2} inducible model to specifically delete Tpl2 from solely type II alveolar epithelial cells. Unfortunately, this model proved not to be useful for epithelial-specific functions of Tpl2. However, early observations utilizing the tamoxifen-inducible cre-system led to an important observation about the off-target immunomodulatory effects of tamoxifen administration. We found that intraperitoneal tamoxifen administration induces significant alterations within the distal lung microenvironment in mice even in the absence of cre-recombinase activity. Cellular infiltrates within the lung included innate and adaptive cells that suggest a broad inflammatory response inducing significant immune cell recruitment. We observed a preponderance of literature across multiple fields that exposed a lack of uniformity due to the empirical nature of tamoxifen efficacy and dosage[309,310] . The wide range of effects have far-reaching implications for any study that employ this methodology. Despite attempts to avoid tamoxifen toxicity on an individual basis, there may be no way to use tamoxifen without triggering off-target effects. The vast alterations that tamoxifen administration can cause suggests that systemic alterations are likely to be present in multiple major organ systems. Despite routine usage in humans as a cancer treatment, tamoxifen effects in mice need to be examined further. Doxycycline-inducible mouse models represent an alternative to tamoxifen-inducible systems; however, doxycycline can affect the microbiome and disrupt mitochondrial metabolism [334]. Therefore, generation of alternative models for inducible deletion are crucial for the future of inducible mouse models due to their importance in understanding functionality of individual genes.

In conclusion, the findings reported here establish that Tpl2 negatively regulates type I and type III IFN production within lung epithelial cells (significantly in AECI and trending in AECII) during influenza infection. Additionally, our findings suggest that Tpl2 functionality within epithelial cells is associated

with pulmonary fibrosis (Fig. 11). Whether the combined trending increases in key fibrotic markers and in Tpl2 epithelial cell-ablated mice are responsible for increased fibrosis or whether Tpl2 ablation in epithelial cells promotes fibrosis via a distinct mechanism remains to be determined. The current findings contribute to a greater understanding of how innate immune responses, specifically interferons, are regulated during viral infections. These studies may reveal potential therapeutic pathways that may be beneficial for treating respiratory diseases.

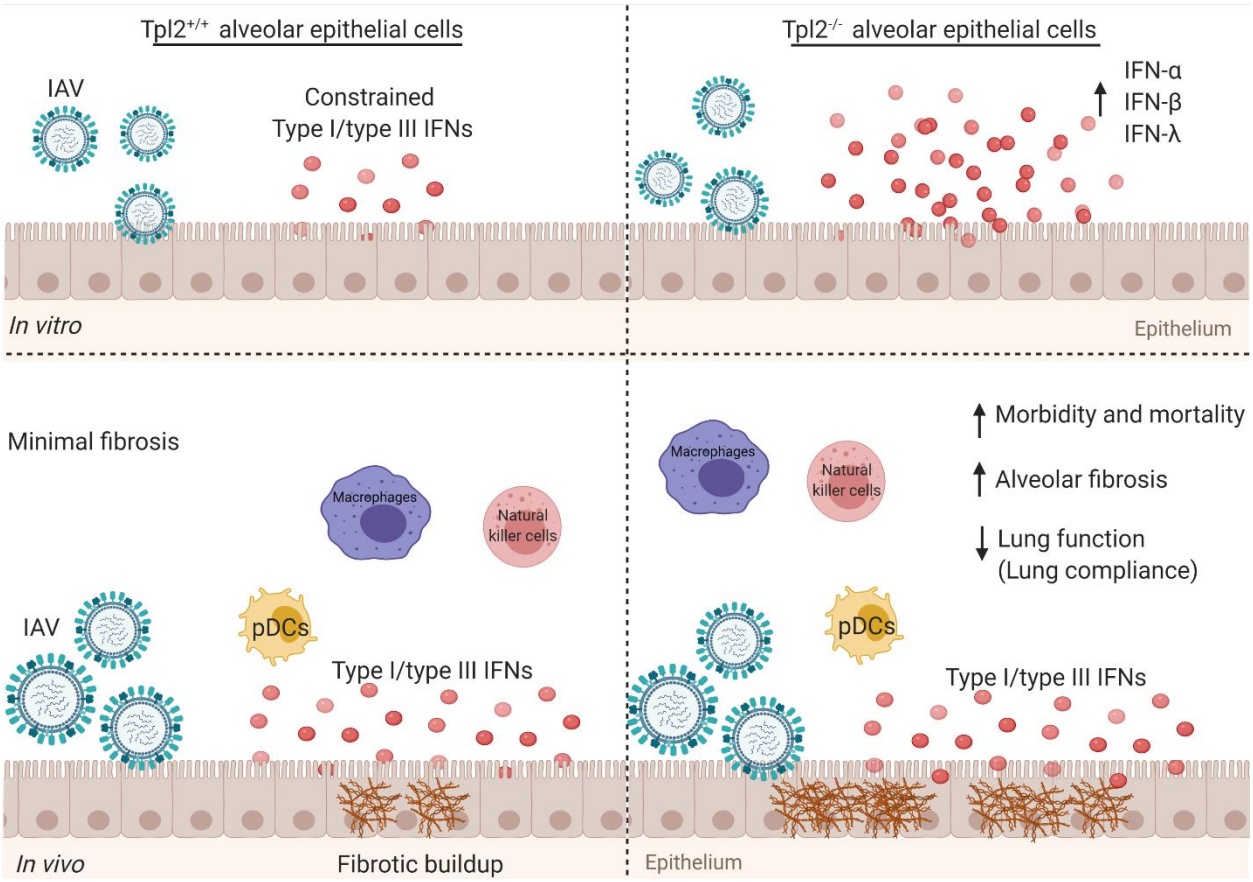

Figure 15. Tpl2 expressed within epithelial cells constrains interferons, pulmonary fibrosis, and morbidity during IAV. Image created with Biorender.com. *In vitro (top panels)*, when Tpl2 inhibition is localized to the alveolar epithelial cells, Tpl2 functions to constrain type I (IFN-α/IFN-β) and type III (IFNλ3) IFN production. *In vivo*, Tpl2 is present within hematopoietic cells that have known roles in interferon production and restriction of viral replication (such as plasmacytoid dendritic cells, macrophages, and natural killer cells). Tpl2's presence in major interferon producing cells may have overshadowed contributions by the epithelial cells. Despite no changes in type I or type III IFNs, mice with Tpl2-deficient alveolar epithelial cells display increased morbidity, mortality, and moderate alveolar fibrosis. Overall, we hypothesize that Tpl2 leads to increased fibrin deposition within the alveolar region, increased dyspnea, and subsequently decreased lung function.

REFERENCES

1. Thompson, W. W. *et al.* Influenza-Associated Hospitalizations in the United States. *JAMA* **292**, 1333 (2004).
2. Sooryanarain, H. & Elankumaran, S. Environmental Role in Influenza Virus Outbreaks. (2014). doi:10.1146/annurev-animal-022114-111017
3. Stegemann-Koniszewski, S. *et al.* Alveolar Type II Epithelial Cells Contribute to the Anti-Influenza A Virus Response in the Lung by Integrating Pathogen- and Microenvironment-Derived Signals. *MBio* **7**, e00276-16 (2016).
4. Cox, N. J. & Subbarao, K. GLOBAL EPIDEMIOLOGY OF INFLUENZA: Past and Present* VIROLOGY AND THE MUTABILITY OF INFLUENZA VIRUSES. *Annu. Rev. Med* **51**, 407–421 (2000).
5. Bouvier, N. M. & Palese, P. The biology of influenza viruses. *Vaccine* **26**, D49 (2008).
6. Goraya, M. U., Wang, S., Munir, M. & Chen, J. L. Induction of innate immunity and its perturbation by influenza viruses. *Protein Cell* **6**, 712–721 (2015).
7. Luo, M. Influenza Virus Entry. in *Advances in experimental medicine and biology* **726**, 201–221 (2012).
8. Harrison, S. C. Viral membrane fusion. *Nat. Struct. Mol. Biol.* **15**, 690–8 (2008).
9. Kielian, M. Mechanisms of Virus Membrane Fusion Proteins. *Annu. Rev. Virol.* **1**, 171–189 (2014).
10. Samji, T. Influenza A: Understanding the Viral Life Cycle. *YALE J. Biol. Med.* **82**, 153–159 (2009).
11. Hutchinson, E. C. & Fodor, E. Transport of the influenza virus genome from nucleus to nucleus. *Viruses* **5**, 2424–46 (2013).
12. Kreijtz, J. H. C. M., Fouchier, R. A. M. & Rimmelzwaan, G. F. Immune responses to influenza virus infection. *Virus Res.* **162**, 19–30 (2011).

13. Lee, M. S. & Kim, Y.-J. Signaling Pathways Downstream of Pattern-Recognition Receptors and Their Cross Talk. *Annu. Rev. Biochem.* **76**, 447–480 (2007).

14. Nan, Y., Nan, G. & Zhang, Y.-J. Interferon induction by RNA viruses and antagonism by viral pathogens. *Viruses* **6**, 4999–5027 (2014).

15. Kumar, V. Toll-like receptors in sepsis-associated cytokine storm and their endogenous negative regulators as future immunomodulatory targets. *International Immunopharmacology* **89**, 107087 (2020).

16. Alexopoulou, L., Holt, A. C., Medzhitov, R. & Flavell, R. A. Recognition of double-stranded RNA and activation of NF-|[kappa]|B by Toll-like receptor 3. *Nature* **413**, 732–738 (2001).

17. Diebold, S. S., Kaisho, T., Hemmi, H., Akira, S. & Reis e Sousa, C. Innate Antiviral Responses by Means of TLR7-Mediated Recognition of Single-Stranded RNA. *Science (80-.).* **303**, (2004).

18. Akira, S. *et al.* A Toll-like receptor recognizes bacterial DNA. *Nature* **408**, 740–745 (2000).

19. Bode, C., Zhao, G., Steinhagen, F., Kinjo, T. & Klinman, D. M. CpG DNA as a vaccine adjuvant. *Expert Rev. Vaccines* **10**, 499–511 (2011).

20. Schlee, M. Master sensors of pathogenic RNA – RIG-I like receptors. *Immunobiology* **218**, 1322–1335 (2013).

21. Perng, Y. C. & Lenschow, D. J. ISG15 in antiviral immunity and beyond. *Nat. Rev. Microbiol.* **16**, 423–439 (2018).

22. Pichlmair, A. *et al.* RIG-I-Mediated Antiviral Responses to Single-Stranded RNA Bearing 5'-Phosphates. *Science (80-.).* **314**, (2006).

23. Hornung, V. *et al.* 5'-Triphosphate RNA Is the Ligand for RIG-I. *Science (80-.).* **314**, (2006).

24. Kato, H. *et al.* Differential roles of MDA5 and RIG-I helicases in the recognition of RNA viruses. *Nature* **441**, 101–105 (2006).

25. Feng, Q. *et al. MDA5 Detects the Double-Stranded RNA Replicative Form in Picornavirus-Infected Cells*. *Cell Reports* **2**, (2012).

26. McCartney, S. A. *et al.* MDA-5 Recognition of a Murine Norovirus. *PLoS Pathog.* **4**, e1000108

(2008).

27. Cole, S. L. & Ho, L. P. Contribution of innate immune cells to pathogenesis of severe influenza virus infection. *Clin. Sci.* **131**, 269–283 (2017).

28. Camp, J. V. & Jonsson, C. B. A role for neutrophils in viral respiratory disease. *Frontiers in Immunology* **8**, 1 (2017).

29. Frank, K. & Paust, S. Dynamic Natural Killer Cell and T Cell Responses to Influenza Infection. *Frontiers in Cellular and Infection Microbiology* **10**, 425 (2020).

30. McGill, J., Heusel, J. W. & Legge, K. L. Innate immune control and regulation of influenza virus infections. *J. Leukoc. Biol.* **86**, 803–812 (2009).

31. Holt, P. G. *et al.* Downregulation of the antigen presenting cell function(s) of pulmonary dendritic cells in vivo by resident alveolar macrophages. *J. Exp. Med.* **177**, 397–407 (1993).

32. Bilyk, N. & Holt, P. G. Cytokine modulation of the immunosuppressive phenotype of pulmonary alveolar macrophage populations. *Immunology* **86**, 231–237 (1995).

33. Strickland, D. H., Thepen, T., Kees, U. R., Kraal, G. & Holt, P. G. Regulation of T-cell function in lung tissue by pulmonary alveolar macrophages. *Immunology* **80**, 266–272 (1993).

34. Colonna, M. *et al.* Plasmacytoid monocytes migrate to inflamed lymph nodes and produce large amounts of type I interferon. *Nat. Med.* **5**, 919–923 (1999).

35. Guillot, L. *et al.* Involvement of toll-like receptor 3 in the immune response of lung epithelial cells to double-stranded RNA and influenza A virus. *J. Biol. Chem.* **280**, 5571–80 (2005).

36. Goritzka, M. *et al.* Alpha/beta interferon receptor signaling amplifies early proinflammatory cytokine production in the lung during respiratory syncytial virus infection. *J. Virol.* **88**, 6128–36 (2014).

37. Swiecki, M. & Colonna, M. The multifaceted biology of plasmacytoid dendritic cells. *Nat. Rev. Immunol.* **15**, 471–85 (2015).

38. Kim, T. S. & Braciale, T. J. Respiratory dendritic cell subsets differ in their capacity to support the induction of virus-specific cytotoxic CD8+ T cell responses. *PLoS One* **4**, e4204 (2009).

39. Wieczorek, M. *et al.* Major Histocompatibility Complex (MHC) Class I and MHC Class II Proteins: Conformational Plasticity in Antigen Presentation. *Front. Immunol.* **8**, 292 (2017).

40. Chen, L. & Flies, D. B. Molecular mechanisms of T cell co-stimulation and co-inhibition. *Nat. Rev. Immunol.* **13**, 227–42 (2013).

41. Hunter, M. C., Teijeira, A. & Halin, C. T Cell Trafficking through Lymphatic Vessels. *Front. Immunol.* **7**, 613 (2016).

42. Swain, S. L., Kai McKinstry, K. & Strutt, T. M. Expanding roles for CD4+ T cells in immunity to viruses. *Nat. Rev. Immunol.* **12**, (2012).

43. Girdlestone, J. & Wing, M. Autocrine activation by interferon-γ of STAT factors following T cell activation. *Eur. J. Immunol.* **26**, 704–709 (1996).

44. Borrow, P. *et al.* CD40L-deficient mice show deficits in antiviral immunity and have an impaired memory CD8+ CTL response. *J. Exp. Med.* **183**, 2129–42 (1996).

45. Sangster, M. Y. *et al.* An early CD4+ T cell-dependent immunoglobulin A response to influenza infection in the absence of key cognate T-B interactions. *J. Exp. Med.* **198**, 1011–21 (2003).

46. Lee, B. O., Hartson, L. & Randall, T. D. CD40-deficient, influenza-specific CD8 memory T cells develop and function normally in a CD40-sufficient environment. *J. Exp. Med.* **198**, 1759–64 (2003).

47. Johnson, S. *et al.* Selected Toll-like receptor ligands and viruses promote helper-independent cytotoxic T cell priming by upregulating CD40L on dendritic cells. *Immunity* **30**, 218–27 (2009).

48. Bourgeois, C., Rocha, B. & Tanchot, C. A Role for CD40 Expression on CD8+ T Cells in the Generation of CD8+ T Cell Memory. *Science (80-.).* **297**, (2002).

49. Topham, D. J., Tripp, R. A. & Doherty, P. C. CD8+ T cells clear influenza virus by perforin or Fas-dependent processes. *J. Immunol.* **159**, 5197–200 (1997).

50. Ishikawa, E., Nakazawa, M., Yoshinari, M. & Minami, M. Role of Tumor Necrosis Factor-Related Apoptosis-Inducing Ligand in Immune Response to Influenza Virus Infection in Mice. *J. Virol.* **79**, 7658–7663 (2005).

51. Brincks, E. L., Katewa, A., Kucaba, T. A., Griffith, T. S. & Legge, K. L. CD8 T cells utilize TRAIL to control influenza virus infection. *J. Immunol.* **181**, 4918–25 (2008).

52. Duan, S. & Thomas, P. G. Balancing Immune Protection and Immune Pathology by CD8+ T-Cell Responses to Influenza Infection. *Front. Immunol.* **7**, (2016).

53. Taylor, P. M. & Askonas, B. A. Influenza nucleoprotein-specific cytotoxic T-cell clones are protective in vivo. *Immunology* **58**, 417–20 (1986).

54. Ramana, C. V *et al.* Inflammatory impact of IFN-γ in CD8+ T cell-mediated lung injury is mediated by both Stat1-dependent and -independent pathways. *Am. J. Physiol. Lung Cell. Mol. Physiol.* **308**, L650-7 (2015).

55. Liu, A. N. *et al.* Perforin-Independent CD8 $^{+}$ T-Cell–Mediated Cytotoxicity of Alveolar Epithelial Cells Is Preferentially Mediated by Tumor Necrosis Factor- α. *Am. J. Respir. Cell Mol. Biol.* **20**, 849–858 (1999).

56. Srikiatkhachorn, A. *et al.* Interference with intraepithelial TNF-α signaling inhibits CD8(+) T-cell-mediated lung injury in influenza infection. *Viral Immunol.* **23**, 639–45 (2010).

57. Knossow, M. & Skehel, J. J. Variation and infectivity neutralization in influenza. *Immunology* **119**, 1–7 (2006).

58. Johansson, B. E., Grajower, B. & Kilbourne, E. D. Infection-permissive immunization with influenza virus neuraminidase prevents weight loss in infected mice. *Vaccine* **11**, 1037–1039 (1993).

59. Kilbourne, E. D. *et al.* Protection of mice with recombinant influenza virus neuraminidase. *J. Infect. Dis.* **189**, 459–61 (2004).

60. Schulman, J. L., Khakpour, M. & Kilbourne, E. D. Protective effects of specific immunity to viral neuraminidase on influenza virus infection of mice. *J. Virol.* **2**, 778–86 (1968).

61. Hashimoto, G., Wright, P. F. & Karzon, D. T. Antibody-dependent cell-mediated cytotoxicity against influenza virus-infected cells. *J. Infect. Dis.* **148**, 785–94 (1983).

62. Noppert, S. J., Fitzgerald, K. A. & Hertzog, P. J. The role of type I interferons in TLR responses.

Immunol. Cell Biol. **85**, 446–457 (2007).

63. Kotenko, S. V. *et al.* IFN-λs mediate antiviral protection through a distinct class II cytokine receptor complex. *Nat. Immunol.* **4**, 69–77

64. Sheppard, P. *et al.* IL-28, IL-29 and their class II cytokine receptor IL-28R. *Nat. Immunol.* **4**, 63–68 (2003).

65. Egli, A. *et al.* IL-28B is a Key Regulator of B- and T-Cell Vaccine Responses against Influenza. *PLoS Pathog.* **10**, e1004556 (2014).

66. Pott, J. *et al.* IFN- determines the intestinal epithelial antiviral host defense. *Proc. Natl. Acad. Sci.* **108**, 7944–7949 (2011).

67. Lazear, H. M., Schoggins, J. W. & Diamond, M. S. Shared and Distinct Functions of Type I and Type III Interferons. *Immunity* **50**, 907–923 (2019).

68. Schneider, W. M., Chevillotte, M. D. & Rice, C. M. Interferon-stimulated genes: A complex web of host defenses. *Annu. Rev. Immunol.* **32**, 513–545 (2014).

69. McNab, F., Mayer-Barber, K., Sher, A., Wack, A. & O'Garra, A. *Type I interferons in infectious disease*. *Nature Reviews Immunology* **15**, 87–103 (Nature Publishing Group, 2015).

70. Platanias, L. C. Mechanisms of type-I- and type-II-interferon-mediated signalling. *Nat. Rev. Immunol.* **5**, 375–386 (2005).

71. Stifter, S. A. S. *et al.* Functional Interplay between Type I and II Interferons Is Essential to Limit Influenza A Virus-Induced Tissue Inflammation. *PLOS Pathog.* **12**, e1005378 (2016).

72. Sommereyns, C. *et al.* IFN-Lambda (IFN-λ) Is Expressed in a Tissue-Dependent Fashion and Primarily Acts on Epithelial Cells In Vivo. *PLoS Pathog.* **4**, e1000017 (2008).

73. Broggi, A., Tan, Y., Granucci, F. & Zanoni, I. IFN-λ suppresses intestinal inflammation by non-translational regulation of neutrophil function. *Nat. Immunol.* **18**, 1084–1093 (2017).

74. Galani, I. E. *et al.* Interferon-λ Mediates Non-redundant Front-Line Antiviral Protection against Influenza Virus Infection without Compromising Host Fitness. *Immunity* **46**, 875-890.e6 (2017).

75. Yin, Z. *et al.* Type III IFNs are produced by and stimulate human plasmacytoid dendritic cells. *J.*

Immunol. **189**, 2735–45 (2012).

76. Lazear, H. M., Nice, T. J. & Diamond, M. S. Interferon-λ: Immune Functions at Barrier Surfaces and Beyond. (2015). doi:10.1016/j.immuni.2015.07.001

77. Ye, L., Schnepf, D. & Staeheli, P. Interferon-λ orchestrates innate and adaptive mucosal immune responses. *Nature Reviews Immunology* **19**, 614–625 (2019).

78. Lenschow, D. J. *et al.* IFN-stimulated gene 15 functions as a critical antiviral molecule against influenza, herpes, and Sindbis viruses. *Proc. Natl. Acad. Sci. U. S. A.* **104**, 1371–1376 (2007).

79. Lu, G. *et al.* ISG15 enhances the innate antiviral response by inhibition of IRF-3 degradation. *Cell. Mol. Biol. (Noisy-le-grand).* **52**, 29–41 (2006).

80. Takeuchi, T., Kobayashi, T., Tamura, S. & Yokosawa, H. Negative regulation of protein phosphatase 2Cβ by ISG15 conjugation. *FEBS Lett.* **580**, 4521–4526 (2006).

81. Jefferies, C. A. *Regulating IRFs in IFN driven disease*. *Frontiers in Immunology* **10**, 325 (Frontiers Media S.A., 2019).

82. Marie, I. Differential viral induction of distinct interferon-alpha genes by positive feedback through interferon regulatory factor-7. *EMBO J.* **17**, 6660–6669 (1998).

83. Lazear, H. M. *et al.* Correction: IRF-3, IRF-5, and IRF-7 Coordinately Regulate the Type I IFN Response in Myeloid Dendritic Cells Downstream of MAVS Signaling. *PLoS Pathog.* **9**, 1003118 (2013).

84. Honda, K. *et al.* IRF-7 is the master regulator of type-I interferon-dependent immune responses. *Nature* **434**, 772–777 (2005).

85. Au, W. C., Moore, P. A., LaFleur, D. W., Tombal, B. & Pitha, P. M. Characterization of the interferon regulatory factor-7 and its potential role in the transcription activation of interferon A genes. *J. Biol. Chem.* **273**, 29210–29217 (1998).

86. Honda, K. & Taniguchi, T. IRFs: Master regulators of signalling by Toll-like receptors and cytosolic pattern-recognition receptors. *Nat. Rev. Immunol.* **6**, 644–658 (2006).

87. Ikushima, H., Negishi, H. & Taniguchi, T. The IRF family transcription factors at the interface of

innate and adaptive immune responses. *Cold Spring Harb. Symp. Quant. Biol.* **78**, 105–116 (2013).

88. Ning, S., Pagano, J. S. & Barber, G. N. IRF7: Activation, regulation, modification and function. *Genes and Immunity* **12**, 399–414 (2011).

89. Marié, I., Durbin, J. E. & Levy, D. E. *Differential viral induction of distinct interferon-α genes by positive feedback through interferon regulatory factor-7. The EMBO Journal* **17**, (1998).

90. Jewell, N. A. *et al.* Lambda Interferon Is the Predominant Interferon Induced by Influenza A Virus Infection In Vivo. *J. Virol.* **84**, 11515–11522 (2010).

91. Mordstein, M. *et al.* Interferon-λ Contributes to Innate Immunity of Mice against Influenza A Virus but Not against Hepatotropic Viruses. *PLoS Pathog.* **4**, e1000151 (2008).

92. Mordstein, M. *et al.* Lambda interferon renders epithelial cells of the respiratory and gastrointestinal tracts resistant to viral infections. *J. Virol.* **84**, 5670–7 (2010).

93. Wang, J. *et al.* Differentiated human alveolar type II cells secrete antiviral IL-29 (IFN-lambda 1) in response to influenza A infection. *J. Immunol.* **182**, 1296–304 (2009).

94. Guo, X. zhi J. & Thomas, P. G. New fronts emerge in the influenza cytokine storm. *Semin. Immunopathol.* **39**, 541–550 (2017).

95. Liu, Q., Zhou, Y. H. & Yang, Z. Q. The cytokine storm of severe influenza and development of immunomodulatory therapy. *Cellular and Molecular Immunology* **13**, 3–10 (2016).

96. Kalil, A. C. & Thomas, P. G. Influenza virus-related critical illness: Pathophysiology and epidemiology. *Critical Care* **23**, (2019).

97. Tisoncik, J. R. *et al.* Into the Eye of the Cytokine Storm. *Microbiol. Mol. Biol. Rev.* **76**, 16–32 (2012).

98. Hwang, I. *et al.* Activation Mechanisms of Natural Killer Cells during Influenza Virus Infection. *PLoS One* **7**, 51858 (2012).

99. Davidson, S., Crotta, S., McCabe, T. M. & Wack, A. Pathogenic potential of interferon αβ in acute influenza infection. *Nat. Commun.* **5**, (2014).

100. Herold, S. *et al.* Lung epithelial apoptosis in influenza virus pneumonia: The role of macrophage-expressed TNF-related apoptosis-inducing ligand. *J. Exp. Med.* **205**, 3065–3077 (2008).

101. Fujikura, D. *et al.* Type-I Interferon is Critical for FasL Expression on Lung Cells to Determine the Severity of Influenza. *PLoS One* **8**, 55321 (2013).

102. Du, M. *et al.* Casein Kinase II Controls TBK1/IRF3 Activation in IFN Response against Viral Infection. *J. Immunol.* **194**, 4477–4488 (2015).

103. Yoshimura, A., Ito, M., Chikuma, S., Akanuma, T. & Nakatsukasa, H. Negative regulation of cytokine signaling in immunity. *Cold Spring Harb. Perspect. Biol.* **10**, (2018).

104. Ivashkiv, L. B. & Donlin, L. T. Regulation of type I interferon responses. *Nat. Rev. Immunol.* **14**, 36–49 (2014).

105. Bilyk, N. & Holt, P. G. Inhibition of the immunosuppressive activity of resident pulmonary alveolar macrophages by granulocyte/macrophage colony-stimulating factor. *J. Exp. Med.* **177**, 1773–1777 (1993).

106. Snelgrove, R. J. *et al.* A critical function for CD200 in lung immune homeostasis and the severity of influenza infection. (2008). doi:10.1038/ni.1637

107. Yoo, J. K., Kim, T. S., Hufford, M. M. & Braciale, T. J. Viral infection of the lung: Host response and sequelae. *Journal of Allergy and Clinical Immunology* **132**, 1263–1276 (2013).

108. Gopal, R. *et al.* Peroxisome proliferator-activated receptor gamma (PPARγ) suppresses inflammation and bacterial clearance during influenza-bacterial super-infection. *Viruses* **11**, (2019).

109. Odegaard, J. I. *et al.* Macrophage-specific PPARγ controls alternative activation and improves insulin resistance. *Nature* **447**, 1116–1120 (2007).

110. Braciale, T. J., Sun, J. & Kim, T. S. Regulating the adaptive immune response to respiratory virus infection. *Nature Reviews Immunology* **12**, 295–305 (2012).

111. Schönrich, G. & Raftery, M. J. The PD-1/PD-L1 axis and virus infections: A delicate balance. *Frontiers in Cellular and Infection Microbiology* **9**, 207 (2019).

112. Takahashi, R. & Yoshimura, A. SOCS1 and regulation of regulatory T cells plasticity. *J. Immunol. Res.* **2014**, (2014).

113. Takahashi, R. *et al.* SOCS1 is essential for regulatory T cell functions by preventing loss of Foxp3 expression as well as IFN-γ and IL-17A production. *J. Exp. Med.* **208**, 2055–2067 (2011).

114. Rothstein, D. M. & Camirand, G. New insights into the mechanisms of Treg function. *Current Opinion in Organ Transplantation* **20**, 376–384 (2015).

115. Hale, B. G., Albrecht, R. A. & García-Sastre, A. Innate immune evasion strategies of influenza viruses. *Future Microbiology* **5**, 23–41 (2010).

116. Sadler, A. J. & Williams, B. R. G. Interferon-inducible antiviral effectors. *Nat. Rev. Immunol.* **8**, 559–68 (2008).

117. Nallagatla, S. R. *et al.* 5'-Triphosphate-Dependent Activation of PKR by RNAs with Short Stem-Loops. *Science (80-.).* **318**, 1455–1458 (2007).

118. Dey, M. *et al.* Mechanistic link between PKR dimerization, autophosphorylation, and eIF2alpha substrate recognition. *Cell* **122**, 901–13 (2005).

119. Guan, R. *et al.* Structural basis for the sequence-specific recognition of human ISG15 by the NS1 protein of influenza B virus. *Proc. Natl. Acad. Sci. U. S. A.* **108**, 13468–13473 (2011).

120. Wang, S. *et al.* Influenza A Virus-Induced Degradation of Eukaryotic Translation Initiation Factor 4B Contributes to Viral Replication by Suppressing IFITM3 Protein Expression. *J. Virol.* **88**, 8375–8385 (2014).

121. Dias, A. *et al.* The cap-snatching endonuclease of influenza virus polymerase resides in the PA subunit. *Nature* **458**, 914–918 (2009).

122. Carr, S. M., Carnero, E., García-Sastre, A., Brownlee, G. G. & Fodor, E. Characterization of a mitochondrial-targeting signal in the PB2 protein of influenza viruses. *Virology* **344**, 492–508 (2006).

123. Graef, K. M. *et al.* The PB2 Subunit of the Influenza Virus RNA Polymerase Affects Virulence by Interacting with the Mitochondrial Antiviral Signaling Protein and Inhibiting Expression of Beta

Interferon. *J. Virol.* **84**, 8433–8445 (2010).

124. Varga, Z. T. *et al.* The influenza virus protein PB1-F2 inhibits the induction of type i interferon at the level of the MAVS adaptor protein. *PLoS Pathog.* **7**, 1002067 (2011).

125. Krammer, F. *et al.* Influenza. *Nature Reviews Disease Primers* **4**, 1–21 (2018).

126. Gantke, T., Sriskantharajah, S. & Ley, S. C. Regulation and function of TPL-2, an IκB kinase-regulated MAP kinase kinase kinase. *Cell Res.* **21**, 131–45 (2011).

127. Patriotis, C., Makris, A., Bear, S. E. & Tsichlis, P. N. Tumor progression locus 2 (Tpl-2) encodes a protein kinase involved in the progression of rodent T-cell lymphomas and in T-cell activation. *Biochemistry* **90**, 2251–2255 (1993).

128. Ceci, J. D. *et al.* Tpl-2 is an oncogenic kinase that is activated by carboxy-terminal truncation. *Genes Dev.* **11**, 688–700 (1997).

129. Gándara, M. L., López, P., Hernando, R., Castaño, J. G. & Alemany, S. The COOH-terminal domain of wild-type Cot regulates its stability and kinase specific activity. *Mol. Cell. Biol.* **23**, 7377–90 (2003).

130. Tsatsanis, C. *et al.* Tpl2 and ERK transduce antiproliferative T cell receptor signals and inhibit transformation of chronically stimulated T cells. *Proc. Natl. Acad. Sci.* **105**, 2987–2992 (2008).

131. Aoki, M. *et al.* The human cot proto-oncogene encodes two protein serine/threonine kinases with different transforming activities by alternative initiation of translation. *J. Biol. Chem.* **268**, 22723–32 (1993).

132. Banerjee, A., Gugasyan, R., McMahon, M. & Gerondakis, S. Diverse Toll-like receptors utilize Tpl2 to activate extracellular signal-regulated kinase (ERK) in hemopoietic cells. *Proc. Natl. Acad. Sci. U. S. A.* **103**, 3274–9 (2006).

133. Dumitru, C. D. *et al.* TNF-alpha induction by LPS is regulated posttranscriptionally via a Tpl2/ERK-dependent pathway. *Cell* **103**, 1071–83 (2000).

134. Mielke, L. A. *et al.* Tumor Progression Locus 2 (Map3k8) Is Critical for Host Defense against Listeria monocytogenes and IL-1 Production. *J. Immunol.* **183**, 7984–7993 (2009).

135. Watford, W. T. *et al.* Tpl2 kinase regulates T cell interferon-γ production and host resistance to *Toxoplasma gondii*. *J. Exp. Med.* **205**, 2803–2812 (2008).

136. Hatziapostolou, M., Polytarchou, C., Panutsopulos, D., Covic, L. & Tsichlis, P. N. Proteinase-Activated Receptor-1-Triggered Activation of Tumor Progression Locus-2 Promotes Actin Cytoskeleton Reorganization and Cell Migration. *Cancer Res.* **68**, 1851–1861 (2008).

137. Das, S. *et al.* Tpl2/Cot Signals Activate ERK, JNK, and NF-κB in a Cell-type and Stimulus-specific Manner. *J. Biol. Chem.* **280**, 23748–23757 (2005).

138. Eliopoulos, A. G., Wang, C.-C., Dumitru, C. D. & Tsichlis, P. N. Tpl2 transduces CD40 and TNF signals that activate ERK and regulates IgE induction by CD40. *EMBO J.* **22**, 3855–64 (2003).

139. Kyrmizi, I. *et al.* Tpl2 kinase regulates FcγR signaling and immune thrombocytopenia in mice. *J. Leukoc. Biol.* **94**, 751–7 (2013).

140. Lang, V. *et al.* ABIN-2 forms a ternary complex with TPL-2 and NF-kappa B1 p105 and is essential for TPL-2 protein stability. *Mol. Cell. Biol.* **24**, 5235–48 (2004).

141. Luciano, B. S., Hsu, S., Channavajhala, P. L., Lin, L.-L. & Cuozzo, J. W. Phosphorylation of Threonine 290 in the Activation Loop of Tpl2/Cot Is Necessary but Not Sufficient for Kinase Activity. *J. Biol. Chem.* **279**, 52117–52123 (2004).

142. Cho, J. & Tsichlis, P. N. Phosphorylation at Thr-290 regulates Tpl2 binding to NF-kappaB1/p105 and Tpl2 activation and degradation by lipopolysaccharide. *Proc. Natl. Acad. Sci. U. S. A.* **102**, 2350–5 (2005).

143. Roget, K. *et al.* IκB kinase 2 regulates TPL-2 activation of extracellular signal-regulated kinases 1 and 2 by direct phosphorylation of TPL-2 serine 400. *Mol. Cell. Biol.* **32**, 4684–90 (2012).

144. Kane, L. P., Mollenauer, M. N., Xu, Z., Turck, C. W. & Weiss, A. Akt-dependent phosphorylation specifically regulates Cot induction of NF-kappa B-dependent transcription. *Mol. Cell. Biol.* **22**, 5962–74 (2002).

145. Rousseau, S. *et al.* TPL2-mediated activation of ERK1 and ERK2 regulates the processing of pre-TNFα in LPS-stimulated macrophages. *J. Cell Sci.* **121**, (2008).

146. Kaiser, F. *et al.* TPL-2 negatively regulates interferon-β production in macrophages and myeloid dendritic cells. *J. Exp. Med.* **206**, 1863–1871 (2009).

147. Senger, K. *et al.* The kinase TPL2 activates ERK and p38 signaling to promote neutrophilic inflammation. *Sci. Signal.* **10**, (2017).

148. Li, X. *et al.* Tumor progression locus 2 (Tpl2) activates the mammalian Target of Rapamycin (mTOR) pathway, inhibits Forkhead Box P3 (FoxP3) expression, and limits regulatory T cell (Treg) immunosuppressive functions. *J. Biol. Chem.* **291**, (2016).

149. Kuriakose, T. *et al.* Tumor Progression Locus 2 Promotes Induction of IFNλ, Interferon Stimulated Genes and Antigen-Specific CD8+ T Cell Responses and Protects against Influenza Virus. *PLOS Pathog.* **11**, e1005038 (2015).

150. McNab, F. W. *et al.* TPL-2-ERK1/2 Signaling Promotes Host Resistance against Intracellular Bacterial Infection by Negative Regulation of Type I IFN Production. *J. Immunol.* **191**, 1732–1743 (2013).

151. Xiao, N. *et al.* The Tpl2 Mutation Sluggish Impairs Type I IFN Production and Increases Susceptibility to Group B Streptococcal Disease . *J. Immunol.* **183**, 7975–7983 (2009).

152. Hirata, K. *et al.* Inhibition of Tumor Progression Locus 2 Protein Kinase Decreases Lipopolysaccharide-Induced Tumor Necrosis Factor α Production Due to the Inhibition of the Tip-Associated Protein Induction in RAW264.7 Cells. *Biol. Pharm. Bull.* **33**, 1233–1237 (2010).

153. Schmid, S., Mordstein, M., Kochs, G., García-Sastre, A. & tenOever, B. R. Transcription Factor Redundancy Ensures Induction of the Antiviral State. *J. Biol. Chem.* **285**, 42013–42022 (2010).

154. Schmid, S., Sachs, D. & tenOever, B. R. Mitogen-activated protein kinase-mediated licensing of interferon regulatory factor 3/7 reinforces the cell response to virus. *J. Biol. Chem.* **289**, 299–311 (2014).

155. Xiao, Y. *et al.* TPL2 mediates autoimmune inflammation through activation of the TAK1 axis of IL-17 signaling. *J. Exp. Med.* **211**, 1689–1702 (2014).

156. Martel, G., Bérubé, J. & Rousseau, S. The Protein Kinase TPL2 Is Essential for ERK1/ERK2

Activation and Cytokine Gene Expression in Airway Epithelial Cells Exposed to Pathogen-Associated Molecular Patterns (PAMPs). *PLoS One* **8**, e59116 (2013).

157. Cox, R. J., Brokstad, K. A. & Ogra, P. Influenza Virus: Immunity and Vaccination Strategies. Comparison of the Immune Response to Inactivated and Live, Attenuated Influenza Vaccines. *Scand. J. Immunol.* **59**, 1–15 (2004).

158. Sato, S. & Kiyono, H. The mucosal immune system of the respiratory tract. *Curr. Opin. Virol.* **2**, 225–232 (2012).

159. Schenck, L. P., Surette, M. G. & Bowdish, D. M. E. Composition and immunological significance of the upper respiratory tract microbiota. *FEBS Lett.* **590**, 3705–3720 (2016).

160. Diamond, G., Legarda, D. & Ryan, L. K. The innate immune response of the respiratory epithelium. *Immunol. Rev.* **173**, 27–38 (2000).

161. Sahin-Yilmaz, A. & Naclerio, R. M. Anatomy and Physiology of the Upper Airway. doi:10.1513/pats.201007-050RN

162. Whitsett, J. A. & Alenghat, T. *Respiratory epithelial cells orchestrate pulmonary innate immunity*. **16**, 27–35 (Nature Publishing Group, 2015).

163. May, A. & Tucker, A. Understanding the development of the respiratory glands. *Dev. Dyn.* **244**, 525–539 (2015).

164. Basil, M. C. *et al.* The Cellular and Physiological Basis for Lung Repair and Regeneration: Past, Present, and Future. *Cell Stem Cell* **26**, 482–502 (2020).

165. Tata, A. *et al.* Myoepithelial Cells of Submucosal Glands Can Function as Reserve Stem Cells to Regenerate Airways after Injury. *Cell Stem Cell* **22**, 668-683.e6 (2018).

166. Whitsett, J. A., Kalin, T. V., Xu, Y. & Kalinichenko, V. V. Building and regenerating the lung cell by cell. *Physiol. Rev.* **99**, 513–554 (2019).

167. Siebel, C. & Lendahl, U. Notch signaling in development, tissue homeostasis, and disease. *Physiol. Rev.* **97**, 1235–1294 (2017).

168. Rokicki, W., Rokicki, M., Wojtacha, J. & Dżeljijli, A. The role and importance of club cells (Clara

cells) in the pathogenesis of some respiratory diseases. *Kardiochirurgia i torakochirurgia Pol. = Polish J. cardio-thoracic Surg.* **13**, 26–30 (2016).

169. Wang, S.-Z., Rosenberger, C. L., Bao, Y.-X., Stark, J. M. & Harrod, K. S. Clara Cell Secretory Protein Modulates Lung Inflammatory and Immune Responses to Respiratory Syncytial Virus Infection. *J. Immunol.* **171**, (2014).

170. Rajavelu, P. *et al.* Airway epithelial SPDEF integrates goblet cell differentiation and pulmonary Th2 inflammation. *J. Clin. Invest.* **125**, 2021–2031 (2015).

171. Whitsett, J. A. Airway epithelial differentiation and mucociliary clearance. in *Annals of the American Thoracic Society* **15**, S143–S148 (American Thoracic Society, 2018).

172. Kuo, C. S. & Krasnow, M. A. Formation of a Neurosensory Organ by Epithelial Cell Slithering. *Cell* **163**, 394–405 (2015).

173. Branchfield, K. *et al.* Pulmonary neuroendocrine cells function as airway sensors to control lung immune response. *Science (80-.).* **351**, 707–710 (2016).

174. Liu, Q. *et al.* Lung regeneration by multipotent stem cells residing at the bronchioalveolar-duct junction. *Nat. Genet.* **51**, 728–738 (2019).

175. Giangreco, A., Reynolds, S. D. & Stripp, B. R. Terminal bronchioles harbor a unique airway stem cell population that localizes to the bronchoalveolar duct junction. *Am. J. Pathol.* **161**, 173–182 (2002).

176. Bender Kim, C. F. *et al.* Identification of bronchioalveolar stem cells in normal lung and lung cancer. *Cell* **121**, 823–835 (2005).

177. Crapo, J. D., Barry, B. E., Gehr, P., Bachofen, M. & Weibel, E. R. Cell number and cell characteristics of the normal human lung. *Am. Rev. Respir. Dis.* **126**, 332–7 (1982).

178. Rozycki, H. J. Potential contribution of type I alveolar epithelial cells to chronic neonatal lung disease. *Front. Pediatr.* **2**, 45 (2014).

179. Kasper, M. & Barth, K. Potential contribution of alveolar epithelial type i cells to pulmonary fibrosis. *Bioscience Reports* **37**, 20171301 (2017).

180. Williams, M. C. ALVEOLAR TYPE I CELLS: Molecular Phenotype and Development. *Annu. Rev. Physiol* **65**, 669–95 (2003).

181. Rosenberger, C. M. *et al.* Characterization of innate responses to influenza virus infection in a novel lung type I epithelial cell model. *J. Gen. Virol.* **95**, 350–362 (2014).

182. Wong, M. M. H. *et al.* Differential Response of Primary Alveolar Type I and Type II Cells to LPS Stimulation. *PLoS One* **8**, e55545 (2013).

183. Mason, R. J. Biology of alveolar type II cells. *Respirology* **11**, 12–15 (2006).

184. Voorhout, W. F. *et al.* Immunocytochemical localization of surfactant protein D (SP-D) in type II cells, Clara cells, and alveolar macrophages of rat lung. *J. Histochem. Cytochem.* **40**, 1589–97 (1992).

185. Kalina, M., Mason, R. J. & Shannon, J. M. Surfactant Protein C Is Expressed in Alveolar Type II Cells but Not in Clara Cells of Rat Lung. *Am. J. Respir. Cell Mol. Biol.* **6**, 594–600 (1992).

186. Yokohira, M. *et al.* Characteristics of surfactant proteins in tumorigenic and inflammatory lung lesions in rodents. *Journal of Toxicologic Pathology* **31**, 231–240 (2018).

187. Kurath-Koller, S., Resch, B., Kraschl, R., Windpassinger, C. & Eber, E. Surfactant Protein B Deficiency Caused by Homozygous C248X Mutation-A Case Report and Review of the Literature. *AJP Rep.* **5**, e53-9 (2015).

188. Melton, K. R. *et al.* SP-B deficiency causes respiratory failure in adult mice. *Am. J. Physiol. - Lung Cell. Mol. Physiol.* **285**, L543–L549 (2003).

189. Clark, J. C. *et al.* Targeted disruption of the surfactant protein B gene disrupts surfactant homeostasis, causing respiratory failure in newborn mice. *Proc. Natl. Acad. Sci. U. S. A.* **92**, 7794–8 (1995).

190. Glasser, S. W. *et al.* Persistence of LPS-Induced Lung Inflammation in Surfactant Protein-C–Deficient Mice. *Am. J. Respir. Cell Mol. Biol.* **49**, 845–854 (2013).

191. Augusto, L., Le Blay, K., Auger, G., Blanot, D. & Chaby, R. Interaction of bacterial lipopolysaccharide with mouse surfactant protein C inserted into lipid vesicles. *Am. J. Physiol.*

Lung Cell. Mol. Physiol. **281**, L776-85 (2001).

192. Glasser, S. W. *et al.* Macrophage dysfunction and susceptibility to pulmonary Pseudomonas aeruginosa infection in surfactant protein C-deficient mice. *J. Immunol.* **181**, 621–8 (2008).

193. Glasser, S. W. *et al.* Surfactant protein C-deficient mice are susceptible to respiratory syncytial virus infection. *AJP Lung Cell. Mol. Physiol.* **297**, L64–L72 (2009).

194. Rubio, S. *et al.* Pulmonary surfactant protein A (SP-A) is expressed by epithelial cells of small and large intestine. *J. Biol. Chem.* **270**, 12162–9 (1995).

195. Haagsman, H. P. *et al.* The major lung surfactant protein, SP 28-36, is a calcium-dependent, carbohydrate-binding protein. *J. Biol. Chem.* **262**, 13877–80 (1987).

196. Wright, J. R. Immunoregulatory functions of surfactant proteins. *Nat. Rev. Immunol.* **5**, 58–68 (2005).

197. Sato, M. *et al.* Direct binding of Toll-like receptor 2 to zymosan, and zymosan-induced NF-kappa B activation and TNF-alpha secretion are down-regulated by lung collectin surfactant protein A. *J. Immunol.* **171**, 417–25 (2003).

198. Wu, H. *et al.* Surfactant proteins A and D inhibit the growth of Gram-negative bacteria by increasing membrane permeability. *J. Clin. Invest.* **111**, 1589–1602 (2003).

199. LeVine, A. M. *et al.* Surfactant Protein-A Binds Group B Streptococcus Enhancing Phagocytosis and Clearance from Lungs of Surfactant Protein-A–Deficient Mice. *Am. J. Respir. Cell Mol. Biol.* **20**, 279–286 (1999).

200. Watford, W. T., Ghio, A. J. & Wright, J. R. Complement-mediated host defense in the lung. *Am. J. Physiol. - Lung Cell. Mol. Physiol.* **279**, (2000).

201. Watford, W. T., Wright, J. R., Hester, C. G., Jiang, H. & Frank, M. M. Surfactant Protein A Regulates Complement Activation. *J. Immunol.* **167**, 6593–6600 (2001).

202. van Iwaarden, F., Welmers, B., Verhoef, J., Haagsman, H. P. & van Golde, L. M. G. Pulmonary Surfactant Protein A Enhances the Host-defense Mechanism of Rat Alveolar Macrophages. *Am. J. Respir. Cell Mol. Biol.* **2**, 91–98 (1990).

203. Tenner, A. J., Robinson, S. L., Borchelt, J. & Wright, J. R. Human pulmonary surfactant protein (SP-A), a protein structurally homologous to C1q, can enhance FcR- and CR1-mediated phagocytosis. *J. Biol. Chem.* **264**, 13923–8 (1989).

204. Kabha, K. *et al.* SP-A enhances phagocytosis of Klebsiella by interaction with capsular polysaccharides and alveolar macrophages.

205. Watford, W. T., Smithers, M. B., Frank, M. M. & Wright, J. R. Surfactant protein A enhances the phagocytosis of C1q-coated particles by alveolar macrophages. *Am. J. Physiol. - Lung Cell. Mol. Physiol.* **283**, (2002).

206. Schagat, T. L., Wofford, J. A. & Wright, J. R. Neutrophils Macrophage Phagocytosis of Apoptotic Surfactant Protein A Enhances Alveolar Surfactant Protein A Enhances Alveolar Macrophage Phagocytosis of Apoptotic Neutrophils. *J Immunol Ref.* **166**, 2727–2733 (2001).

207. Rosseau, S. *et al.* Surfactant protein A down-regulates proinflammatory cytokine production evoked by Candida albicans in human alveolar macrophages and monocytes. *J. Immunol.* **163**, 4495–502 (1999).

208. Reidy, M. F. & Wright, J. R. Surfactant protein A enhances apoptotic cell uptake and TGF-β1 release by inflammatory alveolar macrophages. *Am. J. Physiol. - Lung Cell. Mol. Physiol.* **285**, (2003).

209. Stamme, C., Walsh, E. & Wright, J. R. Surfactant Protein A Differentially Regulates IFN- -and LPS-Induced Nitrite Production by Rat Alveolar Macrophages. *Am. J. Respir. Cell Mol. Biol* **23**, 772–779 (2000).

210. Benne, C. A. *et al.* Interactions of surfactant protein A with influenza A viruses: binding and neutralization. *J. Infect. Dis.* **171**, 335–41 (1995).

211. Hartshorn, K. L. *et al.* Mechanisms of anti-influenza activity of surfactant proteins A and D: comparison with serum collectins. *Am. J. Physiol.* **273**, L1156-66 (1997).

212. Levine, A. M., Whitsett, J. A., Hartshorn, K. L., Crouch, E. C. & Korfhagen, T. R. Surfactant Protein D Enhances Clearance of Influenza A Virus from the Lung In Vivo. *J Immunol* **167**, 5868–

5873 (2001).

213. Armstrong, L. *et al.* Expression of functional toll-like receptor-2 and -4 on alveolar epithelial cells. *Am. J. Respir. Cell Mol. Biol.* **31**, 241–245 (2004).

214. Monick, M. M. *et al.* Respiratory Syncytial Virus Up-regulates TLR4 and Sensitizes Airway Epithelial Cells to Endotoxin. *J. Biol. Chem.* **278**, 53035–53044 (2003).

215. Glasser, S. W. *et al.* Genetic replacement of surfactant protein-C reduces respiratory syncytial virus induced lung injury. *Respir. Res.* **14**, 19 (2013).

216. Dahlin, K. *et al.* Identification of genes differentially expressed in rat alveolar type I cells. *Am. J. Respir. Cell Mol. Biol.* **31**, 309–316 (2004).

217. Uehara, A., Fujimoto, Y., Fukase, K. & Takada, H. Various human epithelial cells express functional Toll-like receptors, NOD1 and NOD2 to produce anti-microbial peptides, but not proinflammatory cytokines. *Mol. Immunol.* **44**, 3100–3111 (2007).

218. Cleaver, J. O. *et al.* Lung epithelial cells are essential effectors of inducible resistance to pneumonia. *Mucosal Immunol.* **7**, 78–88 (2014).

219. Van Maele, L. *et al.* Airway structural cells regulate TLR5-mediated mucosal adjuvant activity. *Mucosal Immunol.* **7**, 489–500 (2014).

220. Hammad, H. *et al.* House dust mite allergen induces asthma via Toll-like receptor 4 triggering of airway structural cells. *Nat. Med.* **15**, 410–416 (2009).

221. Sha, Q., Truong-Tran, A. Q., Plitt, J. R., Beck, L. A. & Schleimer, R. P. Activation of Airway Epithelial Cells by Toll-Like Receptor Agonists. *Am. J. Respir. Cell Mol. Biol.* **31**, 358–364 (2004).

222. Liu, P. *et al.* Retinoic acid-inducible gene I mediates early antiviral response and Toll-like receptor 3 expression in respiratory syncytial virus-infected airway epithelial cells. *J. Virol.* **81**, 1401–11 (2007).

223. Ioannidis, I., Ye, F., McNally, B., Willette, M. & Flaño, E. Toll-like receptor expression and induction of type I and type III interferons in primary airway epithelial cells. *J. Virol.* **87**, 3261–70

(2013).

224. Khaitov, M. R. *et al.* Respiratory virus induction of alpha-, beta- and lambda-interferons in bronchial epithelial cells and peripheral blood mononuclear cells. *Allergy Eur. J. Allergy Clin. Immunol.* **64**, 375–386 (2009).

225. Chioma, O. S. & Drake, W. P. Focus: Infectious Diseases: Role of Microbial Agents in Pulmonary Fibrosis. *Yale J. Biol. Med.* **90**, 219 (2017).

226. Nalysnyk, L., Cid-Ruzafa, J., Rotella, P. & Esser, D. Incidence and prevalence of idiopathic pulmonary fibrosis: Review of the literature. *European Respiratory Review* **21**, 355–361 (2012).

227. Wynn, T. A. & Ramalingam, T. R. Mechanisms of fibrosis: Therapeutic translation for fibrotic disease. *Nature Medicine* **18**, 1028–1040 (2012).

228. Kim, K. K. *et al.* Efferocytosis of apoptotic alveolar epithelial cells is sufficient to initiate lung fibrosis. *Cell Death Dis.* **9**, 1–12 (2018).

229. van den Brand, J. M. A., Haagmans, B. L., van Riel, D., Osterhaus, A. D. M. E. & Kuiken, T. The pathology and pathogenesis of experimental severe acute respiratory syndrome and influenza in animal models. *Journal of Comparative Pathology* **151**, 83–112 (2014).

230. George, P. M., Wells, A. U. & Jenkins, R. G. Pulmonary fibrosis and COVID-19: the potential role for antifibrotic therapy. *The Lancet Respiratory Medicine* **8**, 807–815 (2020).

231. Davey, A., McAuley, D. F. & O'Kane, C. M. Matrix metalloproteinases in acute lung injury: Mediators of injury and drivers of repair. *European Respiratory Journal* **38**, 959–970 (2011).

232. Matthay, M. A., Ware, L. B. & Zimmerman, G. A. The acute respiratory distress syndrome. *Journal of Clinical Investigation* **122**, 2731–2740 (2012).

233. Matthay, M. A. & Zemans, R. L. The acute respiratory distress syndrome: Pathogenesis and treatment. *Annu. Rev. Pathol. Mech. Dis.* **6**, 147–163 (2011).

234. Ware, L. B. & Matthay, M. A. The Acute Respiratory Distress Syndrome. *N. Engl. J. Med.* **342**, 1334–1349 (2000).

235. Dos Santos, C. C. Advances in mechanisms of repair and remodelling in acute lung injury.

Intensive Care Medicine **34**, 619–630 (2008).

236. Williamson, J. D., Sadofsky, L. R. & Hart, S. P. Experimental Lung Research The pathogenesis of bleomycin-induced lung injury in animals and its applicability to human idiopathic pulmonary fibrosis. (2014). doi:10.3109/01902148.2014.979516

237. Reinert, T., Baldotto, C. S. da R., Nunes, F. A. P. & Scheliga, A. A. de S. Bleomycin-Induced Lung Injury. *J. Cancer Res.* **2013**, 1–9 (2013).

238. Laskin, D. L., Malaviya, R. & Laskin, J. D. Role of Macrophages in Acute Lung Injury and Chronic Fibrosis Induced by Pulmonary Toxicants. *Toxicological Sciences* **168**, 287–301 (2019).

239. Zannikou, M. *et al.* MAP3K8 Regulates Cox-2–Mediated Prostaglandin E $_2$ Production in the Lung and Suppresses Pulmonary Inflammation and Fibrosis. *J. Immunol.* ji2000862 (2020). doi:10.4049/jimmunol.2000862

240. Wang, T. *et al.* Arachidonic acid metabolism and kidney inflammation. *International Journal of Molecular Sciences* **20**, (2019).

241. Park, J. Y., Pillinger, M. H. & Abramson, S. B. Prostaglandin E2 synthesis and secretion: The role of PGE2 synthases. *Clin. Immunol.* **119**, 229–240 (2006).

242. Roulis, M. *et al.* Intestinal myofibroblast-specific Tpl2-Cox-2-PGE2 pathway links innate sensing to epithelial homeostasis. *Proc. Natl. Acad. Sci. U. S. A.* **111**, E4658-67 (2014).

243. Dudek, S. E., Nitzsche, K., Ludwig, S. & Ehrhardt, C. Influenza A viruses suppress cyclooxygenase-2 expression by affecting its mRNA stability. *Sci. Rep.* **6**, (2016).

244. Harper, K. A. & Tyson-Capper, A. J. Complexity of COX-2 gene regulation. *Biochemical Society Transactions* **36**, 543–545 (2008).

245. Steer, S. A. & Corbett, J. A. The Role and Regulation of COX-2 during Viral Infection. *Viral Immunology* **16**, 447–460 (2003).

246. Savard, M. *et al.* EBV Suppresses Prostaglandin E 2 Biosynthesis in Human Monocytes . *J. Immunol.* **164**, 6467–6473 (2000).

247. Mertz, D. *et al.* Pregnancy as a risk factor for severe outcomes from influenza virus infection: A

systematic review and meta-analysis of observational studies. *Vaccine* **35**, 521–528 (2017).

248. Wang, X. *et al.* Global burden of respiratory infections associated with seasonal influenza in children under 5 years in 2018: a systematic review and modelling study. *Lancet Glob. Heal.* **8**, e497–e510 (2020).

249. Wilhelm, M. Influenza in Older Patients: A Call to Action and Recent Updates for Vaccinations. *Am. J. Manag. Care* **24**, S15–S24 (2018).

250. Anderson, E. J. *et al.* Outcomes of Immunocompromised Adults Hospitalized With Laboratory-confirmed Influenza in the United States, 2011-2015. *Clin. Infect. Dis.* **70**, 2121–2151 (2020).

251. Iuliano, A. D. *et al.* Estimates of global seasonal influenza-associated respiratory mortality: a modelling study. *Lancet* **391**, 1285–1300 (2018).

252. Konala, V. M. *et al.* Co-infection with Influenza A and COVID-19. *Eur. J. Case Reports Intern. Med.* **7**, 1 (2020).

253. Lee, A. J. & Ashkar, A. A. The dual nature of type I and type II interferons. *Frontiers in Immunology* **9**, 2061 (2018).

254. Killip, M. J., Fodor, E. & Randall, R. E. Influenza virus activation of the interferon system. *Virus Res.* **209**, 11–22 (2015).

255. Shim, J. M., Kim, J., Tenson, T., Min, J. Y. & Kainov, D. E. Influenza virus infection, interferon response, viral counter-response, and apoptosis. *Viruses* **9**, (2017).

256. Chen, X. *et al.* Host immune response to influenza A virus infection. *Frontiers in Immunology* **9**, 320 (2018).

257. Jewell, N. A. *et al.* Lambda interferon is the predominant interferon induced by influenza A virus infection in vivo. *J. Virol.* **84**, 11515–22 (2010).

258. Sommereyns, C. *et al.* IFN-Lambda (IFN-λ) Is Expressed in a Tissue-Dependent Fashion and Primarily Acts on Epithelial Cells In Vivo. *PLoS Pathog.* **4**, e1000017 (2008).

259. Egli, A., Santer, D. M., O ’shea, D., Tyrrell, D. L. & Houghton, M. The impact of the interferon-lambda family on the innate and adaptive immune response to viral infections. **51**, (2014).

260. Crotta, S. *et al.* Type I and Type III Interferons Drive Redundant Amplification Loops to Induce a Transcriptional Signature in Influenza-Infected Airway Epithelia. *PLoS Pathog.* **9**, e1003773 (2013).

261. Ank, N. *et al.* An important role for type III interferon (IFN-lambda/IL-28) in TLR-induced antiviral activity. *J. Immunol.* **180**, 2474–85 (2008).

262. Mordstein, M. *et al.* Lambda Interferon Renders Epithelial Cells of the Respiratory and Gastrointestinal Tracts Resistant to Viral Infections. *J. Virol.* **84**, 5670–5677 (2010).

263. Sun, Y., Jiang, J., Tien, P., Liu, W. & Li, J. IFN-λ: A new spotlight in innate immunity against influenza virus infection. *Protein and Cell* **9**, 832–837 (2018).

264. Dumitru, C. D. *et al.* TNF-α Induction by LPS Is Regulated Posttranscriptionally via a Tpl2/ERK-Dependent Pathway. *Cell* **103**, 1071–1083 (2000).

265. López-Pelaéz, M. *et al.* Cot/tpl2-MKK1/2-Erk1/2 controls mTORC1-mediated mRNA translation in Toll-like receptor-activated macrophages. *Mol. Biol. Cell* **23**, 2982–2992 (2012).

266. Li, X. *et al.* Tumor Progression Locus 2 (Tpl2) Activates the Mammalian Target of Rapamycin (mTOR) Pathway, Inhibits Forkhead Box P3 (FoxP3) Expression, and Limits Regulatory T Cell (Treg) Immunosuppressive Functions *. (2016). doi:10.1074/jbc.M116.718783

267. Watford, W. T. *et al.* Ablation of Tumor Progression Locus 2 Promotes a Type 2 Th Cell Response in Ovalbumin-Immunized Mice. *J. Immunol.* **184**, 105–113 (2010).

268. Koliaraki, V., Roulis, M. & Kollias, G. Tpl2 regulates intestinal myofibroblast HGF release to suppress colitis-associated tumorigenesis. *J. Clin. Invest.* **122**, 4231–42 (2012).

269. Van Acker, G. J. D. *et al.* Tumor progression locus-2 is a critical regulator of pancreatic and lung inflammation during acute pancreatitis. *J. Biol. Chem.* **282**, 22140–9 (2007).

270. Rodríguez-Castillo, J. A. *et al.* Understanding alveolarization to induce lung regeneration. *Respiratory Research* **19**, (2018).

271. Wert, S. E., Glasser, S. W., Korfhagen, T. R. & Whitsett, J. A. Transcriptional elements from the human SP-C gene direct expression in the primordial respiratory epithelium of transgenic mice.

Dev. Biol. **156**, 426–443 (1993).

272. Rawlins, E. L. & Perl, A.-K. The a"MAZE"ing world of lung-specific transgenic mice. *Am. J. Respir. Cell Mol. Biol.* **46**, 269–82 (2012).

273. Costa, R. H., Kalinichenko, V. V. & Lim, L. Transcription factors in mouse lung development and function. *American Journal of Physiology - Lung Cellular and Molecular Physiology* **280**, 823–838 (2001).

274. Rankin, S. A. & Zorn, A. M. Gene regulatory networks governing lung specification. *J. Cell. Biochem.* **115**, 1343–1350 (2014).

275. Sinha, M. & Lowell, C. Isolation of Highly Pure Primary Mouse Alveolar Epithelial Type II Cells by Flow Cytometric Cell Sorting. *BIO-PROTOCOL* **6**, (2016).

276. Acuff, N. V., Li, X., Elmore, J., Rada, B. & Watford, W. T. Tpl2 promotes neutrophil trafficking, oxidative burst, and bacterial killing. *J. Leukoc. Biol.* jlb.3A0316-146R (2017). doi:10.1189/jlb.3A0316-146R

277. Kuriakose, T., Rada, B. & Watford, W. T. Tumor progression locus 2-dependent oxidative burst drives phosphorylation of extracellular signal-regulated kinase during TLR3 and 9 signaling. *J. Biol. Chem.* **289**, 36089–36100 (2014).

278. Rosenberger, C. M. *et al.* Characterization of innate responses to influenza virus infection in a novel lung type I epithelial cell model. *J. Gen. Virol.* **95**, 350–62 (2014).

279. Baer, A. & Kehn-Hall, K. Viral concentration determination through plaque assays: Using traditional and novel overlay systems. *J. Vis. Exp.* 52065 (2014). doi:10.3791/52065

280. Fumoto, K. *et al.* Mark1 regulates distal airspace expansion through type I pneumocyte flattening in lung development. *J. Cell Sci.* **132**, (2019).

281. Kaiser, F. *et al.* TPL-2 negatively regulates interferon-beta production in macrophages and myeloid dendritic cells. *J. Exp. Med.* **206**, 1863–71 (2009).

282. Dumitru, C. D. *et al.* TNF-␣ Induction by LPS Is Regulated Posttranscriptionally via a

Tpl2/ERK-Dependent Pathway. *Cell* **103**, 1071–1083 (2000).

283. Gridley, T. & Groves, A. K. Overview of genetic tools and techniques to study notch signaling in mice. *Methods in Molecular Biology* **1187**, 47–61 (2014).

284. Bao, J., Ma, H. Y., Schuster, A., Lin, Y. M. & Yan, W. Incomplete cre-mediated excision leads to phenotypic differences between Stra8-iCre; Mov10l1lox/lox and Stra8-iCre; Mov10l1lox/Δ mice. *Genesis* **51**, 481–490 (2013).

285. Rock, J. R. *et al.* Multiple stromal populations contribute to pulmonary fibrosis without evidence for epithelial to mesenchymal transition. **108**, E1475–E1483 (2011).

286. Rutigliano, J. A. *et al.* Highly Pathological Influenza A Virus Infection Is Associated with Augmented Expression of PD-1 by Functionally Compromised Virus-Specific CD8+ T Cells. *J. Virol.* **88**, 1636–1651 (2014).

287. Topaz, G. *et al.* The association between red cell distribution width and poor outcomes in hospitalized patients with influenza. *J. Crit. Care* **41**, 166–169 (2017).

288. Dengler, L. *et al.* Cellular Changes in Blood Indicate Severe Respiratory Disease during Influenza Infections in Mice. *PLoS One* **9**, e103149 (2014).

289. Gil, M. P. *et al.* Regulating type 1 IFN effects in CD8 T cells during viral infections: Changing STAT4 and STAT1 expression for function. *Blood* **120**, 3718–3728 (2012).

290. Schmidt, M. E. & Varga, S. M. The CD8 T cell response to respiratory virus infections. *Frontiers in Immunology* **9**, (2018).

291. Mineo, G. *et al.* Post-ARDS pulmonary fibrosis in patients with H1N1 pneumonia: role of follow-up CT. *Radiol. Medica* **117**, 185–200 (2012).

292. Hu, X. & Huang, X. Alleviation of inflammatory response of pulmonary fibrosis in acute respiratory distress syndrome by puerarin via transforming growth factor (TGF-b1). *Med. Sci. Monit.* **25**, 6523–6531 (2019).

293. Meduri, G. U. & Eltorky, M. A. Understanding ARDS-associated fibroproliferation. *Intensive Care Med.* **41**, 517–520 (2015).

294. Vougioukalaki, M., Kanellis, D. C., Gkouskou, K. & Eliopoulos, A. G. Tpl2 kinase signal transduction in inflammation and cancer. *Cancer Lett.* **304**, 80–89 (2011).

295. Li, L. F., Liao, S. K., Huang, C. C., Hung, M. J. & Quinn, D. A. Serine/threonine kinase-protein kinase B and extracellular signal-regulated kinase regulate ventilator-induced pulmonary fibrosis after bleomycin-induced acute lung injury: A prospective, controlled animal experiment. *Crit. Care* **12**, R103 (2008).

296. Kannan, Y. *et al.* TPL-2 Regulates Macrophage Lipid Metabolism and M2 Differentiation to Control TH2-Mediated Immunopathology. *PLoS Pathog.* **12**, (2016).

297. Eslam, M. *et al.* IFN-λ3, not IFN-λ4, likely mediates IFNL3-IFNL4 haplotype-dependent hepatic inflammation and fibrosis. *Nat. Genet.* **49**, 795–800 (2017).

298. Metwally, M. *et al.* IFNL3 genotype is associated with pulmonary fibrosis in patients with systemic sclerosis. *Sci. Rep.* **9**, 1–5 (2019).

299. Heery, M., Corbett, P. & Zelkowitz, R. Precautions for Patients Taking Tamoxifen. *J. Adv. Pract. Oncol.* **9**, 78–83 (2018).

300. Wibowo, E., Pollock, P. A., Hollis, N. & Wassersug, R. J. Tamoxifen in men: a review of adverse events. *Andrology* **4**, 776–788 (2016).

301. Goldhirsch, A. *et al.* Progress and promise: Highlights of the international expert consensus on the primary therapy of early breast cancer 2007. *Ann. Oncol.* **18**, 1133–1144 (2007).

302. Viani, G. A., Bernardes Da Silva, L. G. & Stefano, E. J. Prevention of gynecomastia and breast pain caused by androgen deprivation therapy in prostate cancer: Tamoxifen or radiotherapy? *Int. J. Radiat. Oncol. Biol. Phys.* **83**, e519–e524 (2012).

303. Chlebowski, R. T., Kim, J. & Haque, R. Adherence to endocrine therapy in breast cancer adjuvant and prevention settings. *Cancer Prevention Research* **7**, 378–387 (2014).

304. Yoo, J. J. *et al.* Risk of fatty liver after long-term use of tamoxifen in patients with breast cancer. *PLoS One* **15**, (2020).

305. Candelaria, M., Hurtado-Monroy, R., Vargas-Viveros, P., Carrillo-Muñnoz, S. & Duenas-

Gonzalez, A. Tamoxifen-associated vasculitis in a breast cancer patient. *World Journal of Surgical Oncology* **5**, 9 (2007).

306. Behjati, S. & Frank, M. The Effects of Tamoxifen on Immunity. *Curr. Med. Chem.* **16**, 3076–3080 (2009).

307. Baum, M. *et al.* Anastrozole Alone or in Combination with Tamoxifen versus Tamoxifen Alone for Adjuvant Treatment of Postmenopausal Women with Early-Stage Breast Cancer: Results of the ATAC (Arimidex, Tamoxifen Alone or in Combination) Trial Efficacy and Safety Update Ana. *Cancer* **98**, 1802–1810 (2003).

308. van Hellemond, I., Geurts, S. & Tjan-Heijnen, V. Current Status of Extended Adjuvant Endocrine Therapy in Early Stage Breast Cancer. *Current Treatment Options in Oncology* **19**, (2018).

309. Rawlins, E. L. & Perl, A. K. The a"MAZE"ing world of lung-specific transgenic mice. *American Journal of Respiratory Cell and Molecular Biology* **46**, 269–282 (2012).

310. Patel, S. H. *et al.* Low-dose tamoxifen treatment in juvenile males has long-term adverse effects on the reproductive system: Implications for inducible transgenics. *Sci. Rep.* **7**, (2017).

311. Sthoeger, Z. M., Zinger, H. & Mozes, E. Beneficial effects of the anti-oestrogen tamoxifen on systemic lupus erythematosus of (NZBxNZW)F1 female mice are associated with specific reduction of IgG3 autoantibodies. *Ann. Rheum. Dis.* **62**, 341–346 (2003).

312. Wu, W. M., Suen, J. L., Lin, B. F. & Chiang, B. L. Tamoxifen alleviates disease severity and decreases double negative T cells in autoimmune MRL-lpr/lpr mice. *Immunology* **100**, 110–118 (2000).

313. Wu, W., Lin, B., Su, Y., Suen, J. & Chiang, B. Tamoxifen Decreases Renal Inflammation and Alleviates Disease Severity in Autoimmune NZB/W F1 Mice. *Scand. J. Immunol.* **52**, 393–400 (2000).

314. Bebo, B. F. *et al.* Treatment with selective estrogen receptor modulators regulates myelin specific T-cells and suppresses experimental autoimmune encephalomyelitis. *Glia* **57**, 777–790 (2009).

315. Animals, N. R. C. (US) C. for the U. of the G. for the & Laboratory, C. and U. of. *Guide for the*

Care and Use of Laboratory Animals. *Guide for the Care and Use of Laboratory Animals* (National Academies Press, 2011). doi:10.17226/12910

316. McClean, C. M. & Tobin, D. M. Macrophage form, function, and phenotype in mycobacterial infection: Lessons from tuberculosis and other diseases. *Pathogens and Disease* **74**, 68 (2016).

317. Gutiérrez-Jiménez, C. *et al.* Persistence of brucella abortus in the bone marrow of infected mice. *J. Immunol. Res.* **2018**, (2018).

318. Dellière, S. *et al.* Understanding pathogenesis and care challenges of immune reconstitution inflammatory syndrome in fungal infections. *Journal of Fungi* **4**, (2018).

319. Shah, S. *et al.* Cutting Edge: Mycobacterium tuberculosis but Not Nonvirulent Mycobacteria Inhibits IFN- and AIM2 Inflammasome-Dependent IL-1 Production via Its ESX-1 Secretion System. *J. Immunol.* **191**, 3514–3518 (2013).

320. Russell, D. G., Cardona, P. J., Kim, M. J., Allain, S. & Altare, F. Foamy macrophages and the progression of the human tuberculosis granuloma. *Nature Immunology* **10**, 943–948 (2009).

321. Greaves, P., Goonetilleke, R., Nunn, G., Topham, J. & Orton, T. *Two-Year Carcinogenicity Study of Tamoxifen in Alderley Park Wistar-derived Rats*. *CANCER RESEARCH* **53**, (1993).

322. Huh, W. J. *et al.* Tamoxifen induces rapid, reversible atrophy, and metaplasia in mouse stomach. *Gastroenterology* **142**, 21 (2012).

323. Keeley, T. M., Horita, N. & Samuelson, L. C. Tamoxifen-Induced Gastric Injury: Effects of Dose and Method of Administration. *CMGH* **8**, 365–367 (2019).

324. Moon, H.-G. *et al.* Airway Epithelial Cell-Derived Colony Stimulating Factor-1 Promotes Allergen Sensitization. *Immunity* **49**, 275-287.e5 (2018).

325. Ye, R. *et al.* Impact of tamoxifen on adipocyte lineage tracing: Inducer of adipogenesis and prolonged nuclear translocation of Cre recombinase. *Mol. Metab.* **4**, 771–778 (2015).

326. Madisen, L. *et al.* A robust and high-throughput Cre reporting and characterization system for the whole mouse brain. *Nat. Neurosci.* **13**, 133–140 (2010).

327. Glaab, T., Taube, C., Braun, A. & Mitzner, W. Invasive and noninvasive methods for studying

pulmonary function in mice. *Respiratory Research* **8**, 63 (2007).

328. Bates, J. H. T. CORP: Measurement of lung function in small animals. *Journal of Applied Physiology* **123**, 1039–1046 (2017).

329. Agarwal, A. K., Raja, A. & Brown, B. D. Chronic Obstructive Pulmonary Disease. (2020).

330. Saxena, N. Restrictive lung disease. in *The Perioperative Medicine Consult Handbook* 199–202 (Springer International Publishing, 2015). doi:10.1007/978-3-319-09366-6_32

331. Criée, C. P. *et al.* Body plethysmography - Its principles and clinical use. *Respiratory Medicine* **105**, 959–971 (2011).

332. Lim, R. *et al.* Measuring respiratory function in mice using unrestrained whole-body plethysmography. *J. Vis. Exp.* 51755 (2014). doi:10.3791/51755

333. Castro, D. & Keenaghan, M. Arterial Blood Gas. (2020).

334. Wüst, R. C. I., Houtkooper, R. H. & Auwerx, J. Confounding factors from inducible systems for spatiotemporal gene expression regulation. *Journal of Cell Biology* **219**, (2020).